

# **INVESTIGATIONS ON THE ROLE OF GREEN SYNTHESIZED IRON NANOPARTICLES IN THE FENTON'S OXIDATION OF TRICLOSAN IN WASTEWATER**

Thesis

Submitted in partial fulfillment of the requirements for the degree of

**DOCTOR OF PHILOSOPHY**

By

**RASHMISHREE K N**

**(Reg. No: 155123CV15P01)**



**DEPARTMENT OF CIVIL ENGINEERING**

**NATIONAL INSTITUTE OF TECHNOLOGY KARNATAKA, SURATHKAL**

**SRINIVASNAGAR, MANGALURU -575 025**

**December 2023**

**INVESTIGATIONS ON THE ROLE OF  
GREEN SYNTHESIZED IRON  
NANOPARTICLES IN THE FENTON'S  
OXIDATION OF TRICLOSAN IN  
WASTEWATER**

**Thesis**

Submitted in partial fulfillment of the requirements for the degree of

**DOCTOR OF PHILOSOPHY**

By

**RASHMISHREE K N**

**(Reg. No: 155123CV15P01)**

Under the guidance of

**Dr. S. SHRIHARI**

**&**

**Dr. ARUN KUMAR THALLA**



**DEPARTMENT OF CIVIL ENGINEERING**

**NATIONAL INSTITUTE OF TECHNOLOGY KARNATAKA, SURATHKAL**

**SRINIVASNAGAR, MANGALURU -575 025**

**December 2023**

## DECLARATION

By the Ph.D. Research Scholar

I hereby declare that the Research Thesis entitled "*INVESTIGATIONS ON THE ROLE OF GREEN SYNTHESIZED IRON NANOPARTICLES IN THE FENTON'S OXIDATION OF TRICLOSAN IN WASTEWATER*" which is being submitted to the National Institute of Technology Karnataka, Surathkal in partial fulfillment of the requirements for the award of the Degree of Doctor of Philosophy in Environmental Engineering in the Department of Civil Engineering is a bonafide report of the research work carried out by me. The material contained in this Research Synopsis has not been submitted to any University or Institution for the award of any degree.



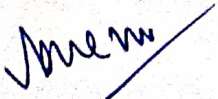
Rashmishree K N (155123CV15P01)  
Department of Civil Engineering

Place: NITK-Surathkal

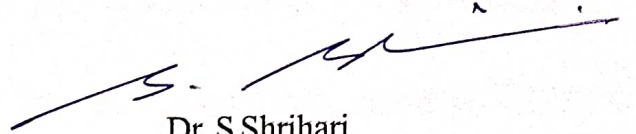
Date: 08/12/2023

## CERTIFICATE

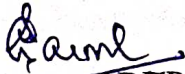
This is to certify that the Research Thesis entitled "*INVESTIGATIONS ON THE ROLE OF GREEN SYNTHESIZED IRON NANOPARTICLES IN THE FENTON'S OXIDATION OF TRICLOSAN IN WASTEWATER*" submitted by RASHMISHREE K N (Register Number: 155123CV15P01) as the record of the research work carried out by her, is accepted as the Research Thesis submission in partial fulfillment of the requirements for the award of the degree of Doctor of Philosophy.



Dr. Arun Kumar Thalla  
Professor  
Department of Civil Engineering  
NITK, Surathkal



Dr. S Shrihari  
Professor  
Department of Civil Engineering  
NITK, Surathkal



Chairman - DRPC  
Department of Civil Engineering  
NITK, Surathkal

**Chairman (DRPC)**  
**Department of Civil Engineering**  
**National Institute of Technology Karnataka**  
**Surathkal, Mangalore - 575 025, Karnataka, INDIA**



## CONTENTS

ABSTRACT.....	iv
LIST OF FIGURES.....	viii
LIST OF TABLES.....	xi
NOMENCLATURE .....	xii
<b>CHAPTER 1 .....</b>	<b>1</b>
<b>INTRODUCTION.....</b>	<b>1</b>
1.1 GENERAL .....	1
1.2 OBJECTIVES .....	7
1.3 MOTIVATION FOR THE RESEARCH.....	7
1.4 STRUCTURE OF THE THESIS .....	9
<b>CHAPTER 2 .....</b>	<b>11</b>
<b>LITERATURE REVIEW .....</b>	<b>11</b>
2.1 GENERAL .....	11
2.2 EXPOSURE OF TRICLOSAN IN THE ENVIRONMENT .....	13
2.3 AVAILABLE TREATMENT TECHNOLOGIES FOR TRICLOSAN REMOVAL .....	16
2.3.1 Physical Treatment Methods.....	16
2.3.2 Biological Treatment Methods.....	17
2.3.3 Advanced Oxidation Process .....	18
2.3.3.1 Fenton’s Oxidation.....	20
2.4 DEGRADATION OF TRICLOSAN USING NANOPARTICLES.....	22
2.5 GREEN SYNTHESIZED NANOPARTICLES FOR THE POLLUTANT REMOVAL.....	23

2.6 FENTONS OXIDATION PROCESS USING LATERITE IRON.....	25
2.7 BIO-FENTON OXIDATION .....	27
2.8 SUMMARY OF THE LITERATURE REVIEW .....	28
<b>CHAPTER 3 .....</b>	<b>31</b>
<b>MATERIALS AND METHODS .....</b>	<b>31</b>
3.1 MATERIALS .....	31
3.1.1 List of Chemicals Utilized .....	31
3.1.2 Raw Laterite Soil Sample.....	32
3.2 METHODOLOGY .....	32
3.2.1 Extraction of Iron from Laterite Soil.....	32
3.2.2 Preparation of Leaf Extract .....	33
3.3 SYNTHESIS AND CHARACTERIZATION OF IRON NANOPARTICLES .....	33
3.4 ANALYTICAL METHODS .....	34
3.5 FENTON’S OXIDATION OF TRICLOSAN.....	34
3.6 BIO-FENTON’S OXIDATION OF TRICLOSAN.....	34
3.6.1 Production of Hydrogen Peroxide Based on Enzyme Activity .....	35
<b>CHAPTER 4 .....</b>	<b>37</b>
<b>RESULTS AND DISCUSSION .....</b>	<b>37</b>
4.1 CHARACTERIZATION OF RAW LATERITE SOIL .....	37
4.2 CHARACTERIZATION OF GREEN LATERITE-BASED IRON NANOPARTICLES (GLaFeNPs).....	39
4.2.1 Characterization of Synthesized GLaFeNPs .....	39
4.3 FENTON’S OXIDATION OF TRICLOSAN.....	44
4.3.1 Fenton’s Degradation of Triclosan by GPsLaNP .....	44
4.3.2 Fenton’s Degradation of Triclosan by GMpLaNP .....	46

4.3.3	Effect of Hydrogen Peroxide on Fenton’s Oxidation of Triclosan.....	48
4.3.3.1	<i>Effect of Hydrogen Peroxide on GPsLaNP.....</i>	49
4.3.3.2	<i>Effect of Hydrogen Peroxide on GMpLaNP.....</i>	51
4.3.4	Effect of Initial Concentration of Triclosan on Fenton’s Oxidation .....	52
4.3.4.1	<i>Effect of initial Concentration of triclosan on Fenton’s Oxidation using GPsLaNP</i>	53
4.3.4.2	<i>Effect of initial Concentration of triclosan on Fenton’s Oxidation using GMpLaNP</i>	55
4.3.5	Effect of pH on Fenton’s Oxidation of Triclosan.....	56
4.3.6	Effect of Treatment Time on Fenton’s Oxidation of Triclosan.....	58
4.3.7	Effect of Iron on Fenton’s Oxidation of Triclosan.....	59
4.3.8	Degradation Kinetics.....	62
4.3.9	Reuse and Recoverability Studies .....	64
4.4	BIO-FENTON’S OXIDATION OF TRICLOSAN.....	65
4.4.1	Optimization of Hydrogen Peroxide Production From Glucose Oxidase and Glucose .....	66
4.4.2	Bio Fenton’s Process of Triclosan Using GPsLaNP and GMpLaNP.....	67
4.4.3	Degradation Kinetics for Bio-Fenton Process.....	68
<b>CHAPTER 5</b>	.....	<b>71</b>
<b>SUMMARY AND CONCLUSIONS</b>	.....	<b>71</b>
<b>SCOPE FOR THE FUTURE WORK</b>	.....	<b>72</b>

## LIST OF FIGURES

Figure 2.1: Structure of triclosan.....	13
Figure 2.2: Environmental fate and effects of TCS.....	14
Figure 3.1: Location of Raw Lateritic soil sample.....	32
Figure 3.2: Green synthesised laterite iron nanoparticles (a) <i>Psidium guajava</i> leaf extract(b) <i>Macaranga peltata</i> leaf extract (c) Laterite extract (d) synthesized nano iron particles.....	33
Figure 4.1: Raw Laterite Particles a) Scanning Electron Microscopic images b) EDS images .....	38
Figure 4.2: XRD Images of Raw Laterite Particles.....	39
Figure 4.3: Scanning Electron Microscopic images of Green laterite Iron oxide Nanoparticles (GLaFeNPs) a) <i>Psidium guajava</i> Laterite Iron Oxide Nanoparticles (GPsLaNP) b) <i>Macaranga peltata</i> Laterite Iron Oxide Nanoparticles (GMpLaNP) showing the morphological appearance .....	41
Figure 4.4: EDS images of Green laterite Iron oxide Nanoparticles (GLaFeNPs) a) <i>Psidium guajava</i> Laterite Iron Oxide Nanoparticles (GPsLaNP) b) <i>Macaranga peltata</i> Laterite Iron Oxide Nanoparticles (GMpLaNP).....	41
Figure 4.5: XRD Images of Green laterite Iron oxide Nanoparticles (GLaFeNPs) a) <i>Psidium guajava</i> Laterite Iron Oxide Nanoparticles (GPsLaNP) b) <i>Macaranga peltata</i> Laterite Iron Oxide Nanoparticles (GMpLaNP) representing the corresponding peaks	42
Figure 4.6: FTIR Images of Green laterite Iron oxide Nanoparticles (GLaFeNPs) a) <i>Psidium guajava</i> Laterite Iron Oxide Nanoparticles (GPsLaNP) b) <i>Macaranga peltata</i> Laterite Iron Oxide Nanoparticles (GMpLaNP) representing the corresponding peaks	43

Figure 4.7: Oxidative degradation of Triclosan at different GPsLaNP dosages with variation in H <sub>2</sub> O <sub>2</sub> a) 100 mg/L of H <sub>2</sub> O <sub>2</sub> b) 200 mg/L of H <sub>2</sub> O <sub>2</sub> c) 300 mg/L of H <sub>2</sub> O <sub>2</sub> d) 400 mg/L of H <sub>2</sub> O <sub>2</sub> .....	46
Figure 4.8: Oxidative degradation of Triclosan at different GMpLaNP dosages with variation in H <sub>2</sub> O <sub>2</sub> a) 100 mg/L of H <sub>2</sub> O <sub>2</sub> b) 200 mg/L of H <sub>2</sub> O <sub>2</sub> c) 300 mg/L of H <sub>2</sub> O <sub>2</sub> d) 400 mg/L of H <sub>2</sub> O <sub>2</sub> .....	48
Figure 4.9: Effect of Hydrogen Peroxide during Fenton's oxidation of Triclosan with GPsLaNP at a) 0.01 g/L b) 0.1 g/L c) 1 g/L .....	50
Figure 4.10: Effect of Hydrogen peroxide during Fenton's oxidation of Triclosan with GMpLaNP at a) 0.01 g/L b) 0.1 g/L c) 1 g/L .....	52
Figure 4.11: Effect of Initial concentration of Triclosan during Fenton's oxidation with <i>Psidium guajava</i> Laterite Iron Oxide Nanoparticles (GPsLaNP) .....	54
Figure 4.12: Effect of Initial concentration of Triclosan during Fenton's oxidation with <i>Macaranga peltata</i> Laterite Iron Oxide Nanoparticles (GMpLaNP).....	56
Figure 4.13: Effect of pH during Fenton's oxidation with a) <i>Psidium guajava</i> Laterite Iron Oxide Nanoparticles (GPsLaNP) b) <i>Macaranga peltata</i> Laterite Iron Oxide Nanoparticles (GMpLaNP).....	57
Figure 4.14: Total Iron variation during Fenton's oxidation of Triclosan with a) <i>Psidium guajava</i> Laterite Iron Oxide Nanoparticles (GPsLaNP) b) <i>Macaranga peltata</i> Laterite Iron Oxide Nanoparticles (GMpLaNP) .....	60
Figure 4.15: Ferrous Iron variation during Fenton's oxidation of Triclosan with a) <i>Psidium guajava</i> Laterite Iron Oxide Nanoparticles (GPsLaNP) b) <i>Macaranga peltata</i> Laterite Iron Oxide Nanoparticles (GMpLaNP) .....	51

Figure 4.16: Ferric Iron variation during Fenton’s oxidation of Triclosan with a) <i>Psidium guajava</i> Laterite Iron Oxide Nanoparticles (GPsLaNP) b) <i>Macaranga peltata</i> Laterite Iron Oxide Nanoparticles (GMpLaNP) .....	61
Figure 4.17: Linear fit for Fenton’s oxidation of Triclosan with a) <i>Psidium guajava</i> Laterite Iron Oxide Nanoparticle (GPsLaNP) b) <i>Macaranga peltata</i> Laterite Iron Oxide Nanoparticle (GMpLaNP) .....	63
Figure 4.18: Reusability on Fenton’s oxidation of Triclosan with a) <i>Psidium guajava</i> Laterite Iron Oxide Nanoparticles GPsLaNP b) <i>Macaranga peltata</i> Laterite Iron Oxide Nanoparticles GMpLaNP .....	65
Figure 4.19: Production of H <sub>2</sub> O <sub>2</sub> with different concentrations of glucose (a) 1000U/L Enzyme (b) 2000U/L Enzyme.....	67
Figure 4.20: Oxidative degradation of Triclosan by Bio-Fenton process a) <i>Psidium guajava</i> Laterite Iron Oxide Nanoparticles (GPsLaNP) b) <i>Macaranga peltata</i> Laterite Iron Oxide Nanoparticles (GMpLaNP) .....	68
Figure 4.21: Linear fit for Bio Fenton’s oxidation of Triclosan with a) <i>Psidium guajava</i> Laterite Iron Oxide Nanoparticles (GPsLaNP) b) <i>Macaranga peltata</i> Laterite Iron Oxide Nanoparticles (GMpLaNP).....	69

## LIST OF TABLES

Table 2.1: Occurrence of Triclosan in various water bodies .....	15
Table 4.1 Chemical composition of Raw Lateritic soil.....	38
Table 4.2: Elemental composition of GPsLaNP and GMpLaNP .....	40
Table 4.3: Degradation of triclosan by GPsLaNP with different catalyst loading .....	45
Table 4.4: Degradation of triclosan by GMpLaNP with different catalyst loading.....	47
Table 4.5: Maximum degradation of triclosan by GPsLaNP.....	49
Table 4.6: Maximum degradation of triclosan by GMpLaNP.....	51
Table 4.7: Degradation of initial concentration of triclosan by GPsLaNP .....	53
Table 4.8: Degradation of Initial concentration of triclosan by GMpLaNP .....	55
Table 4.9: Maximum degradation of triclosan at various pH.....	58
Table 4.10: Reusability of GLaFeNPs on Fenton's oxidation of Triclosan .....	64
Table 4.11: Overview of Fenton's oxidation of Triclosan with a different iron nanoparticles .....	65
Table 4.12: Bio-Fenton's degradation of triclosan at various pH .....	68

## NOMENCLATURE

<b>Name</b>	<b>Fullform</b>
AB 113	Azo dye
Al <sub>2</sub> O <sub>3</sub>	aluminium oxides
AOP	Advanced Oxidation Process
BDD	Boron-doped diamond
BF	Bio-Fenton
BiFeOMNP	Bismuth ferrite magnetic nanoparticle
BOD	Biochemical oxygen Demand
CDEO	Conductive-Diamond Electrochemical Oxidation
COD	Chemical oxygen demand
DAD	Diode array detector
ECs	Emerging contaminants
EDC	Endocrine-disrupting chemicals
Fe <sup>2+</sup>	Ferrous
Fe <sub>2</sub> O <sub>3</sub>	Iron oxides
Fe <sup>3+</sup>	Ferric
FTIR	Fourier Transform Infrared Spectroscopy
GLFeNP's	Green synthesized laterite iron nanoparticles
GMpLaNP	Green synthesized laterite-based Makarangapeltata nanoparticles
GO	Graphene oxide
GOD	Glucose oxidase
GPsLaNP	Green synthesized laterite-based Psidiumguajava nanoparticles
H <sub>2</sub> O <sub>2</sub>	Hydrogen Peroxide
HA	Humic acid
HCl	Hydrochloric acid
HPLC	High performance liquid chromatography
Ni	Nickel
NMs	Nanomaterials
NOM	Natural organic matter
NPs	Nanoparticles

O <sub>2</sub>	Oxygen
OH	Hydroxyl radical
PPCPs	Pharmaceutical and Personal Care Products
Sep	Sepolite
Si <sub>2</sub> O <sub>3</sub>	Silica
TCE	Trichloroethylene
TCS	Triclosan
TiO <sub>2</sub>	Titanium oxide
UV	Ultraviolet
WWTP	Wastewater treatment plant
XRD	X Ray Diffraction

# CHAPTER 1

## INTRODUCTION

### 1.1 GENERAL

Water is essential for all living beings. Rivers, lakes, oceans, and underground aquifers are the sources of water from which it is drawn for various purposes like domestic, irrigation, and industrial. But with the advancement in industrialization and urbanization, the utility of water has enormously increased and it is impossible to fulfill the water demand from various sources. Therefore it is very essential to treat the generated wastewater and utilize the same. Hence treated wastewater has become one of the important alternative sources of water.

Bioaccumulation of Pharmaceutical and Personal Care Products (PPCPs) in the water system is of major concern in the field of Environmental technology. Instances pointing to the reappearance of traces of Pharmaceutical and Personal Care compounds like ibuprofen, aspirin, primidone, triclosan carbamazepine, etc in the treated water indicate the system failure in the removal of these micropollutants. Pharmaceutical Active compounds are complex molecules polar in nature with molecular weights ranging from 200 to 1000 Da (Pal, 2018).

Special concern has lately been provided to what could be known as "emerging pollutants," which are generally uncontrolled substances that could be candidates for prospective management based on research on their potential health hazards and analyzing data on their prevalence. Pharmaceuticals and personal care products (PPCP) and endocrine-disrupting chemicals (EDC) are recently considered emerging contaminants that are unregulated or can be regularized in the future. Sewage effluents and hospital and animal waste are the point sources and agricultural run-off, wash-off from roadways, and underground contaminations are the non-point sources of PPCPs. If EDCs and PPCPs are present in water, it will adversely affect the reproductive and health effects of humans and other living things. In recent decades, the amount of chemicals

found in the aquatic environment has increased significantly. In this approach, active components in personal care products are part of a wide set of bioactive compounds that are attracting greater exposure as possible environmental contaminants (Sanchez-Prado et al., 2006).

Triclosan (TCS, 5-chloro-2-(2,4-dichloro phenoxy)-phenol), is an antimicrobial and antifungal agent found in most personal care products. Triclosan is among the most frequently identified as an arising contaminant and is being used in a variety of personal grooming products such as mouthwash, body washes, antiperspirants, hair products, and beauty products, as well as products such as plastic cookware and shoes, and usable garments such as fully functioning footwear and undies. Not only it is visible in industrial effluent and sewage treatment plants but also in potable and drinking water sources. Major concern of TCS use recently developed, owing to its prevalence not just in WWTP of industrial effluent, but in human milk (Ogutverici et al., 2016). Because of its significant antimicrobial action, its global production reaches 1500 tonnes per year (Liu et al., 2016). It has been claimed that it is extremely hazardous to certain aquatic creatures. The usage of Triclosan has increased in recent years. Triclosan is an endocrine-disrupting agent which has been found in breast milk, urine, and plasma. Recently Triclosan has raised serious environmental concerns because of both its toxicity to some aquatic organisms and the formation of more toxic byproducts (Methatham et al., 2012; Song et al., 2012; Liu et al., 2014).

The standard wastewater treatment techniques are unable to provide a dependable barrier against triclosan, it is proposed to implement extra advanced treatment technologies in places where a chronic pollution problem has been identified or is expected. The various technologies such as ozonation and advanced oxidation processes, membrane bioreactors, membrane filtration, and activated carbon adsorption, indicate that chemical oxidation with ozone is an extremely effective treatment process for a wide variety of new organic pollutants such as pesticides, pharmaceutical drugs, care products, emulsifiers, microbial pollutants, and normal fatty acids. Ozonation has lately emerged as a critical method for

the oxidizing and destruction of a diverse spectrum of organic contaminants in wastewater (Ikehata et al., 2006). It has been shown that it is an excellent post-treatment method for medicines and personal care items (Ikehata et al., 2008; Wert et al., 2009).

In Advanced Oxidation Process (AOP) hydroxyl radicals will be formed and it has a strong oxidizing property and the ability to degradation of pollutants. Because of the tremendous oxidizing activity of AOPs, which are commonly described as oxidation processes that create hydroxyl radicals, are responsible for organic degradation. As a result, they may oxidize and accumulate nearly every organic molecule, producing CO<sub>2</sub> and inorganic ions. The predominance of AOP systems requires a combination of oxidants and irradiation (O<sub>3</sub>/H<sub>2</sub>O<sub>2</sub>/UV) or a catalyst and irradiation (Fe<sup>2+</sup>/H<sub>2</sub>O<sub>2</sub>; UV/TiO<sub>2</sub>).

The common shortcoming of such methods is the high demand for electrical energy for equipment such as ozonation, (Ultraviolet) UV lamps, and so on, which frequently makes such treatments economically inefficient. This is why, even though AOPs are widely recognized for their ability to oxidize and mineralize practically any organic pollutant, commercial uses are still limited. Catalysis and solar energy might be used to improve future uses of these technologies. As a result, research is increasingly focused (Malato et al., 2007) on the two AOPs that can be driven by solar radiation, i.e., light with a wavelength greater than 300 nm, homogeneous catalysis through the photo-Fenton reactions and heterogeneous catalysis by UV/TiO<sub>2</sub>.

To prevent contamination of the environment, it is vital to create an ecologically safe and quick process for triclosan biodegradation. Recent research has focused on the pathways of triclosan degradation. Sonoelectrochemical (Ren et al., 2014), photoelectrocatalytic (Liu et al., 2013), oxidative (Song et al., 2012), and electro-Fenton degradation (Sirés et al., 2007) are some of the triclosan degradation techniques. Research in the literature has proposed ways of completing the remediation of triclosan-containing municipal wastewater. This developing contaminant can be chemically oxidized using chlorine

(Inaba et al., 2006), ozonation, or UV/TiO<sub>2</sub> photocatalysis (Klamerth et al., 2010; Rafqah et al., 2006).

Fenton's reagent could provide a realistic solution for emerging contaminants that are generally at extremely low concentrations, provided that the overall organic load of the effluent to be treated is likewise within a low range, allowing the procedure to be completed with relatively modest H<sub>2</sub>O<sub>2</sub> doses. Fenton was most extensively used in wastewater treatment by radical oxidation and flocculation. Ferrous ions accelerate the breakdown of H<sub>2</sub>O<sub>2</sub> into OH and the generation of extra radicals capable of totally oxidizing organic molecules. Nonetheless, there is a paucity of knowledge on the potential application of Fenton's oxidation as a post-treatment for the degradation of triclosan as well as other developing chlorinated contaminants (Klamerth et al., 2009).

Nanotechnology has enormous promise for improving efficiency in modern water and wastewater treatment. Because of its distinctive qualities, such as high adsorption activity, reactivity, and environmentally friendly nature, nanotechnology is a viable technique for implementing new and effective solutions to a variety of environmental concerns (Malakootian et al., 2019; Zinatloo-Ajabshir et al., 2016). Nanomaterials have great promise in environment cleansing, water purification, and treatment of wastewater. From the perspective of both resource sustainability and environmental remediation, nanomaterials (NMs) have been presented as an efficient, cost-effective, and environmentally acceptable alternative to conventional treatment materials (Qu et al., 2013). Nanomaterials are employed as adsorbents, catalysts, photocatalysts, and so on. Because of their magnetic and catalytic capabilities, iron oxide nanoparticles (NPs) are widely employed in the chemical and electronic sectors. Iron oxide nanoparticles have recently seen increased usage in the treatment of hazardous waste and the remediation of polluted soil, surface, and groundwater. Iron oxide nanoparticles are now being investigated in the adsorption process to remove developing contaminants.

Green nanoparticle synthesis has many benefits over previous techniques, such as being considerably simpler, not harming the environment, and also being extremely cost-

effective. The benefit of green synthesized NPs is that they do not demand synthetic reducing agents, which are environmentally harmful. Additionally, such a technique eliminates the necessity of external capping and stabilizing chemicals. Iron nanoparticles possess excellent mechanical properties, are non-toxic, and also have a tendency to form oxides. Fe NPs are also called magnetic nanoparticles due to their enormous surface area, high thermal stability, and magnetic properties (Arabi et al., 2016). Iron is abundantly available, less expensive, and its magnetism feature has assisted in the synthesis of NPs with enormous application potential in environment separation. Green route approaches have reduced significantly agglomeration, which has long been a concern in the chemical production of NPs. The polyphenolic concentration and endogenous proteins, especially in leaf extracts and microbe synthesizing, act as a stabilizer and coating agent over the formed NPs, minimizing aggregation. Either ferrous sulphate or ferric chloride salts will be added as a precursor for the synthesis of nanomaterials, which add extra chlorides and sulphates to the treatment method. To avoid either ferrous sulphate or ferric chloride salts as a precursor, locally available laterite as a source of iron and plant extract was used for the synthesis of nanoparticles.

Natural laterite iron replacement for the commercial iron catalyst is one of the acceptable attempts made by many researchers (Manu and Mahamood, 2011; Bhaskar et al., 2021; Sangami and Manu, 2019). Laterite soil by its characteristic has 30-40% of iron which makes it a naturally available iron rich mineral. The investigation on the usage of laterite iron as a catalyst in its natural form, iron leached from laterite soil by chemical method, bioleached laterite iron, and nanoparticles synthesized from leached laterite iron confirms its role as a catalyst in the Fentons oxidation (Bhaskar et al., 2021b; Sangami and Manu, 2017). *Psidium guajava*, a tropical plant extensively rich in phytochemicals such as alkaloids, flavonoids, and polyphenols is used for the synthesis of nanoparticles. Polyphenols present in the plant extracts are proven to actively act as a capping agent around the particles reducing their size and increasing their surface area (Madubuonu et al., 2020). The interaction of various organic functional groups with the precursor used with the *Psidium guajava* makes it one of the prominent plants used in the green

synthesis of a wide variety of nanoparticles (Madubuonu et al., 2020). A plant widely found in the Western Ghats in India is *Makaranga peltata*. It has been found to contain bergenin derivatives, polyphenols, as well as other flavonoids and diterpinoids. (Verma et al., 2013). *Makaranga peltata* leaf extract is used for the synthesis of silver, copper, and zinc nanoparticles (Vazhacharickal et al., 2018). Properties of nanoparticles like size, shape, and surface area depend on the plant extract and the precursor used in the process of synthesis.

A few researchers have synthesized the gold, titanium oxide, silver, tin oxide, zinc oxide, copper oxide, zero-valent iron nanoparticles using *Psidium guajava* which was used to remove various dyes like reactive yellow 186, vinyl disulphone RY 186, methylene blue, Nile blue, RY 160 and many more. (Patil and Rane, 2020). There is no literature available on nanoparticle synthesis using *Makaranga peltata* leaf extract and laterite iron as a precursor for its application in Fenton's degradation of triclosan.

The bio-Fenton (BF) is a process in which hydrogen peroxide is generated, when the enzyme reacts with the glucose. In addition to being sustainable, bio-Fenton can produce hydrogen peroxide in situ, which reduces overall expenses and reduces power consumption. In wastewater treatment, this process is relatively recent, and has been used mainly to treat dye effluents, such as Malachite green and Acid blue 113 (Kahoush et al. 2018). Organic pollutant like trichloroethylene have also been removed by the bio-Fenton process (Ravi et al., 2020).

The present study aims to degrade the triclosan using green synthesized laterite-based *Psidium guajava* nanoparticles (GPsLaNP) and green synthesized laterite-based *Makaranga peltata* nanoparticles (GMpLaNP) by Fenton's process.

## 1.2 OBJECTIVES

- Main objective
  - The primary objective of the current study is the degradation of triclosan from wastewater by Fenton's Oxidation using green synthesized laterite iron nanoparticles (GLFeNP's).
- Specific objectives
  - To extract iron from laterite soil and to synthesize, and characterize Green Laterite based Iron Nano Particles (GLFeNP's).
  - To study the influence of GLFeNP's, H<sub>2</sub>O<sub>2</sub> dosage, pH, and initial triclosan concentration on the degradation of the target compound in Fenton's Oxidation.
  - To study the reaction kinetics of triclosan degradation.
  - To optimize the bio-Fenton's for *Psidium guajava* Laterite Iron Oxide Nano Particles (GPsLaNP) and *Macaranga peltata* Laterite Iron Oxide Nanoparticles (GMpLaNP).

## 1.3 MOTIVATION FOR THE RESEARCH

Wastewater from pharmaceutical and personal care industries are characterized by high concentration of organic contaminants, high biochemical oxygen demand (BOD) concentration, high chemical oxygen demand (COD) concentration, high suspended solids, and different BOD/COD value in wastewater (Luo et al., 2019). Many research is evident on the presence of pharmaceutical and personal care compounds in surface water, groundwater, and drinking water (Vieno et al., 2007; Mutiyar et al., 2018). The presence of PPCP's pose a potential threat to an aquatic environment. Ibuprofen, diclofenac, and carbamazepine are toxic to fish species like *Corbicula fluminca* on 3 days of exposure while its toxicity on *Pimephales promelas* varies with an exposure period of 109 days.

Ibuprofen and sulfamethoxazole at a concentration of 0.1 µg/L induce over-expression of glutathione s-transferase p1 gene in humans for a period of 24h exposure. Carbamazepine at a rate of 0.005 µg/L and ciprofloxacin at a rate of 0.5 µg/L may cause antagonistic synergistic interactions for a period of 48h exposure in humans (Vasquez et al., 2014). Triclosan enters the wastewater treatment plants when it is discharged from wastewater (Yin et al., 2022). It found not only in water bodies, but also in human blood, plasma, and urine (Dann and Hontela, 2011). There are several health risks associated with Triclosan, an antibacterial compound. Hence it is necessary to remove the triclosan.

Although many treatment technologies have been developed in recent decades for the degradation of PPCPs, they are confined to relatively few chemical groups. In addition, the occurrence of resistance to complete degradation led to failure in the treatment of these compounds. Apart from conventional and biological treatment, advanced oxidation processes like Fenton's are proven to be effective in treating recalcitrant organic pollutants. Fenton's process is a simple method to produce hydroxyl radicals having a relative oxidation power of 2.05 at an ambient temperature and pressure. Fenton oxidation is a highly efficient, most economical, and easily available treatment method (Srivastav et al., 2019).

The nanotechnological approach in the treatment of organic compounds is proven to be the most effective technology (Boukhessaim et al., 2022; (Boukhessaim et al., 2022; Ibrahim et al., 2016)). Cost-effectiveness of such nano catalyst-based Fenton oxidation needs more investigation as the efficiency is based on the morphological and chemical composition of the nano iron particles. In this view, the present study encompasses the extraction and usage of laterite iron as a precursor in the synthesis of nano iron particles for its application in Fenton's oxidation as a catalyst. The study also extends the application of nano iron catalyst in bio-Fenton's oxidation nullifying the addition of hydrogen peroxide.

## **1.4 STRUCTURE OF THE THESIS**

Chapter 1 provides an introduction to the emerging contaminants, Triclosan, and their effects on the environment and the treatment methods involved, the motivation for the research, and the objective of the research.

Chapter 2 provides the exposure, environmental concern of triclosan, literature summary on treatment techniques involved to treat the triclosan by advanced oxidation process. Degradation of Triclosan by Fenton's process and bio-Fenton process by conventional iron and green synthesized iron is discussed in detail.

Chapter 3 gives the details about the materials, methodology, analytical techniques used.

Chapter 4 deals with the results and discussion on the synthesis of nanoparticles and its characterization using leaf extract and laterite extract and its application as a catalyst in the Fenton and bio-Fenton process for the degradation of Triclosan.

Chapter 5 gives the conclusion drawn from the objectives based on the experimental results, also the scope and future work is presented.



## **CHAPTER 2**

### **LITERATURE REVIEW**

Chapter 2 focuses on the literature related to triclosan and other PPCPs and their applications. The exposure of triclosan in the environment, occurrence of triclosan in water and the available treatment methods to degrade the triclosan are involved in the degradation are discussed.

#### **2.1 GENERAL**

Chemicals that are emerging contaminants can include medicines, personal care products, household cleaning products, lawn care products, agricultural products, etc. These will get introduced into water bodies if it is not removed during the treatment and it will cause a detrimental effect on aquatic life and human beings.

Endocrine Disrupting Compounds (EDCs) are widely present and include natural oestrogens as well as synthesized xenoestrogens phthalates and many others that have already been discovered to impact hormone activity in the endocrine system (Jobling et al., 1998; Desbrow et al., 1998; Folmar et al., 1996) revealed sewage effluent as a significant source of natural estrogenic substances in the water habitats, garnering substantial interest during the last 2 decades. (Liu and Liu, 2004) discovered equivalent oestrogen findings when photolysis processes were increased with MP lights and at greater pH levels. A study conducted by Linden et al., (2007) investigated the EDC breakdown intermediates following AOP (UV/H<sub>2</sub>O<sub>2</sub>) that discovered no change in oestrogenic activity.

In recent years, there has been a strong interest personal care products identified in various aqueous matrices. Though normally present in low quantities, long-term exposure to such substances, offers a promising risk to both the environment and humankind. In addition to pharmaceutically active compounds, personal care products, endocrine disruptors, and their metabolites, per and polyfluoroalkyl substances, artificial

sweeteners, industrial wastes, food additives, flame retardants, heavy metals, pesticides, fertilizers, disinfectants by-products, illicit drugs, steroids, antibiotic-resistant bacteria, antibiotic-resistant genes are among the emerging contaminants (ECs) (Jagini et al., 2019; Renganathan et al., 2021). The presence of ecologically unfavorable compounds in the environment grows dramatically (Wooten, 2012). As a result, pharmaceutical residues will be a significant burden on wastewater treatment plants. According to studies, conventional (waste water treatment plant) WWTP does not effectively disintegrate PPCPs and in pharmaceutical preparations active ingredients (Okuda et al., 2008), demanding additional treatment to fulfill water reuse conditions. In studying AOPs for eliminating in pharmaceutical preparations active ingredients, Klavarioti et al., (2009) reported that, pollutants in surface and groundwater rapidly decreased below the limit of detection.

Triclosan (TCS, 5-chloro-2-(2,4-dichlorophenoxy)-phenol), is among the most frequently identified as an arising contaminant, is being used in a variety of personal grooming products such as mouthwash, body washes, antiperspirants, hair products, and beauty products, as well as products such as plastic cookware and shoes, and usable garments such as fully functioning footwear and undies. Triclosan is visible not only in industrial effluent and sewage treatment plants but also in water bodies. Because of its significant antimicrobial action, its global production reaches 1500 tonnes per year (Liu et al., 2016). Triclosan has recently sparked severe environmental concerns due to its toxicity to various aquatic creatures as well as the development of more harmful metabolites (Song et al., 2012; Liu et al., 2014; Methatham et al., 2012). Table 2.1 summarizes the triclosan concentrations in various water sources. Triclosan may be directly photo transformed to create 2,8-dichloro dibenzo-p-dioxin, which is carcinogenic (Yang et al., 2011). The structure of triclosan is seen in Figure 2.1. The table below depicts the presence of triclosan in numerous water bodies.

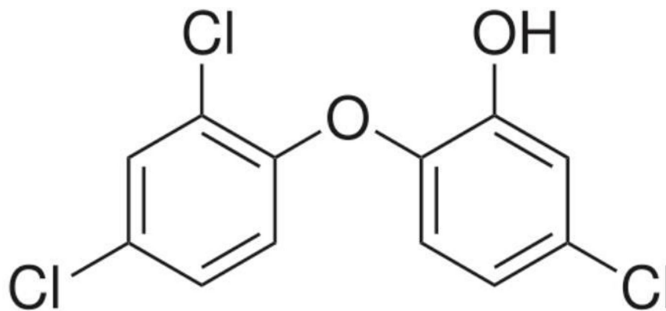


**Figure 2.1: Structure of triclosan**  
(Oztamer and Cokay, 2017)

## 2.2 EXPOSURE OF TRICLOSAN IN THE ENVIRONMENT

The extensive usage and inadequate removal of triclosan in WWTPs create a multitude of entry points for the chemical into the environment. Triclosan has already been identified as one of the most regularly observed chemicals in solid and water environmental compartments (Singer et al., 2002). Lindström *et al.* (2002) discovered triclosan levels of up to 70 µg/L in lakes and a river in Switzerland. Whereas triclosan levels in the Ruhr River in Germany varied between 11-98 µg/L, substantial quantities of triclosan were observed in rivers getting WWTP effluents (Bester, 2005). Whenever administered to land, triclosan can divide into sewage sludge during treating wastewater and then transfer to soil.

High triclosan concentrations were observed in a field using biosolid in land application (Langdon et al., 2012). Moreover, triclosan was found in the marine sediment of Barker Inlet, South Australia, with quantities ranging from 5-27 µg/g (Fernandes et al., 2011). There is an average concentration of 1 to 10 mg/L of TCS in wastewater from WWTPs, due to the washing down the drain of up to 96% of TCS in consumer products (Yueh and Tukey, 2016). A direct photolysis reaction may occur when TCS and chlorinated derivatives are discharged into surface waters through WWTP effluents, leading to the formation of 2, 4-dichlorophenol and polychlorodibenzo-p-dioxins (PCDDs), including 1, 2, 8 trichlorodibenzo-p-dioxin (1, 2,-TriCDD), 1, 2, 3, 8, tetrachlorodibenzo-p-dioxin (1, 2, 3, 8), 2, 3, 7 trichlorodibenzo-p-dioxin (2, 7-TriCDD), and 2, 8-dichloro-dibenzo-p

dioxin (Buth et al., 2009; Fiss et al., 2008). However, exposing triclosan to sunlight or (ultraviolet) UV irradiation in photocatalytic activity can result in the development of very hazardous and long-lasting chlorinated byproducts such as 2, 8-dichlorodibenzo-p-dioxin. When sewage sludge is applied to agricultural land which contains triclosan, it accumulates and persists in biosolid (Chalew and Halden, 2009; Heidler and Halden, 2007).

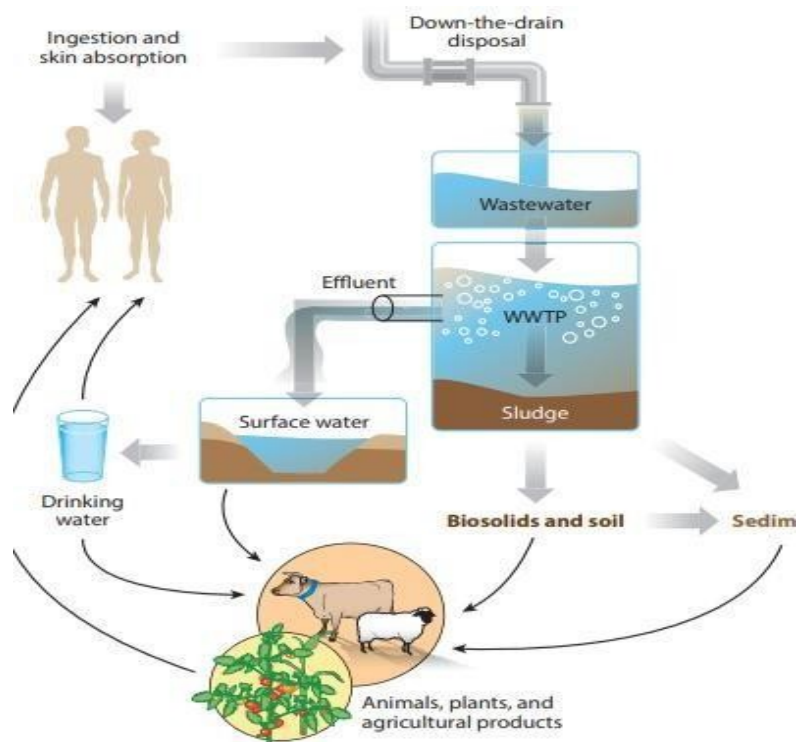


**Figure 2.2 Environmental fate and effects of TCS**  
(Yueh and Tukey, 2016)

Aquatic biota, such as snails, algae, fish, and marine mammals, have been detected to accumulate TCS contamination both in aquatic and terrestrial environments (Yueh and Tukey, 2016). A study conducted by Wilson et al., (2003) proved that as a consequence of WWTP effluent being disposed of in water ecosystems, TCS might have an impact on the structure and function of algal communities. Invertebrates, fish, and activated-sludge microorganisms were used in an experiment conducted by Orvos et al., (2002) to study

triclosan's aquatic toxicity. TCS was found to be toxic to algae, with an EC50 of 1.4 g/L and a no-observed effect concentration of 0.69 g/L after 96 hours. During adult and early stages of development, TCS causes deleterious effects on zebrafish (Oliveira et al., 2009).

**Table 2.1: Occurrence of Triclosan in various water bodies**

Source	Concentration of TCS	Reference
Surface Water	1.4–40,000 ng/l	Dhillon et. al;(2015); Kumar et. al., (2015)
Sea Water	<0.001–100 ng/l	
Wastewater Influent	20–86,161 ng/l	
Wastewater Effluent	23–5370 ng/l	
Pore Water	0.201–328.8 µg/l	
Raw Drinking Water (U.S.)	8.8 ng/l	Snyder (2008)
Australian WWTPs effluent	23 - 434 ng/l	Ying and Kookana (2007)
Switzerland WWTPs effluent	42 - 213 ng/l	
USA WWTPs effluent	35 - 2700 ng/l	
UK WWTPs effluent	340 - 1100 ng/l	
surface water of Australia	75 ng/l	
Indian Rivers	3800- 5160ng/l	Ramaswamy et al., (2011)

Triclosan is an endocrine disrupting agent which has been found not only in aquatic biota but also in the breast milk, urine (Calafat et al., 2008), plasma (Allmyr et al., 2006) of humans (Dann and Hontela, 2011; Yueh and Tukey, 2016). A research conducted by Calafat et al., (2008) found that 74.6% of 2,517 participants were found to have TCS concentrations ranging from 2.40 to 3.79 grams/liter in urine samples, with the highest levels occurring among young adults in their twenties and those in higher socioeconomic positions. In 51 out of 62 samples taken from the Breast Milk Banks in California and Texas, researchers found TCS at concentrations ranging from 100 to 2,100 g/kg lipid

(Dayan, 2007). According to the survey conducted on pregnant women in Canada found triclosan concentration in their urine. Higher socioeconomic status and older age were associated with increased urinary TCS concentrations (Arbuckle et al., 2015). In a health risk assessment study, higher levels of TCS were reported to be associated with the use of daily care products containing TCS in a population of Swedish women (Allmyr et al., 2006).

## **2.3 AVAILABLE TREATMENT TECHNOLOGIES FOR TRICLOSAN REMOVAL**

Triclosan is an endocrine-disrupting agent due to its highly ecotoxic nature. Triclosan if found in water bodies, wastewater, humans, flora, and fauna, it is necessary to treat the triclosan. The available treatment methods like physical, biological, and advanced oxidation methods to degrade the triclosan are discussed below.

### **2.3.1 Physical Treatment Methods**

Nakada et al. (2007) evaluated the removal rates of 24 active pharmaceutical chemicals utilizing sand filtering and advanced oxidation at an operating municipality sewerage system. Sand filtering alone did not result in efficient removal, however ozonation was a successful approach for removing the target contaminant (triclosan removal was up to 80%). With the use of a blend of activated sludge process, sand filtering, and advanced oxidation the triclosan was removed at a rate of greater than 90%. A study conducted by Leal et al., (2011) reported that 95% of triclosan was removed by adsorption onto granular activated carbon. An acidic condition facilitated triclosan removal better than an alkaline condition using activated carbon, kaolinite, and montmorillonite sorbents (Behera et al., 2010).

Liu et al. (2014) tested whether triclosan could be effectively removed from waste paddy straw-derived hydrochar. This analysis revealed that waste paddy straw-derived hydrochar is a viable predecessor for the production of high magnetized activated carbon in the removal of contaminants from real water matrices.

Ogutverici et al. (2016) evaluated triclosan elimination by nanofiltration (NF) through natural organic matter interaction (NOM). The results revealed that NOM had a favorable effect on TCS elimination due to the development of a TCS–HA (Humic Acid) complex, which restricts TCS permeability across the membrane. TCS elimination increased as the NOM concentration of the surface water increased.

### **2.3.2 Biological Treatment Methods**

This is one of the treatment processes that use microorganisms to oxidize pollutant in waste water into organic matter. For waste water treatment, microorganisms demand more oxygen (Akhbari et al., 2019). This procedure is primarily concerned with the elimination of organic contaminants. Using well-constructed wetlands, three different types of aquatic plants were tested for their effectiveness in removing TCS (Liu et al., 2016). There was a significant improvement in removing TCS from water, as all removal efficiencies were greater than 97 %. By constructing wetlands with different types of plants, Zhao et al., (2015) studied the variation of the bacterial community and the microbial removal mechanisms of TCS removal. Over 90% of TCS was removed from constructed wetlands, and TCS negatively affected bacterial diversity and abundance.

Using *Sphingopyxis* strain KCY1, a wastewater isolate produced stoichiometric amounts of chloride during the complete degradation of triclosan (Lee et al., 2012). *Aspergillus versicolor* has been investigated for its ability to degrade triclosan by Ertit Taştan and Donmez, (2015). At 7.5 mg/L triclosan concentration, *Aspergillus versicolor* achieved a maximum biodegradation yield of 71.91%. A ubiquitous green alga, *Chlorella pyrenoidosa*, was used in the study conducted by Wang et al., (2013) to remove and biodegrade triclosan from water. More than 50% of the triclosan was quickly removed by algal uptake within one hour of exposure to algal cells at concentrations from 100 to 800 ng /mL. 77.2% of triclosan was eliminated from the medium after 96 hours of exposure to 800 ng /mL algal cells.

### 2.3.3 Advanced Oxidation Process

Highly effective technologies such as advanced oxidation processes (AOP) are all cited as being ideal for micropollutant removal. Martinez et al. (2014) examined the elimination of triclosan by (titanium oxide)  $\text{TiO}_2$  immobilized by the synthesis of dense  $\text{TiO}_2$  films on mesoporous stones, providing a photocatalytic activity that occupies a Pyrex® CPC container. In photocatalytic oxidation, two sets of parameters were investigated for the elimination of triclosan. Initially, by retaining persulfate as a strong electron acceptor the removal of triclosan was high but when the pH was maintained neutral, the persulfate concentration had no effect on removal efficiency, but it became a water pollutant in treated water.

A study was conducted to integrate ultraviolet (UV) and ultraviolet irradiance with Conductive-Diamond Electrochemical Oxidation (CDEO) to accelerate the degradation of caffeine and triclosan pollutants in wastewater. It's been observed that triclosan removal is more than 60%. The mixture of UV light and US irradiations using CDEO tends to enhance triclosan degradation (Saez et al., 2014).

Aqueous ozonation was used to remove triclosan in a study performed by Chen et al., (2012). The experiment was carried out for various triclosan to ozone molar ratios, and the clearance rate ranged from 94 to 99.9%. The treatment procedure may completely remove triclosan and convert it to the corresponding products: 2,4-dichlorophenol, chlorocatechol, mono-hydroxy-triclosan, and di-hydroxy triclosan.

Utilizing simulated solar UV irradiation, Martinez-Zapata et al., (2013) analyzed the removal of triclosan by photodegradation in solutions containing Fe(III) and in the lack and existence of humic acids. The best conditions for TCS breakdown in direct photolysis was at basic pH (i.e. 9), a ferric iron dosage of 2mg/l in the lack of HA.

Chen et al., (2016) extensively investigated the potential use of potassium permanganate as an oxidizing agent for the reduction of triclosan (TCS) in sewage treatment. The

triclosan concentration of 20 mg/L was completely degraded within 120s, with an optimized condition of pH = 8.0, [TCS]<sub>0</sub>: [KMnO<sub>4</sub>]<sub>0</sub> = 1:2.5, and T = 25 °C.

An investigation was conducted by Orhon et al., (2017) to determine how efficiently ozonation could remove triclosan from surface water. It was found that continuous ozonation at 5 mg/L was required to completely eliminate triclosan from surface water containing 1 to 5 mg/L of triclosan.

Anupama and Shrihari (2018) studied the removal of triclosan from wastewater by both homogeneous AOP by O<sub>3</sub>/UV and heterogeneous AOP using TiO<sub>2</sub>/UV. It is observed that, when compared with heterogeneous condition, at homogeneous condition the removal is higher and it has reached greater than 90%.

Fidelis et al. (2019) discussed the photocatalytic reaction in the degradation of Triclosan utilizing the immobilized catalyst Fe/Nb<sub>2</sub>O<sub>5</sub>. The results showed that the immobilized Fe/Nb<sub>2</sub>O<sub>5</sub> catalysts were effective at degrading Triclosan.

According to the Constantin et al., (2018) investigation, a heterogeneous photocatalysis was used in wastewater treatment with TCS to produce non-toxic compounds like carboxylic acid and HCl while converting target pollutants and their byproducts. A composite of Ag/BiVO<sub>4</sub>/rGO was synthesized to degrade the triclosan. It is observed that under UV light complete degradation of triclosan in 100 minutes with 1 mg/mL photocatalyst (Li et al., 2019).

The electrochemical dechlorination of triclosan using a composite electrode made from palladium/polypyrrole-reduced graphene oxide/foamed nickel was examined by Zhang et al., (2020). After 100 minutes, 100% of TCS removal was observed under the polymerized potential of 0.7V.

Chandra Pragada and Thalla, (2021) synthesized an immobilized Fe<sub>2</sub>O<sub>3</sub>-TiO<sub>2</sub>/PVP to degrade the triclosan. An 83.27% degradation efficiency was achieved by using a solar

photocatalytic reactor to degrade triclosan (TCS) in treated grey water discharged from the anaerobic-aerobic treatment system.

### ***2.3.3.1 Fenton's Oxidation***

Many AOPs utilize oxidants and irradiation ( $O_3/H_2O_2/UV$ ) or a catalyst and irradiation ( $Fe^{2+}/H_2O_2$ ;  $UV/TiO_2$ ). The main drawback of such techniques is the large demand for electrical energy for apparatus like ozonators, UV light generation, etc, which often renders such remedies commercially ineffective. Fenton is regarded as one of the most successful alternative advanced treatment procedures for removing a wide range of harmful micropollutants from refractory/toxic wastewater (Pignatello et al., 2006). The interaction of aqueous ferrous ions with hydrogen peroxide ( $H_2O_2$ ) produces the hydroxyl radical (OH), which can eliminate refractory and harmful organic contaminants in wastewater (Neyens and Baeyens, 2003). In 1894, Fenton discovered the Fenton reaction and observed that ferrous ( $Fe^{2+}$ ) ions could activate  $H_2O_2$  to oxidize tartaric acid.

It was effective in its use as an oxidizing procedure for the destruction of hazardous organics. Fenton was most extensively used in wastewater treatment by radical oxidation and flocculation. Ferrous ions accelerate the breakdown of  $H_2O_2$  into OH and the generation of extra radicals capable of totally oxidizing organic molecules. Photo-Fenton degrades low concentration organic contaminants more effectively. Because excessive concentrations of organic contaminants reduce the absorption radiation of ferrous compounds, a greater radiation duration, as well as a greater  $H_2O_2$  dose, are required. Excessive  $H_2O_2$  may readily absorb OH. Several chemical compounds, including ethylene diamine tetraacetic acid (EDTA), Ethylenediamine-N,N'-disuccinic acid (EDDS), oxalate, as well as other organic acids, were introduced to functionalize the  $Fe^{3+}$  during photocatalytic activity to improve Fenton and photo-Fenton efficiency. In the Fenton process, most organic pollutants are almost completely oxidized by OH radicals (Prousek, 1995).

Sirés et al., (2007) examined the effective degradation of triclosan at pH 3 using electro fenton process using undivided electrolytic cells with a Pt or boron-doped diamond (BDD) anode and a carbon felt or (oxygen) O<sub>2</sub> diffusion cathode. Klammerth et al.,(2009) investigated the degradation of triclosan at lower concentration (0.1 mg/L, 0.3 µmol/L) using solar photo fenton and (titanium oxide) TiO<sub>2</sub> photocatalysis. The result showed that triclosan was more effectively removed from solar photo fenton than with TiO<sub>2</sub> photocatalysis.

Methatham et al., (2012) investigated the possibility of continuous electro-regeneration of ferrous ions by removing triclosan completely using Fenton's reagent in conjunction with an electrochemical system. Maintaining the current densities of 0.15 mA cm<sup>2</sup> with 4 mM H<sub>2</sub>O<sub>2</sub>, 0.1 mM Fe<sup>2+</sup>, and pH 3.

Song et al. (Song et al., 2012) analyzed the deterioration of triclosan in the presence of H<sub>2</sub>O<sub>2</sub> as an oxidizer and bismuth ferrite magnetic nanoparticles (BiFeO<sub>3</sub> MNPs) as catalysts at pH 6.0 at ambient temperature. The inclusion of BiFeO<sub>3</sub> MNPs (0.5 g/L) enhanced the triclosan elimination to 82.7% with the presence of H<sub>2</sub>O<sub>2</sub>. The addition of EDTA (0.5 mmol/l) resulted in almost complete triclosan degradation in 30 minutes.

Luo et al., (2017) examined the efficiency of triclosan (TCS) transformation at 254 nm in the presence of H<sub>2</sub>O<sub>2</sub>. The effects of oxidant dose, TCS concentration, and pH were also investigated. When the H<sub>2</sub>O<sub>2</sub> dose was 1 mmol/L, the measured pseudo-first-order rate constant for TCS breakdown was raised. However, when H<sub>2</sub>O<sub>2</sub> concentrations were above 1 mmol/L, dropped as H<sub>2</sub>O<sub>2</sub> dose due to the effects of radical scavenging by H<sub>2</sub>O<sub>2</sub>.

Oztamer and Çokay (2017) evaluated the elimination of triclosan using the photo-Fenton technique and to detect the production of by-products following the oxidation. It has been found that the optimal combination of H<sub>2</sub>O<sub>2</sub>/Fe(II)/TCS for removing maximum amounts of triclosan (98.5%) within 60 minutes is 50/2/0.1.

Peng et al., (2019) investigated the synthesis and characterization of iron nanoparticles employing *Ginkgo biloba* leaf extract as a green stabilising agent to produce the Fe/Co

bimetallic nanoparticles in order to eradicate triclosan from aqueous solution. The results obtained showed that the lower concentration of graphene oxide (GO) (2.0mg/L) exhibit significant effect on the triclosan degradation. It was reported that as the pH and starting TCS content were increased, the removal rate dropped. Removal of triclosan by  $\text{Fe}^{3+}/\text{H}_2\text{O}_2$  in aqueous GO showed 90% removal efficiency even at lower GO concentration.

The electro-Fenton breakdown of Triclosan in aqueous solution was measured using a cylindrical vessel with polarization carbon cloth electrodes and a cation exchange resin. As a consequence, triclosan degradation was very efficient (above 95%), and the nature and magnitude of the ionic strength of the electrolytic solution had the strongest influence on the process, despite the reasonable effect of all variables and their interactions (García-Espinoza et al., 2019). Using  $\text{Fe}_3\text{O}_4$  nanoparticles and PMS, So et al., (2019) investigated the removal of TCS. It is observed that complete degradation of triclosan within 60 minutes with optimum dosage of [TCS:PMS] at 1:25 and  $\text{Fe}_3\text{O}_4$  dosage of 0.750 g/L.

## **2.4 DEGRADATION OF TRICLOSAN USING NANOPARTICLES**

For the removal of pollutants, the use of nanomaterials and nanocomposites will be a viable solution. Nanomaterials play a significant part in current research for the effective remediation of waste water. Because of nanoparticle's unique properties, including high adsorption activity, reactivity, and environmental friendliness, nanotechnology has the potential to provide innovative solutions for environmental challenges. Many researchers have studied the application of nanoparticle for the degradation of triclosan.

Under optimal experimental conditions, green synthesized bimetallic iron/nickel nanoparticles (Fe/Ni NPs) were used to effectively eradicate triclosan (TCS) with removal efficiencies of 75.8 percent. A pseudo second order kinetic equation ( $R^2 > 0.998$ ) as well as the Freundlich isotherm ( $R^2 > 0.905$ ) fit pollutant adsorption well. In contrary, the degradation kinetics fitted a pseudo first order concept. As a result, TCS

removal demanded a mixture of adsorption and reduction techniques. Eventually, a triclosan removal method was established. Therefore, Fe/Ni NPs have the highest potential to reduce TCS in aqueous medium instantaneously in a variety of scenarios (Lin et al., 2019).

Gao et al., (2019) examined the triclosan adsorption and degradation by Ginkgo biloba L. stabilized Fe/Co bimetallic nanoparticles. With 6.92 pH initial value, 5% Co loading, 0.56 g/L NPs dosage, and 7.0 mg/L CO<sub>2</sub>, TCS removal efficiency reached 89.74% in 5 min. Based on the results, pseudo-second-order kinetics were observed for the removal of TCS.

Cusioli et al., (2021) examined triclosan adsorption using seed husks from Moringa oleifera Lam, which had been functionalized with iron oxide nanoparticles. The kinetic study found that the adsorption equilibrium reached in 600 minutes with an adsorptive capacity of 29.57 mg /g, and the best fit was the pseudo-first-order equation, and the isotherm models were altered in the Langmuir model, obtaining a peak capacity values of 103.45 mg /g.

A study conducted on sepiolite-supported bimetallic Fe/Ni (Sep-Fe/Ni) nanoparticles were used to remove triclosan. The triclosan removal was observed as 93.9% for 5 mg/L concentration of triclosan at a pH of 3.1 and the optimized dose of the Sep-Fe/Ni was 2g/L (Ren et al., 2021).

## **2.5 GREEN SYNTHESIZED NANOPARTICLES FOR THE POLLUTANT REMOVAL**

Green methods of micro-pollutant treatment are adopted as they are easier to extract from natural sources and are more effective than traditional methods of treatment. Green methods are the materials or components used in the treatment are taken from natural extracts like leaves, bio-enzymes, secondary metabolites and others. Various researches have been conducted until now whereby plant extracts as well as microbial extracts have been used in the development of nanoparticles like iron based or titanium dioxide based,

that can oxidize pollutants. The main reason for using green synthesized nanoparticles is because of their sustainability, cost-effective, higher level of efficiency in pollutant degradation, and reducing the time for reaction (Devatha et al., 2016; Shahwan et al., 2011). The benefit of green synthesized nanoparticles is that they do not demand synthetic reducing agents, which are environmentally harmful. Additionally, such a technique eliminates the necessity of external capping and stabilizing chemicals.

Iron nanoparticles possess excellent mechanical properties, are non-toxic, and also have a tendency to form oxides. Iron nanoparticles are also called magnetic nanoparticles due to their enormous surface area, high thermal stability, and magnetic properties (Arabi et al., 2016). Iron is abundantly available, less expensive, and its magnetism feature has assisted in the synthesis of nanoparticles with enormous application potential in environment separation (Huber, 2005; Mondal et al., 2020). Green route approaches have reduced agglomeration, which has long been a concern in the chemical production of nanoparticles. The polyphenolic concentration and endogenous proteins, especially in leaf extracts and microbe synthesising, act as a stabilizer and coating agent over the formed nanoparticles, minimising aggregation. To ensure stability and homogenous particle size, the bulk of nanoparticles synthesized via green route approaches are typically retained in aqueous state at a certain pH (Bolade et al., 2020).

Using green synthesized iron nanoparticles, Weng et al., (2020) studied synergic adsorption and Fenton like oxidation for simultaneous removal of ofloxacin and enrofloxacin. With an initial concentration of 50 mg/ L of ofloxacin and enrofloxacin and a dose of 0.8 g/L of iron nanoparticles at 25 °C, removal efficiencies of up to 91.8% (ofloxacin) and 90.7% (enrofloxacin) were achieved.

Iron nanoparticles were synthesized using different leaf extracts from *Mangifera indica*, *Murraya Koenigii*, *Azadiracta indica*, *Magnolia champaca*, and Ferrous sulfate heptahydrate as a precursor. The effectiveness of treatment of domestic waste water was evaluated using the synthesized nanoparticles (Devatha et al., 2016).

Selvaraj et al (2021) analyzed the complete degradation of crystal violet dye in 270 minutes by Fenton's process using synthesized magnetic  $\alpha$ -Fe<sub>2</sub>O<sub>3</sub> nanospheres using *Bridelia retusa* leaf extract. Prabhakar et al. (2017) synthesized iron nanoparticles from extract of both marine and terrestrial weeds and evaluated their efficacy for nitrate and phosphate elimination in eutrophic wastewater treatment. Wang et al. (2014) created spheroidal 20-80 nm iron nanoparticles from dried eucalyptus leaves extract for eutrophic wastewater treatment. Approximately 71.7 percent of total nitrogen and 84.5 percent of COD were reduced from the wastewater during the investigation.

Groiss et al. (2017) synthesized iron oxide nanoparticles from *Cynometra ramiflora* leaves extract and used them in the Fenton-like catalytic degradation of Rhodamine B in the presence of hydrogen peroxide. The breakdown period was lowered to 15 minutes when 1.11 mM nanoparticles were mixed with 2% hydrogen peroxide. This approach produced the lowest volume of sludge, rendering it preferable to certain other Fenton-catalyzed techniques.

## **2.6 FENTONS OXIDATION PROCESS USING LATERITE IRON**

Laterite soil is abundantly available in India. Laterites soil is mainly composed of iron oxides (Fe<sub>2</sub>O<sub>3</sub>), aluminium oxides (Al<sub>2</sub>O<sub>3</sub>), quartz, and kaolinite. Along with these cobalt, nickel, and chromium, titanium oxide in a minor concentration (Chaturvedi and Katoch, 2020). Laterite soil is used as a source of iron in the Fenton's oxidation process. The degradation of paracetamol (Manu and Mahamood, 2011), 2-aminopyridine (2-AP) (Karale et al., 2013), sodium azide (Khataee and Pakdehi, 2014), azo dye (Khataee et al., 2015), 2-Nitroaniline, 3-nitroaniline and 4-nitroaniline (Amritha and Manu, 2018), dicamba and ametryn (Bhaskar et al., 2019; Sangami and Manu, 2019) methylene blue (Bhaskar et al., 2022) were studied using laterite soil as a source of iron in the fenton's oxidation process.

In a study conducted by Khataee and Pakdehi (2014) a heterogeneous Fenton process with natural laterite as a catalyst was applied to the treatment of sodium azide aqueous

solution. Sodium azide was removed with 97% efficiency after 60 minutes with the optimum conditions (pH = 3, 1 g/L laterite, and 3 mmol/L H<sub>2</sub>O<sub>2</sub>). The C.I. Acid Red 17 using calcined laterite soil as a source of iron was studied by a heterogeneous photo-Fenton-like process. (Khataee et al., 2015). At 120 minutes, heterogeneous photo-Fenton-like process was found to have the highest decolorization efficiency of 94.71%, compared to heterogeneous Fenton-like process. Iron extracted from laterite soil is used in Fenton and Photo-Fenton processes to degrade 2-aminopyridine (Karale et al., 2013). Maximum removal of 2-aminopyridine was observed at Photo-Fenton processes (100%) with initial concentration of 10mg/L and pH 3. Research shows Fenton and Photo-Fenton treatments using low-cost iron extracted from laterite soil can replace conventional ferrous salts in advanced oxidation processes. The removal of 2-Nitroaniline, 3-nitroaniline, and 4-nitroaniline were observed as 85.3%, 84.3%, and 98.7% respectively for 0.5 mM of initial concentration (Amritha and Manu, 2018).

Sangami and Manu (2017) utilized eucalyptus leaf extracts to produce Fe nanoparticles. Instead of employing iron salts, the low-cost and locally abundant laterite was utilized as a source of iron. The X-Ray diffraction (XRD) results showed the existence of iron as meghemite ( $\gamma$ -Fe<sub>2</sub>O<sub>3</sub>), magnetite (Fe<sub>3</sub>O<sub>4</sub>), and zero valent iron (Fe<sup>0</sup>) iron hydroxides, hematite (Fe<sub>3</sub>O<sub>4</sub>). The results proved that derived iron particles demonstrated effective ametryn breakdown with rapid kinetics.

In a study conducted by Sangami and Manu, (2019) ametryn, dicamba, and 2,4-Dichlorophenoxyacetic acid (2,4-D) were oxidized in water using the synthesized iron nanoparticles (FeNPs) as heterogeneous Fenton catalysts. An extract of Tectona Grandis was used to synthesize iron nanoparticles by locally available low-cost laterite soil, as an iron source. The presence of iron elements was confirmed by XRD and Fourier-transform infrared (FTIR) analysis. With optimal iron nanoparticles and oxidant concentrations of 25.29 mgL<sup>-1</sup> and 430 mgL<sup>-1</sup>, laterite-based nanoparticles significantly enhanced degradation efficiency by 100% in 135 minutes and >86% within 45 minutes.

Bhaskar et al., (2021) investigated ametryn and dicamba degradation efficiency of bioleached laterite iron (BLFe) was analyzed for its catalytic role in the Fenton's oxidation process. The degradation of 94.24% of ametryn and 92.45% of dicamba was observed at an optimum pH of 3.

## **2.7 BIO-FENTON OXIDATION**

Bio-Fenton is a process in which the enzyme is added to nullify the addition of H<sub>2</sub>O<sub>2</sub>. The Bio-Fenton process produces hydroxyl radicals by releasing hydrogen peroxide from enzymatic reactions and reacting it with Fe<sup>2+</sup> ions. This process is used to treat organic pollutants from industrial sources, like textile effluent and pesticide effluent. Biocatalyst concentration, substrate concentration, ferrous ions concentration, temperature, pH of the medium, pollutant concentration these are the important factors and conditions that influence the Bio-Fenton reaction (Kahoush et al., 2018).

Ravi et al., (2020) examined the removal of trichloroethylene (TCE) using the Bio-Fenton process. TCE concentrations in aqueous solutions were almost 97% removed in 30 minutes under pH 3.0 conditions under classical Fenton. It was found that by Bio-Fenton process, 61% removal of TCE in 30 minutes at pH 7 for aqueous solution and 30.2% in groundwater was observed. .

On the surface of the spherical Kissirises Titanium dioxide (TiO<sub>2</sub>) and Fe<sub>3</sub>O<sub>4</sub> magnetite particles were coated and the glucose oxidase enzyme was immobilized on the same to enhance enzyme reusability and it is used as a catalyst. A heterogeneous bio-Fenton catalyst of 2 g /L has been used to achieve 99% decolorization of Malachite Green after 120 minutes at pH 5.5, 20 mM glucose, and 40 °C (Elhami et al., 2015).

The decolourization of Acid Blue 113 (AB 113) textile azo dye was investigated by Eskandarian et al., (2014) using Bio-Fenton process. Under constant temperature and shaking rate (160 rpm), AB 113 was degraded by 91 % in 1 hour at 0.2 mmol/L Fe<sup>2+</sup>, pH 4, 0.02 mol/L glucose, and 3,000 U/L glucose oxidase activity.

Aber et al., (2016) studied the removal of Acid Yellow 12 using immobilization of glucose oxidase on Fe<sub>3</sub>O<sub>4</sub> magnetic nanoparticles. 62.27% of decolourization was observed after 120 minutes with the presence of 0.3 g immobilized enzyme (450 U/g) in 100 cm<sup>3</sup> solution at an optimum condition of pH= 4.5, temperature as 29 °C, initial glucose concentration of 1.5 g/L, and Fe<sup>+2</sup> concentration of 1.4 g/L.

The investigation done by Karimi et al., (2012) achieved 78% removal of malachite green dye during 120 minutes. From the study it was observed that as the concentration of dye increased the decolourization was decreased. The decolourization was increased with increase in concentrations of glucose with constant enzyme rate.

## **2.8 SUMMARY OF THE LITERATURE REVIEW**

It consists of the exposure, occurrence, toxicity level, and environmental concern of triclosan. Many treatment methods like physical, chemical and biological methods for the degradation of triclosan was discussed in detail. Including that advanced oxidation process, Fenton's process, nanoparticles, green synthesized nanoparticles for the removal of pollutant, and bio-Fenton's process were discussed in detail.

It consists of an introduction to the Endocrine Disrupting Compounds, pharmaceutical preparations active ingredients and personal care products, triclosan, and their effect on human and aquatic life. The effect of triclosan on human beings, animals and aquatic life is described in this. The treatment methods like physical, chemical, biological, Fenton's oxidation, green synthesized nanoparticles, green synthesized laterite as a catalyst, and bio-Fenton process were discussed in detail.

For environmental protection, it is essential to prevent and treat TCS contamination, despite its increasing attention. Therefore it is necessary to remove the triclosan which is present in wastewater before disposing of it in water bodies or soil. The treatment methods which were discussed to degrade triclosan have limitations. In the adsorption process, a large quantity of residue will be formed. Hence it is necessary to provide further treatment. Though the toxicity level is high biodegradation is one of the

limitations, hence it is necessary to provide pretreatment. Ozone and UV-H<sub>2</sub>O<sub>2</sub> treatment are more efficient and reliable than Fenton's treatment in AOPs, but it is more expensive since UV lamps consume a lot of energy. Many researchers have concluded that heterogeneous Fenton's oxidation can degrade triclosan. Green synthesized nanoparticles application in the Fenton process showed the better results for the degradation of organic contaminants. Using laterite soil as a source of iron instead of iron salts have reduced the addition of extra sulfates and chlorides to the treatment system. Various nanoparticles were synthesized using both *Psidium guajava* and *Makaranga peltata* leaf extract and used to degrade dyes and organic pollutants. Laterite has many advantages like temperature resistivity, non-toxic, economical and its availability. Hence it can be used as a precursor.



## CHAPTER 3

### MATERIALS AND METHODS

#### 3.1 MATERIALS

A detailed experimental methodology implemented in this present investigation was described in this chapter. The chemicals used for the synthesis, and determination of iron, and hydrogen peroxide are listed below. The procedure adopted for the green synthesis of nanoparticles from leaf extract was presented in detail. The Characterization of the synthesized iron nanoparticles has been analyzed. Morphological characterization like the size and shape of synthesized nanoparticles was confirmed by Fourier Emission Scanning Electron Microscopy (FESEM) with Energy Dispersive X-Ray Analyzer (EDS). The functional group of the nanoparticles was identified with Fourier-transform infrared spectroscopy (FTIR). The mineral phase identification of synthesized nanoparticles was carried out with X-ray diffraction (XRD). The surface area, pore size, and pore volume were analyzed by BET (Brunauer–Emmett–Teller) surface area analysis. The synthesized nanoparticles were used to degrade the triclosan in wastewater. The experimental method and analytical procedure to degrade the Triclosan using the conventional Fenton process and by Bio-Fenton process are explained in detail.

##### 3.1.1 List of Chemicals Utilized

The chemicals used for the synthesis of nanoparticles and triclosan removal were analytical grade reagents. Triclosan ( $\geq 97.0\%$ ) was procured from Sigma Aldrich. Sulphuric acid was procured from Merck India which is used to adjust the pH. Hydrochloric Acid, Hydrogen peroxide, Sodium thiocyanate, potassium thiocyanate, titanium sulfate, 1-10 phenanthroline, ferrous ammonium sulfate, and Sodium carbonate were purchased from Merck India. Glucose oxidase (GOD) from *Aspergillus niger* was purchased from Himedia.

### 3.1.2 Raw Laterite Soil Sample

Raw laterite soil was collected from the National Institute of Technology Karnataka (NITK), Surathkal, India. Soil samples were collected at a depth of 200 cm from the surface. To know the morphology, chemical characteristics, and mineralogy the analysis of the raw laterite soil was conducted.

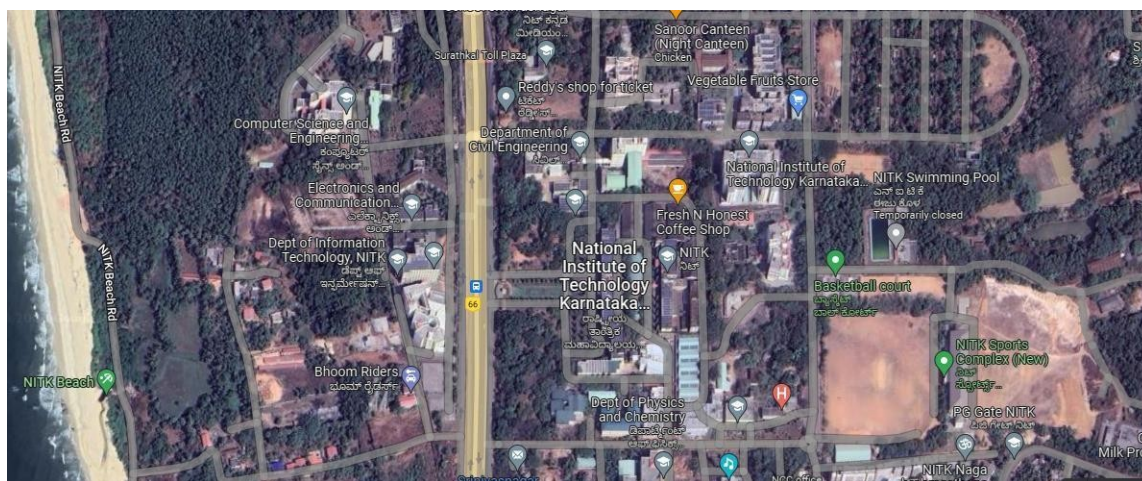


Figure 3.1 Location of Raw Lateritic soil sample

## 3.2 METHODOLOGY

### 3.2.1 Extraction of Iron from Laterite Soil

Laterite soil collected from NITK Campus was dried and crushed to powder. The soil was then passed through a  $150\mu$  sieve. 1g of sieved soil was taken in a glass beaker and 20 ml of 1:1 water and hydrochloric acid (HCl) was added. The solution was mixed gently and was kept for heating on a sand bath for maximum evaporation till a residue formed at the bottom of the beaker. The residue left was baked in an oven for 1 h. Again for the dried residue, 20ml of 1:1 water: HCl was added and heated for 1min, followed by the addition of 20ml hot distilled water. The solution was filtered through a Whatman filter paper (No. 42). The residue left over in the filter paper is ignited in a muffle furnace at a temperature of  $650\text{ }^{\circ}\text{C}$  and the residue left was considered silicon dioxide. The obtained filtrate is a mixture of aluminum and iron oxide and other traces of elements.

The filtrate is diluted to 250 ml and 50% of the liquid was used to obtain  $\text{Al}_2\text{O}_3$  and  $\text{Fe}_2\text{O}_3$  and the remaining sample was used for the extraction of iron (IS 2720 (Part- XXV) – 1982).

### 3.2.2 Preparation of Leaf Extract

*Psidium guajava* and *Macaranga peltata* leaves were washed with distilled water and dried for 2 days in an oven at a temperature of 40 °C. The dried leaves were crushed and ground into powder form. 2.5g of leaf powder was mixed separately with 100 mL of double distilled water taken in a beaker at 80 °C while being continuously stirred for 30 min. Both the solution was allowed to cool to room temperature then filtered using Whatman filter paper and stored at 4 °C for further use (Hussien et al., 2017).

### 3.3 SYNTHESIS AND CHARACTERIZATION OF IRON NANOPARTICLES

The iron nanoparticles were prepared by adding laterite extract as a precursor to the obtained leaf extract in the ratio of 1:1. Formation of black precipitation indicates the synthesis of iron nanoparticles. Then the solution was centrifuged at a speed of 8000 rpm for 15 min. Nanoparticles settled at the bottom after centrifugation and were collected and dried in an oven at 60 °C for 10 h. Dried nanoparticles were stored in an airtight container for further use.

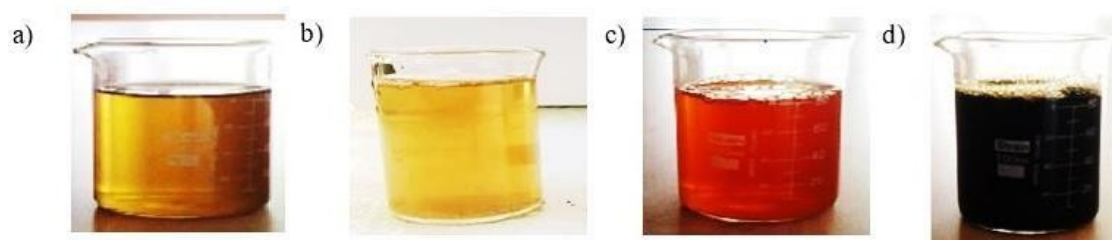


**Figure 3.2. Green synthesized laterite iron nanoparticles (a) *Psidium guajava* leaf extract (b) *Macaranga peltata* leaf extract (c) Laterite extract (d) Synthesized nano iron particles**

### **3.4 ANALYTICAL METHODS**

The concentration of triclosan was measured using High-performance liquid chromatography (HPLC) Agilent 1200 with a C18 reverse phase column (pore size 3.5  $\mu\text{m}$ ,  $100 \times 0.46$  cm), using water and methanol (in the ratio of 58:42) as mobile phase injected with a flow rate of 1.0 ml/min employing diode array detector (DAD) (Anupama and S. Shrihari 2018; Bhaskar et al., 2019). Digital pH meter was used to measure the pH (Hanna make). Ferric iron was measured by potassium thiocyanate method using UV - Vis spectrophotometer (Mellon and Woods, 1941). The ferrous iron was measured using phenanthroline method UV visible spectrophotometer. Total iron concentration was measured by 1,10 phenanthroline method using UV-Spectrophotometer (Mellon and Woods, 1941).  $\text{H}_2\text{O}_2$  was measured using UV-spectrophotometer (Eisenberg, 1943).

### **3.5 FENTON'S OXIDATION OF TRICLOSAN**

Catalytic potential of Green Laterite based Iron Nano Particles (GLFeNP's) in the Fenton's oxidation of Triclosan was evaluated. The stock solution of Triclosan of 1 g/L was prepared to carry out the experiment. A working Triclosan solution with the desired concentration in the range of 2 -10 mg/L was taken in a conical flask and the pH was adjusted using 1N  $\text{H}_2\text{SO}_4$  or 1N NaOH. Synthesized nanoparticles were added to the conical flask and were kept in a shaker for 10 minutes at 180 rpm to ensure proper mixing.  $\text{H}_2\text{O}_2$  was then added to the solution to mark the start of the experiment. Samples were drawn at regular intervals for the analysis during which 1ml of sodium thiosulphate was to halt the reaction (Khan et al., 2009). All the experiments were conducted in triplicates.

### **3.6 BIO-FENTON'S OXIDATION OF TRICLOSAN**

The Triclosan concentration of 2 mg/L was taken in a conical flask, using 1N  $\text{H}_2\text{SO}_4$  or 1N NaOH the pH was adjusted. The optimized dose of Green Laterite based Iron Nano Particles (GLFeNP's) were added to the conical flask maintaining a speed of 180 rpm.

The effect of pH (3, 5.5 and 7) was studied for the degradation of triclosan. Then the desired dose of glucose and glucose oxidase was added to the same to start the experiment. Samples were drawn at regular intervals for the analysis during which 1ml of sodium thiosulphate was to halt the reaction (Khan et al., 2009). All the experiments were conducted in triplicates.

### **3.6.1 Production of Hydrogen Peroxide Based on Enzyme Activity**

As glucose concentrations were varied from 0.5 to 2 g/L with an increment of 0.5 g/L, different concentrations of GOD were used to determine the optimal conditions for H<sub>2</sub>O<sub>2</sub> production. An orbital shaker at 180 rpm was used in these experiments for 48 hours during which samples were collected periodically. Results are based on the average of the three experiments with a standard deviation of less than 5%.



## CHAPTER 4

### RESULTS AND DISCUSSION

The nanoparticles were synthesized from laterite and leaf extract and are characterized and discussed in detail which is used as a catalyst. The laterite soil is used as a source of iron instead of commercially available iron salts for the green synthesis of iron nanoparticles. The experimental investigation was carried out. The studies were conducted on pH, H<sub>2</sub>O<sub>2</sub>, and synthesized nanoparticles dosages for maximum triclosan degradation. Chemical reaction kinetic constants are calculated based on kinetic analysis of triclosan degradation. Bio-Fenton's oxidation studies were carried out for the optimized condition. To ignore the addition of hydrogen peroxide, the bio-Fenton process was studied for the optimized condition of the conventional Fenton process.

#### 4.1 CHARACTERIZATION OF RAW LATERITE SOIL

The chemical composition and morphological characteristics of raw laterite soil were analyzed and reported. Table 4.1 shows the chemical composition of raw laterite soil. Figure 4.1 (a) and Figure 4.2 presents the SEM and XRD images of raw laterite soil, respectively. It is estimated that the raw laterite soil has a high iron content of 45.75 % indicating the richness of the iron content in it (Khataee et al., 2015). This iron content in the raw laterite soil was used for the synthesis of nano iron oxide particles. In the raw laterite soil, elements such as aluminum, silica, and oxygen are also present. The XRD plot confirms the presence of iron oxide with sharp peaks in the raw laterite soil. It exhibits six peaks at  $2\theta$  12.401, 18.347, 21.448, 26.690, 35.7446, and 78.21 corresponding to iron oxide (PDF: 01-079-0007) and two peaks at  $2\theta$  33.189 and 59.988 which corresponds to iron hydride (PDF: 00-043-1321) (Kasthurba et al., 2008; Sangami and Manu, 2017a).

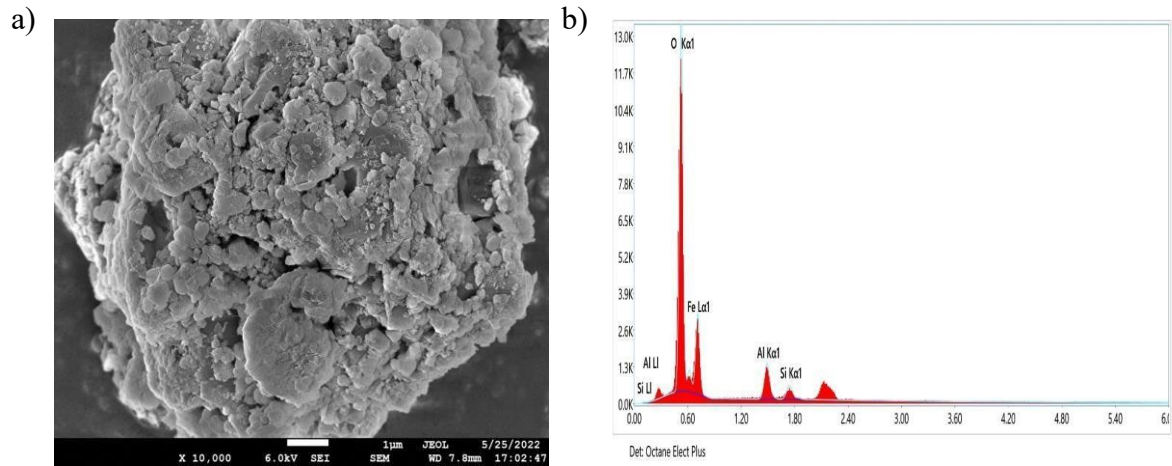


**Figure 4.1. Raw Laterite Particles a) Scanning Electron Microscopic images b) EDS images**

Figure 4.1(b) shows an EDS plot of raw laterite soil, the peak presents the presence of oxygen, iron, aluminium, silica, and other elements in traces (Sangami and Manu, 2017a). Raw laterite soil was found to have 32.3% of iron by weight. Table 4.1 presents the elemental composition of raw laterite soil. The total iron content of the laterite iron extract was found to be 5.02 g/L.

**Table 4.1 Chemical composition of Raw Lateritic soil**

Element	Weight (%)
Iron oxide ( $\text{Fe}_2\text{O}_3$ )	45.75
Aluminium Oxide ( $\text{Al}_2\text{O}_3$ )	19.7
Silica ( $\text{Si}_2\text{O}_3$ )	24.2
Others	10.35

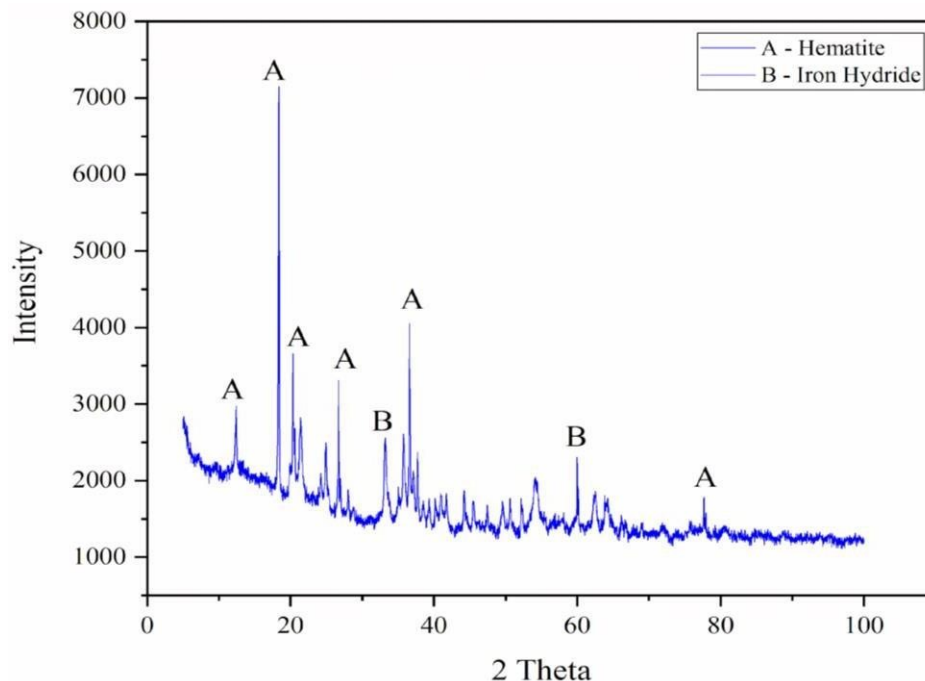


**Figure 4.2 XRD Images of Raw Laterite Particles**

## **4.2 CHARACTERIZATION OF GREEN LATERITE-BASED IRON NANOPARTICLES (GLaFeNPs)**

The mineralogical composition, morphological appearance, surface area, pore volume, and functional group of the green synthesized laterite-based iron nanoparticles (GLaFeNPs) were investigated. The green synthesized laterite-based iron nanoparticles using *Psidium guajava* are represented as *Psidium guajava* Laterite Iron Oxide Nano Particles (GPsLaNP) and the green synthesized laterite-based iron nanoparticles using *Macaranga peltata* leaves are represented as green synthesized *Macaranga peltata* Laterite Iron Oxide Nanoparticles (GMpLaNP) respectively.

### **4.2.1 Characterization of Synthesized GLaFeNPs**

On morphological characterization, iron nanoparticles were seen as agglomerated spherical particles arranged in the group for GPsLaNP and agglomerated spherical particles with a clear edge for GMpLaNP under the scanning electron microscope. The scanning electron micrographic images of GPsLaNP and GMpLaNP are shown in Figure

4.3 (a) and Figure 4.3 (b) respectively. Table 4.2 presents the elemental composition of both GPsLaNP and GMpLaNP. GPsLaNP were found to have 27.6% iron by weight with potassium and chlorine being other elements in trace quantities and GMpLaNP were found to have 19.0% iron by weight with chlorine, potassium, phosphate, silica, and aluminum being other elements in a trace. The EDS image representing the elemental compositions of both GPsLaNP and GMpLaNP are shown in Figure 4.4 (a) and Figure 4.4 (b) respectively. Iron oxide was likely formed in both leaf extracts because Fe and O peaks were observed (Madubuonu et al., 2020; Somchaidee and Tedsree, 2018).

**Table 4.2: Elemental composition of GPsLaNP and GMpLaNP**

Elements	<i>Psidium guajava</i> Laterite Iron Oxide Nano Particles (GPsLaNP) (Weight %)	<i>Macaranga peltata</i> Laterite Iron Oxide Nanoparticles (GMpLaNP) (Weight %)
O	66.7	68.2
Fe	27.6	19.0
Cl	5.1	2.7
K	0.7	1.0
P	-	5.0
Si	-	2.9
Al	-	1.2

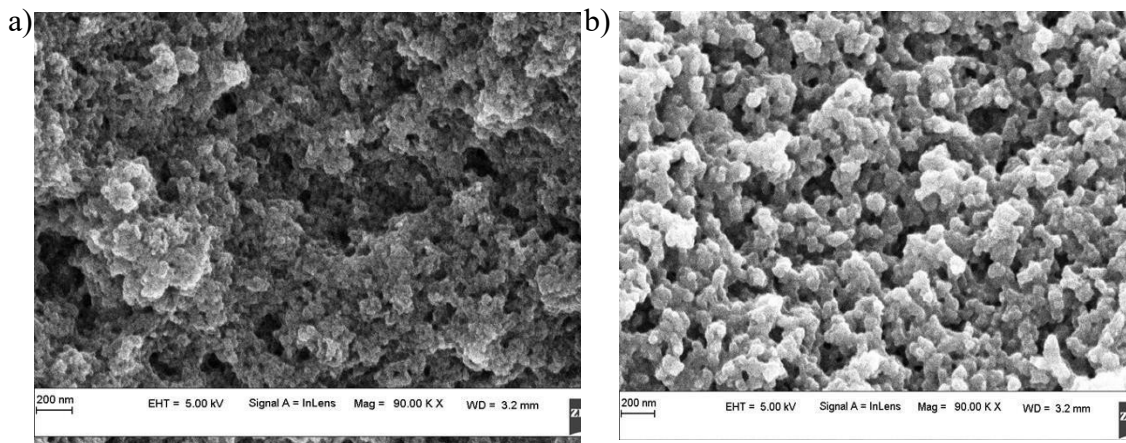


**Figure 4.3** Scanning Electron Microscopic images of Green laterite Iron oxide Nanoparticles (GLaFeNPs) a) *Psidium guajava* Laterite Iron Oxide Nanoparticles (GPsLaNP) b) *Macaranga peltata* Laterite Iron Oxide Nanoparticles (GMpLaNP) showing the morphological appearance

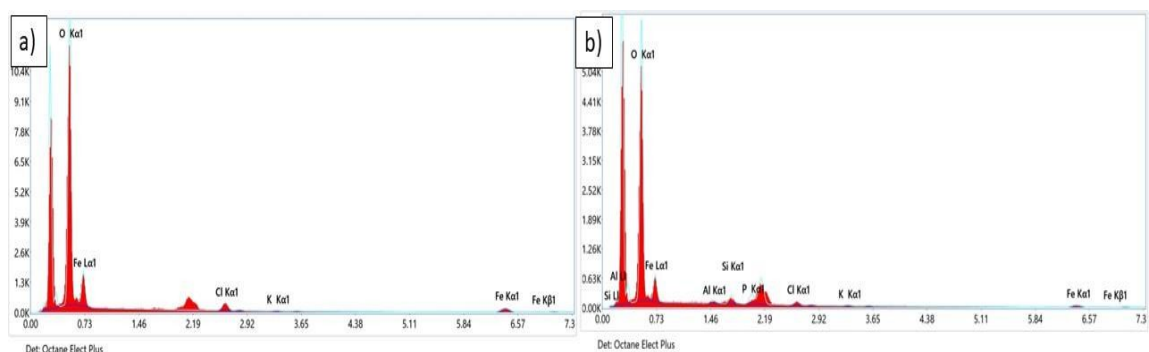


**Figure 4.4** EDS images of Green laterite Iron oxide Nanoparticles (GLaFeNPs) a) *Psidium guajava* Laterite Iron Oxide Nanoparticles (GPsLaNP) b) *Macaranga peltata* Laterite Iron Oxide Nanoparticles (GMpLaNP)

Covering the  $2\theta$  angle from  $2-100^\circ$  X-ray diffraction measurements were performed at room temperature. The XRD images of both GPsLaNP and GMpLaNP are shown in Figure 4.5 (a) and Figure 4.5 (b) respectively. The synthesized GPsLaNP formed four peaks at  $2\theta$  18.315, 35.487, 57.010, and 62.624 corresponding to magnetite (PDF: 01-089-0691), one peak at  $2\theta$  30.336 corresponds to magnesium aluminium iron oxide

(PDF: 01-071-1234) and another one peak at  $2\theta$  43.116 corresponds to copper zinc iron oxide (PDF: 01-077-0012) (Shahwan et al., 2011; Wang et al., 2014). The XRD images of synthesized GMpLaNP exhibit a total of eight peaks at 30.161, 74.2249, 35.54, 62.6638, 35.5184, 43.1402, 53.5493 and 63.6638 corresponding to two peaks at  $2\theta$  30.161 and 74.2249 corresponds to iron silicon oxide (PDF: 01 – 052 – 1140), three peaks at  $2\theta$  35.54, 62.6638 and 74.2249 corresponds to magnetite (PDF: 01 – 088 – 0315) and four peaks at  $2\theta$  35.5184, 43.1402, 53.5493 and 63.6638 corresponds to magnesioferrite (01 – 088 – 1937) (Afsheen et al., 2018; Shahwan et al., 2011; Wang et al., 2014). This indicates the presence of iron particles in the synthesized GLaFeNPs.

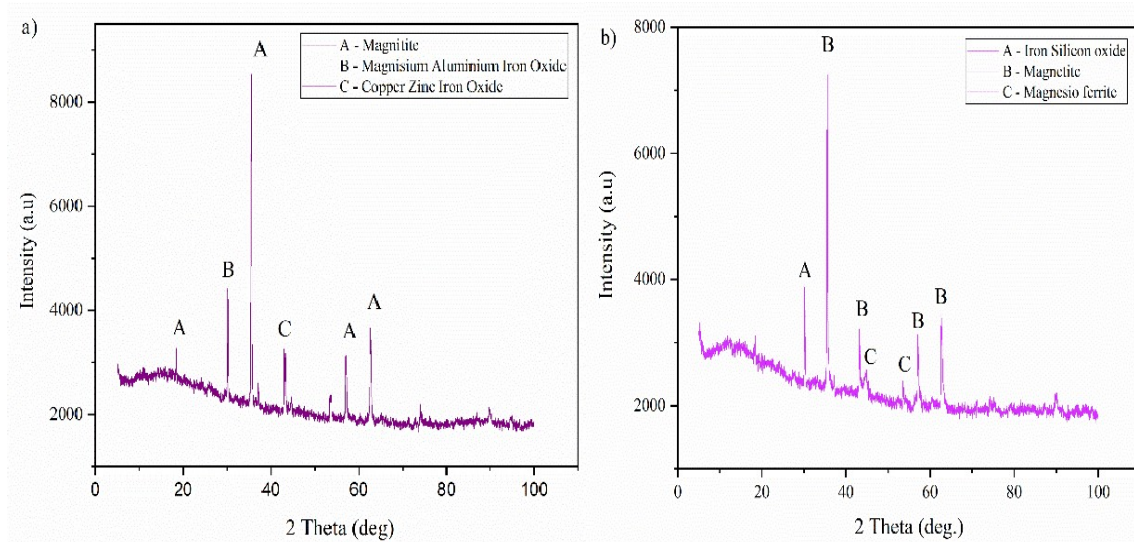


**Figure 4.5 XRD Images of Green laterite Iron oxide Nanoparticles (GLaFeNPs)**  
**a) *Psidium guajava* Laterite Iron Oxide Nanoparticles (GPsLaNP)**  
**b) *Macaranga peltata* Laterite Iron Oxide Nanoparticles (GMpLaNP)**  
**representing the corresponding peaks**

The fourier-transform infrared spectroscopy (FTIR) technique was used to recognize the functional groups, present in the synthesized nanoparticles. From Figure 4.6 (a), it is observed that the FTIR spectra of the GPsLaNP show strong bands at 3323.22, 1640.56, and 525.47 respectively. The peak of 3323.22 corresponds to carbon-to-hydrogen

stretching (C-H), 1640.56 corresponds to carbon-to-carbon double bond stretching (C=C), 525.47 corresponds to iron-to-oxygen bonding (Fe-O) confirming the formation of iron oxide nanoparticles (Anitha et al., 2021; Devatha et al., 2016). Figure 4.6 (b) presents the FTIR spectrum of synthesized GMpLaNP, in which peak 3331.43 corresponds to a secondary amine group (N-H), peak 1638.00 corresponds to double bond stretching (C=C), peak 511.11 corresponds to iron to oxygen bonding (Fe-O), confirming the formation of iron oxide nanoparticles (Devatha et al., 2016; Selvaraj et al., 2021).

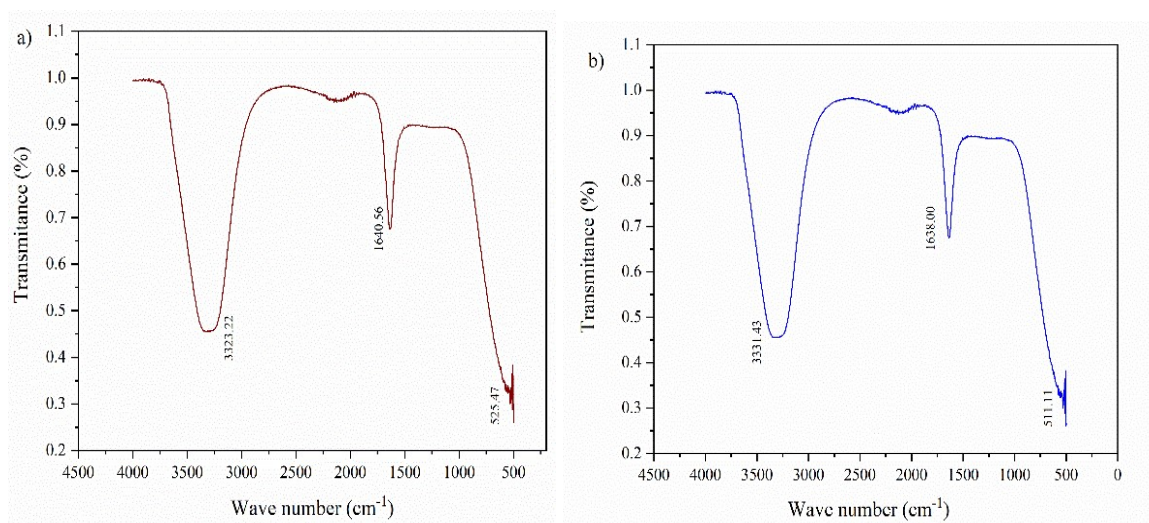


**Figure 4.6 FTIR Images of Green laterite Iron oxide Nanoparticles(GLaFeNPs)**

**a) *Psidium guajava* Laterite Iron Oxide Nanoparticles (GPsLaNP)**

**b) *Macaranga peltata* Laterite Iron Oxide Nanoparticles (GMpLaNP)**

**representing the corresponding peaks**

According to the BET surface area analysis, the surface area and pore volume of GPsLaNP are found to be 11.76m<sup>2</sup>/g and 0.02409 cm<sup>3</sup>/g and GMpLaNP are 11.707 m<sup>2</sup>/g and 0.241 cm<sup>3</sup>/g respectively. The surface area of the obtained GLaFeNPs is two times greater than that of commercially available Fe<sub>2</sub>O<sub>3</sub> (Ahmmad et al., 2013).

### 4.3 FENTON'S OXIDATION OF TRICLOSAN

To optimize the reaction conditions a detailed study was carried out. The Parameters like the concentration of Triclosan, pH, the dosage of synthesized nanoparticles, and the dosage of hydrogen peroxide were considered for the optimization process. For the degradation of Triclosan synthesized iron nanoparticles were used. The laterite is used as a precursor with *Psidium guajava* and *Makaranga peltata* leaf extract instead of commercially available iron salts for the synthesis of nanoparticles. Initially, the known quantity of catalyst was added to the solution. Later the required dose of H<sub>2</sub>O<sub>2</sub> was added to the same after 10 minutes. After adding the H<sub>2</sub>O<sub>2</sub> to the solution, the degradation of the Triclosan was initiated.

#### 4.3.1 Fenton's Degradation of Triclosan by GPsLaNP

This study investigated the degradation of triclosan using GPsLaNP as a catalyst in heterogeneous Fenton-like processes, varying the GPsLaNP dose from 0.01 to 1 g/L. The catalytic action of GPsLaNP with hydrogen peroxide was found in the degradation of triclosan. The triclosan concentration was varied from 2 – 10 mg/L with an increment of 2 mg/L. The maximum removal was observed at 2 mg/L of triclosan concentration. The degradation of triclosan using different dosage of GPsLaNP is presented in figure 4.7. The degradation of triclosan using GPsLaNP with different catalyst loading is presented in Table 4.3. Maximum triclosan removal was found to be 96.5% for GPsLaNP at a catalyst dosage of 1.0 g/L and hydrogen peroxide dosage of 300 mg/L with a rate constant of 0.0226/Min. Degradation efficiency observed with 0.01 g/L and 400 mg/ L of H<sub>2</sub>O<sub>2</sub> was 47.5% and with 0.1 g/L and 200 mg/ L of H<sub>2</sub>O<sub>2</sub> was 69.5% with rate constant 0.006/ Min and 0.0081/ Min respectively. It is observed that the increase in the catalyst dose of GPsLaNP from 0.01g/ L to 0.1 g/L has an increase in the removal efficiency by 22% and 0.1g/L to 1g/L has an increase in the removal efficiency of 27.0% respectively. Also, the k value increased as the dosage of the nanoparticle increased. The present study confirms the active participation of synthesized nanoparticles in the degradation of Triclosan by Fenton's oxidation. Triclosan is degraded by hydroxyl radicals that are

generated while hydrogen peroxide is dissociated through the oxidation and reduction of iron catalysts. An increase in catalyst load is more useful than increasing hydrogen peroxide since iron will increase the speed of the reaction by promoting the generation of more hydroxyl radicals in less time (Andrades et al., 2021; Khataee et al., 2015). The rate of oxidation depends on the dissolution rate of ferrous ion that has leached out from the nanoparticles while adsorption on the surface of the catalyst also contributes to the removal rate. It is the amount of addition of catalyst that indicates the adsorption part of heterogeneous Fenton's oxidation that in turn contributes to the maximum removal of the target compound in the process. This is supported by previous studies (Bhaskar et al., 2019; Chen et al., 2017).

**Table 4.3: Degradation of triclosan by GPsLaNP with different catalyst loading**

Catalyst Loading (g/L)	H <sub>2</sub> O <sub>2</sub> Dosage	% Removal of TCS	Rate Constant /Min
0.01	100	40	0.0038
	200	43	0.0046
	300	37.5	0.0036
	400	47.5	0.006
0.1	100	44.1	0.0033
	200	69.5	0.0081
	300	45.5	0.004
	400	48	0.0046
1	100	82	0.011
	200	77.5	0.0089
	300	96.5	0.0226
	400	84	0.0127

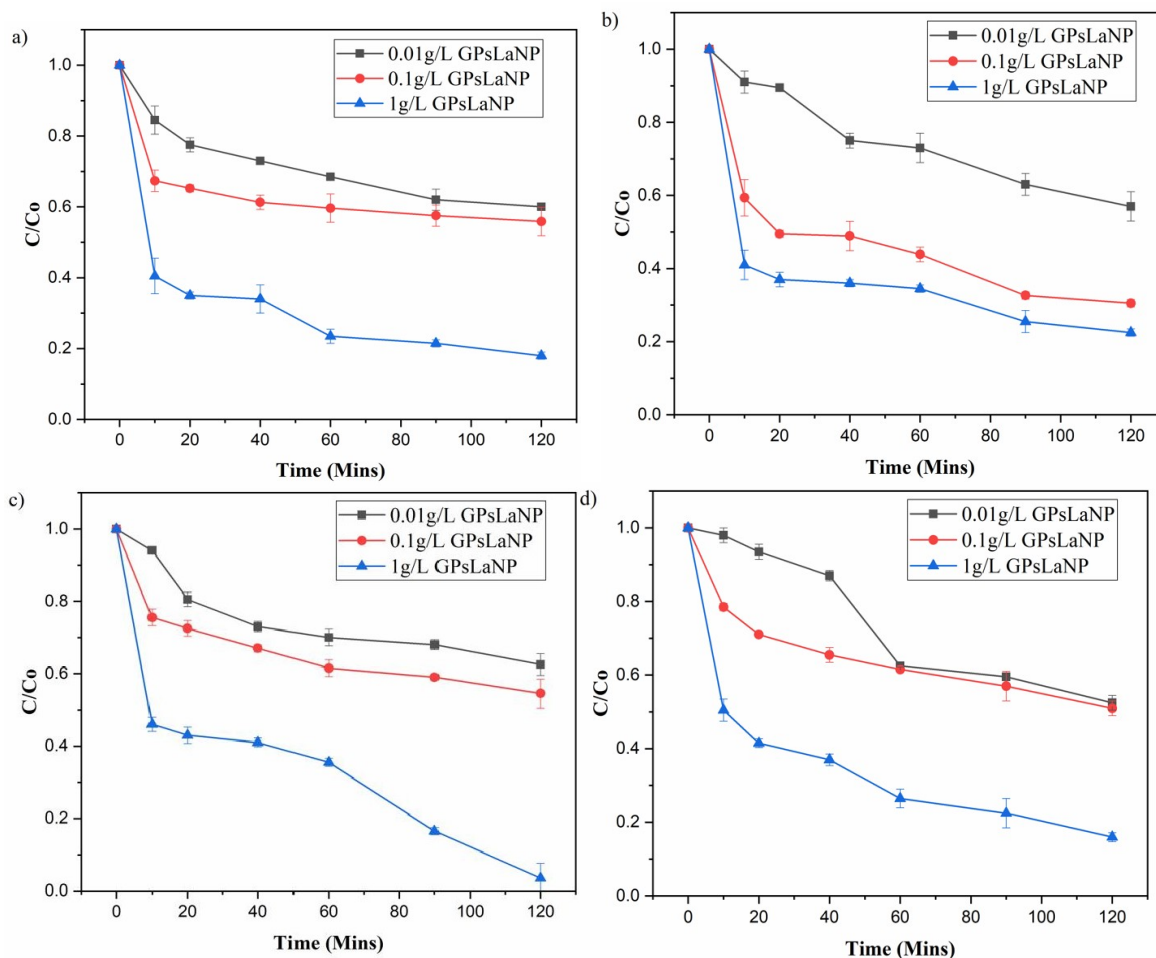


**Figure 4.7: Oxidative degradation of Triclosan at different GPsLaNP dosages with variation in H<sub>2</sub>O<sub>2</sub> a) 100 mg/L of H<sub>2</sub>O<sub>2</sub> b) 200 mg/L of H<sub>2</sub>O<sub>2</sub> c) 300 mg/L of H<sub>2</sub>O<sub>2</sub> d) 400 mg/L of H<sub>2</sub>O<sub>2</sub>**

### 4.3.2 Fenton's Degradation of Triclosan by GMpLaNP

In this study, GMpLaNP loading of 0.01-1.0 g/L was studied to determine the effects of catalyst loading on the degradation of 2 mg/L of triclosan concentration. Figure 4.8 presents the oxidative degradation of triclosan using GMpLaNP. The degradation of triclosan using GMpLaNP is presented in Table 4.4 for 0.01, 0.1 and 1 g/L. It is observed that the increase in the catalyst dose of GMpLaNP from 0.01g/ L to 0.1 g/L has an increase in the removal efficiency of 27% from 0.1g/L to 1g/L has an increase in the removal efficiency of 29.1% respectively. The present study confirms the active

participation of synthesized nanoparticles in the degradation of triclosan by Fenton's oxidation. It is observed that an increased catalyst load is more beneficial than increasing hydrogen peroxide since iron promotes the generation of more hydroxyl radicals in a shorter period, thereby increasing the speed of the reaction (Andrades et al., 2021; So et al., 2019). The rate of oxidation depends on the dissolution rate of ferrous ion that has leached out from the nanoparticles while adsorption on the surface of the catalyst also contributes to the removal rate. It is the amount of catalyst addition that indicates the adsorption part of heterogenous Fenton's oxidation that in turn contributes to the maximum removal of the target compound in the process. This is supported by previous studies (Bhaskar et al., 2019; Chen et al., 2017; Bhaskar et al., 2020).

**Table 4.4: Degradation of triclosan by GMpLaNP with different catalyst loading**

Catalyst Loading (g/L)	H <sub>2</sub> O <sub>2</sub> Dosage	% Removal of TCS	Rate Constant /Min
0.01	100	43	0.0037
	200	40.5	0.0041
	300	30.5	0.0027
	400	26.5	0.0023
0.1	100	60	0.007
	200	58.5	0.0074
	300	63	0.0073
	400	70	0.0087
1	100	84.5	0.0144
	200	82.5	0.0122
	300	99.1	0.0356
	400	86	0.015

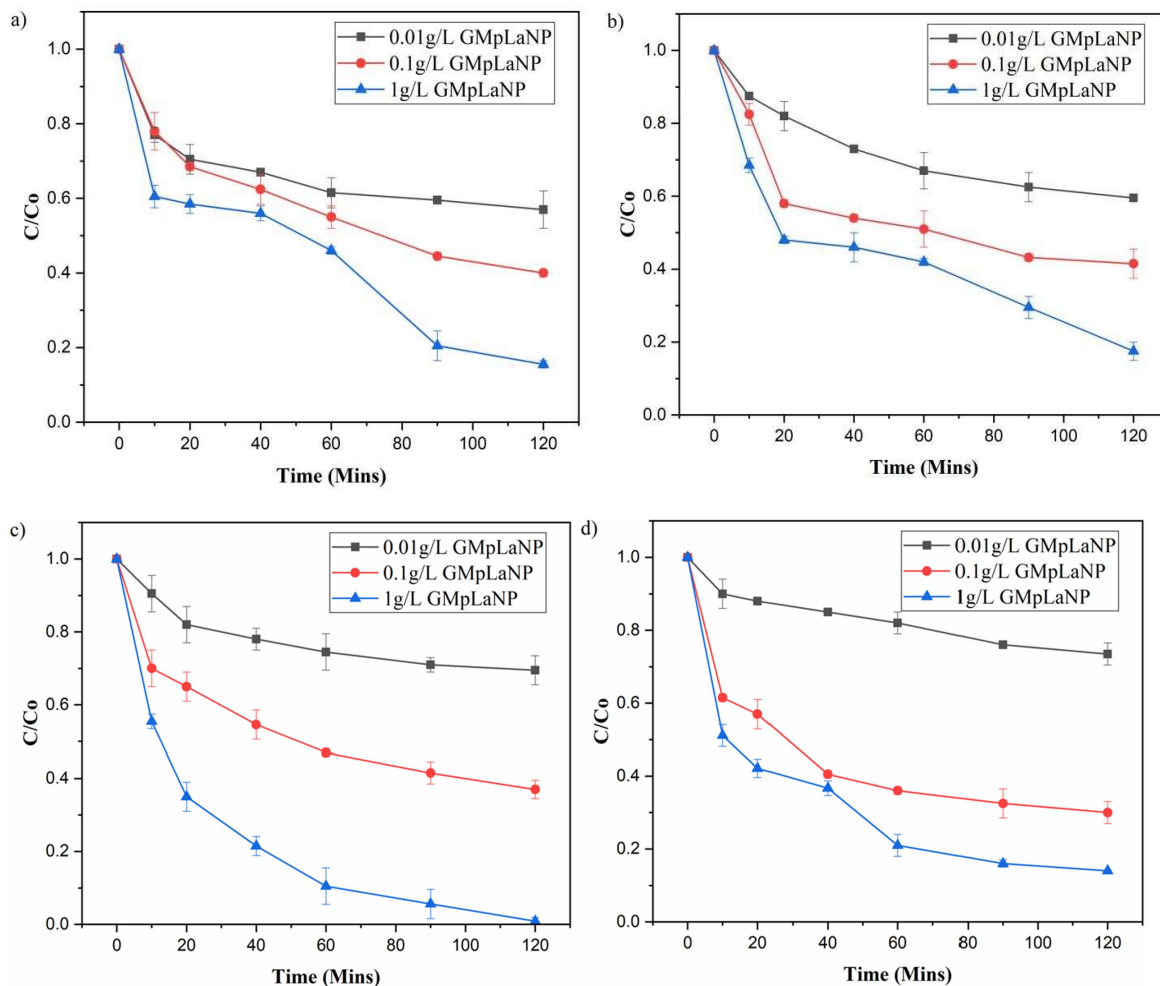


**Figure 4.8: Oxidative degradation of Triclosan at different GMpLaNP dosages with variation in H<sub>2</sub>O<sub>2</sub> a) 100 mg/L of H<sub>2</sub>O<sub>2</sub> b) 200 mg/L of H<sub>2</sub>O<sub>2</sub> c) 300 mg/L of H<sub>2</sub>O<sub>2</sub> d) 400 mg/L of H<sub>2</sub>O<sub>2</sub>**

### 4.3.3 Effect of Hydrogen Peroxide on Fenton's Oxidation of Triclosan

The effect of hydrogen peroxide concentration on the GLaFeNPs is discussed below. The maximum degradation was achieved at 1g/L of GPsLaNP at pH 3 and an initial triclosan concentration of 2 mg/L. The hydrogen peroxide concentration was varied from 100 to 400 mg/L to optimize the H<sub>2</sub>O<sub>2</sub> concentration. The concentration of H<sub>2</sub>O<sub>2</sub> also has a significant impact on the degradation efficiency of pollutants in Fenton's oxidation

process, because H<sub>2</sub>O<sub>2</sub> concentration directly determines the generation of hydroxyl radicals.

#### 4.3.3.1 Effect of Hydrogen Peroxide on GPsLaNP

The radicals are generated from hydrogen peroxide in Fenton's Oxidation. The oxidization of pollutants and their intermediates is done by the hydroxyl radicals and helps in the reduction of pollutants. According to Figure 4.10, the triclosan removal efficiency increased rapidly from 82.5% to 96.5% when the H<sub>2</sub>O<sub>2</sub> concentration increased from 100 mg/L to 300 mg/L. This may be because of the less production of OH radicals at the lower concentration of H<sub>2</sub>O<sub>2</sub> as represented by the reaction shown in equation 4.1. When the concentration of H<sub>2</sub>O<sub>2</sub> increased to 400 mg/L again the removal efficiency was reduced. It may be because of the scavenging effect of OH radicals according to the reactions (Eq. 4.2 and Eq. 4.3) (Chu et al., 2012).



**Table 4.5: Maximum degradation of triclosan by GPsLaNP**

Catalyst Loading (g/L)	H <sub>2</sub> O <sub>2</sub> Dosage	% Removal of TCS	Rate Constant /Min
0.01	400	47.5	0.006
0.1	200	69.5	0.0081
1	300	96.5	0.0226

The degradation of triclosan with different concentrations of  $H_2O_2$  is shown in Figure 4.9. The maximum degradation of triclosan observed at different  $H_2O_2$  concentrations is presented in Table 4.5. Degradation of triclosan is less in the presence of 100 mg/L, 200 mg/L, and 300 mg/L with 1 g/L GPsLaNP. This is likely due to insufficient OH radicals in the aqueous solution. It is observed that the highly reactive OH radicals are scavenged by a higher concentration of  $H_2O_2$ , while the less reactive OOH radicals are generated by the increased  $H_2O_2$ .

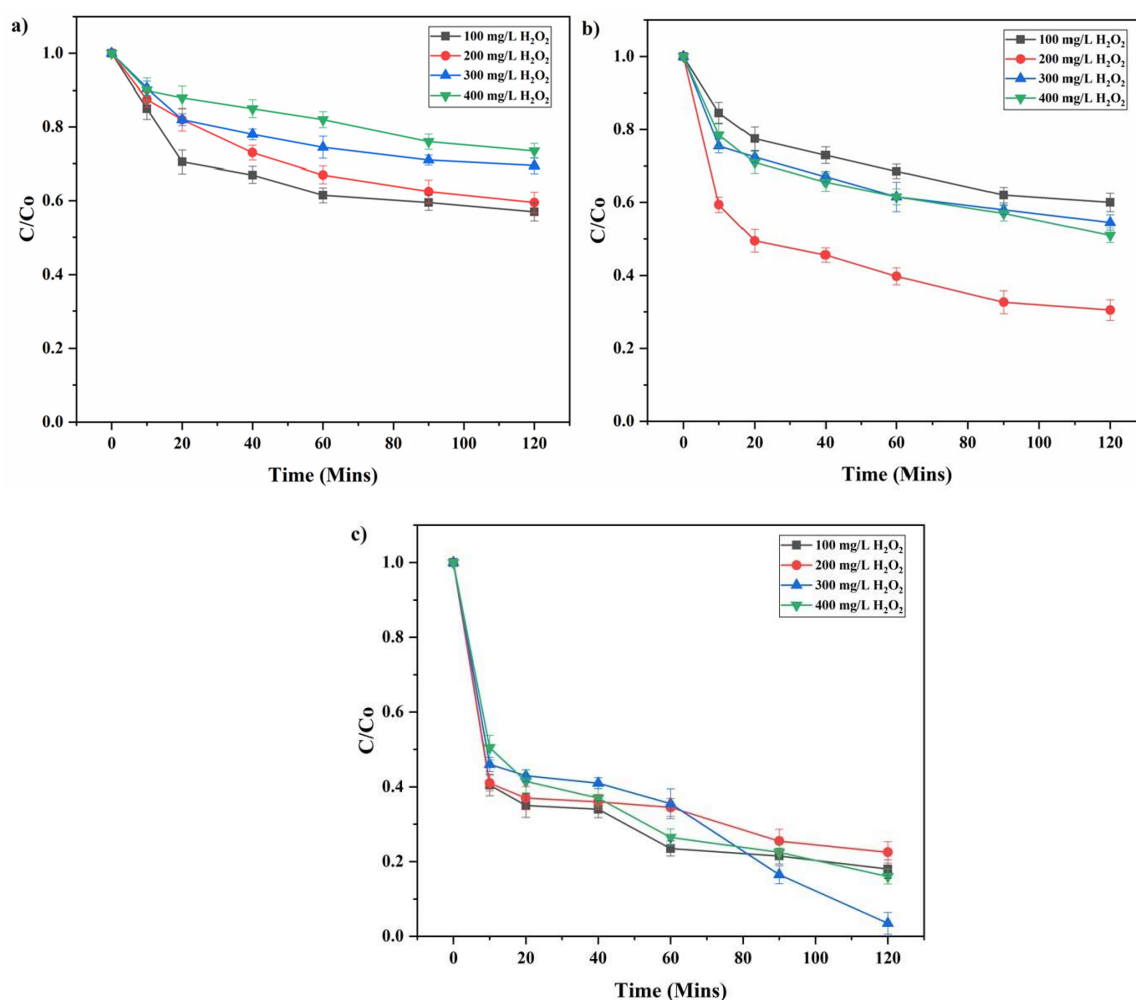


**Figure 4.9: Effect of Hydrogen Peroxide during Fenton's oxidation of Triclosan with GPsLaNP at a) 0.01 g/L b) 0.1 g/L c) 1 g/L**

#### 4.3.3.2 Effect of Hydrogen Peroxide on GMpLaNP

Hydrogen peroxide decomposition produces hydroxyl radicals, which are oxidizing species that are necessary for the Fenton-like process. The effect of hydrogen peroxide with different GMpLaNP dosages is shown in figure 4.10. With the increase in H<sub>2</sub>O<sub>2</sub> dosage from 100 mg/L to 300 mg/L, the removal efficiency was 15.5% higher, with a double rate constant indicating that H<sub>2</sub>O<sub>2</sub> was more readily dissociated with GMpLaNP. With a further increase of 400 mg/L, the rate of hydrogen peroxide variation during Fenton's oxidation of triclosan with GMpLaNP is shown in Figure 4.10 (c) in which the rate constant of GMpLaNP dropped to 0.0160/Min with a removal efficiency of 86%, indicating a scavenging effect. As a result of continuous dissociation during the treatment process, the concentration of hydrogen peroxide decreases until 120 minutes (Kuang et al., 2013). The maximum removal of triclosan with H<sub>2</sub>O<sub>2</sub> dosage is presented in Table 4.6. Increasing the H<sub>2</sub>O<sub>2</sub> dosage to 400 mg/L decreased the removal efficiency by 16.5%, indicating a flushing effect of H<sub>2</sub>O<sub>2</sub>. Initially, the removal of triclosan by 100 mg/L H<sub>2</sub>O<sub>2</sub> was observed to be 60% with a rate constant of 0.007/min. A further increase in H<sub>2</sub>O<sub>2</sub> decreased the removal rate by 1.5% at 200 mg/L. Increasing H<sub>2</sub>O<sub>2</sub> again from 200 to 400 mg/L increased the removal rate by 11.5%. This may be because of the availability of an insufficient amount of OH radicals for the dissociation of the pollutant. It is to note that there is a decrease in the concentration of hydrogen peroxide till 120 mins indicating its continuous dissociation during the treatment process.

**Table 4.6: Maximum degradation of triclosan by GMpLaNP**

Catalyst Loading (g/L)	H <sub>2</sub> O <sub>2</sub> Dosage	% Removal of TCS	Rate Constant /Min
0.01	100	43	0.0037
0.1	400	70	0.0087
1	300	99.1	0.0356

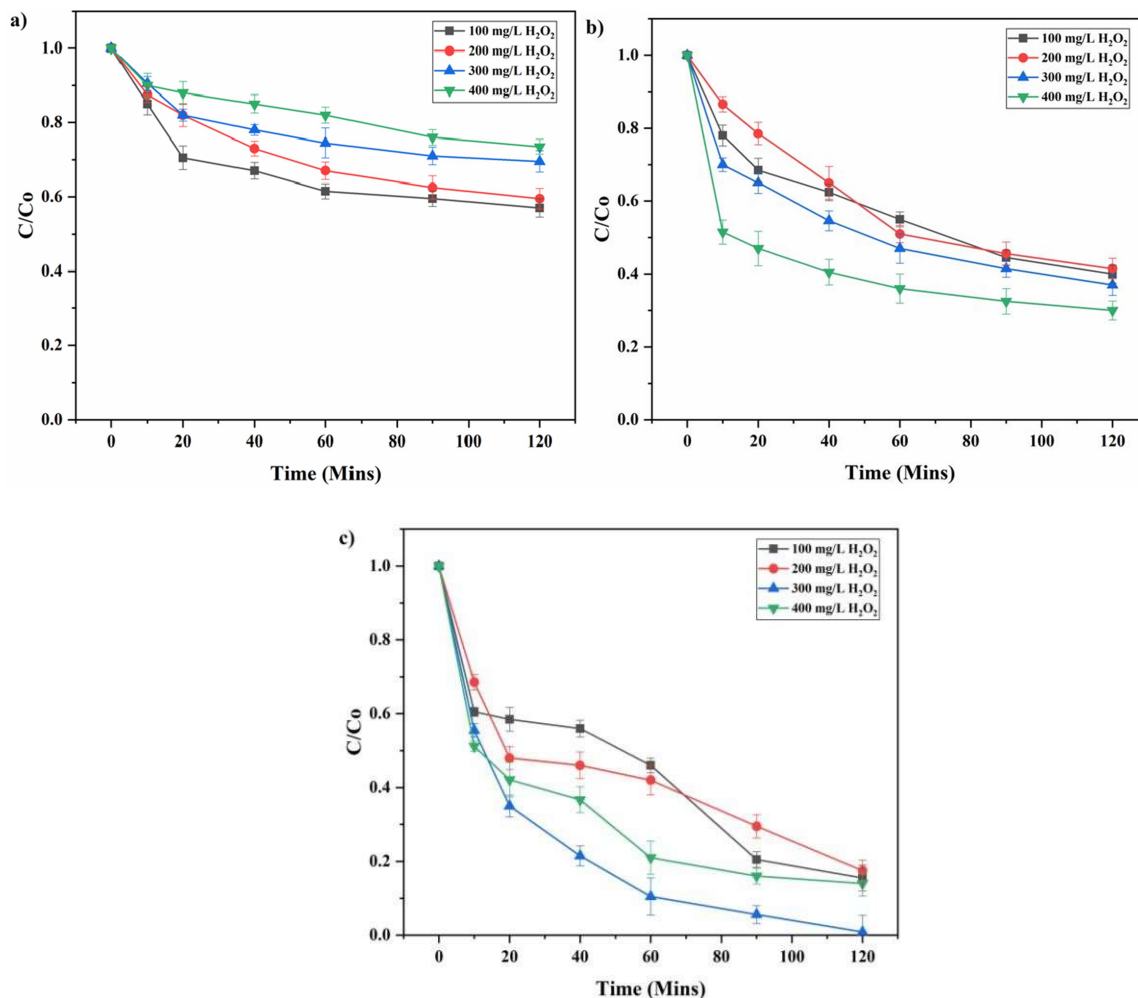


**Figure 4.10: Effect of Hydrogen peroxide during Fenton's oxidation of Triclosan with GMpLaNP at a) 0.01 g/L b) 0.1 g/L c) 1 g/L**

#### 4.3.4 Effect of Initial Concentration of Triclosan on Fenton's Oxidation

The initial concentration of Triclosan was taken as 2mg/L and varied up to 10mg/L with an increment of 2mg/L. It is important to notice that degradation efficiency varies with an organic pollutant's initial concentration. The maximum removal of Triclosan was observed at 2mg/L of Triclosan concentration using GLaFeNPs. This indicates as the concentration of the pollutant increases the removal rate gets decreased.

#### 4.3.4.1 Effect of Initial Concentration of Triclosan on Fenton's Oxidation Using GPsLaNP

Maximum removal was observed at 2 mg/L of initial triclosan concentration for both GPsLaNP and GMpLaNP. This marks the resistance of triclosan for the Fenton's degradation as the concentration of the target compound increases. Figure 4.11 shows the effect of the initial concentration of triclosan on Fenton oxidation with different doses of GPsLaNP. Table 4.7 presents the maximum degradation of triclosan for various initial triclosan concentrations using GPsLaNP.

**Table 4.7: Degradation of initial concentration of triclosan by GPsLaNP**

Catalyst Loading (g/L)	Initial Concentration of TCS (g/L)	% Removal of TCS	H <sub>2</sub> O <sub>2</sub> Dosage
0.01	2	47.5	400
	4	40	
	6	35.8	
	8	34.7	
	10	33	
0.1	2	69.5	200
	4	62	
	6	56.8	
	8	54.8	
	10	50.5	
1	2	69.5	300
	4	62	
	6	56.8	
	8	54.8	
	10	50.5	

The removal was gradually decreased with the increase in the initial triclosan concentration as shown. The results indicate that when the pollutant concentration is increased there will be a reduction in the removal rate (Anupama and Shrihari S, 2018; Orhon et al., 2017).

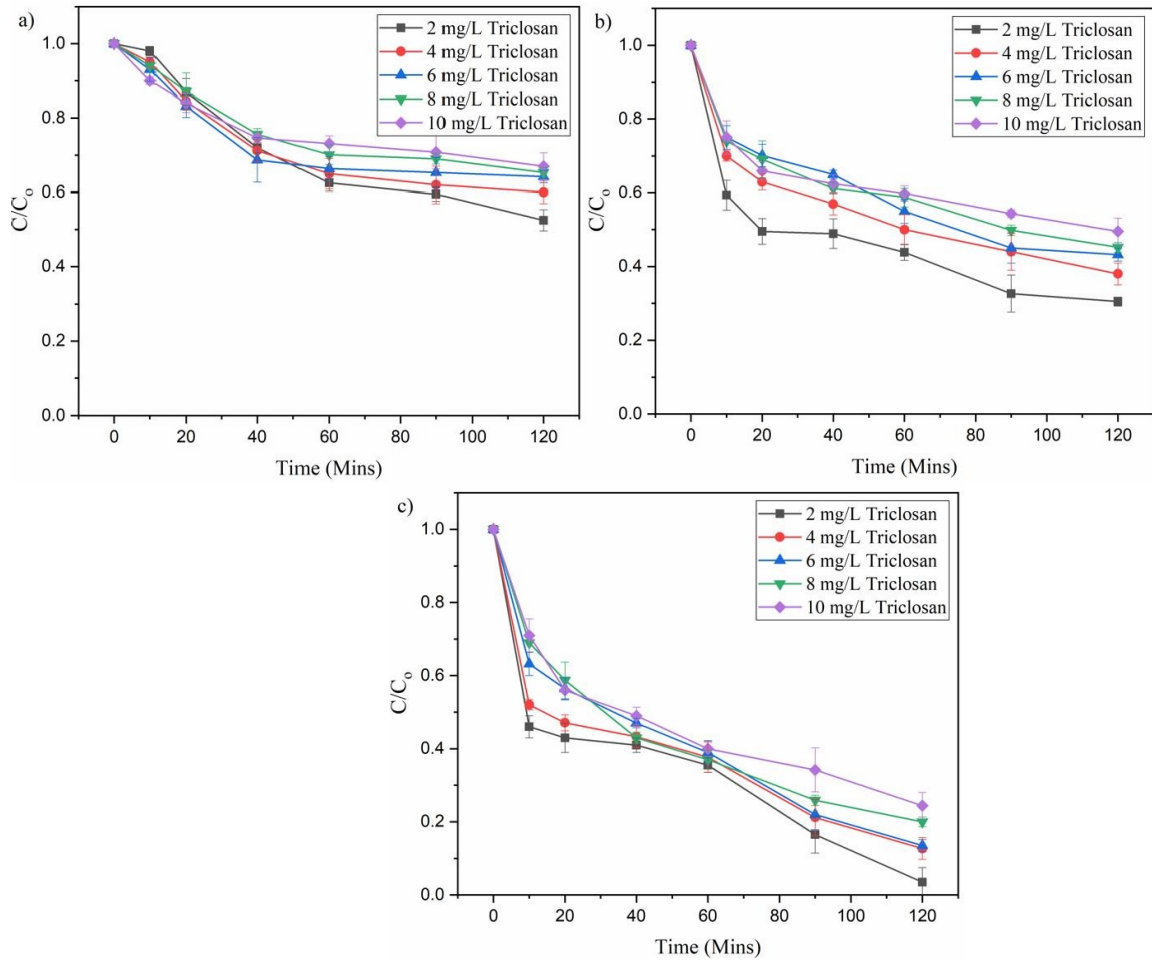


**Figure 4.11: Effect of Initial concentration of Triclosan during Fenton's oxidation with *Psidium guajava* Laterite Iron Oxide Nanoparticles (GPsLaNP)**

#### 4.3.4.2 Effect of Initial Concentration on Fenton's Oxidation Using GMpLaNP

The removal of triclosan at a different initial concentration of triclosan by GMpLaNP is shown in Figure 4.12. Table 4.8 shows the maximum triclosan degradation for different initial triclosan concentrations using GMpLaNP. It is observed that when the concentration of the pollutant is increased, there is a decline in both the removal efficiency and k value.

**Table 4.8: Degradation of Initial concentration of triclosan by GMpLaNP**

Catalyst Loading (g/L)	Initial Concentration of TCS (g/L)	% Removal of TCS	H <sub>2</sub> O <sub>2</sub> Dosage
0.01	2	43	100
	4	41	
	6	38.8	
	8	35.2	
	10	30	
0.1	2	70	400
	4	64.8	
	6	60.5	
	8	57.9	
	10	52.5	
1	2	99.1	300
	4	87.9	
	6	85.5	
	8	80.1	
	10	77	

For GMpLaNP, maximum removal was observed with a 2 mg/L initial concentration of triclosan while with 4 mg/L, 6 mg/L, 8 mg/L, and 10 mg/L the degradation was gradual and considerably low. It is observed that as the concentration increases the removal efficiency decreased, also there is a decline in the rate constant value (Manu and Mahamood, 2011).

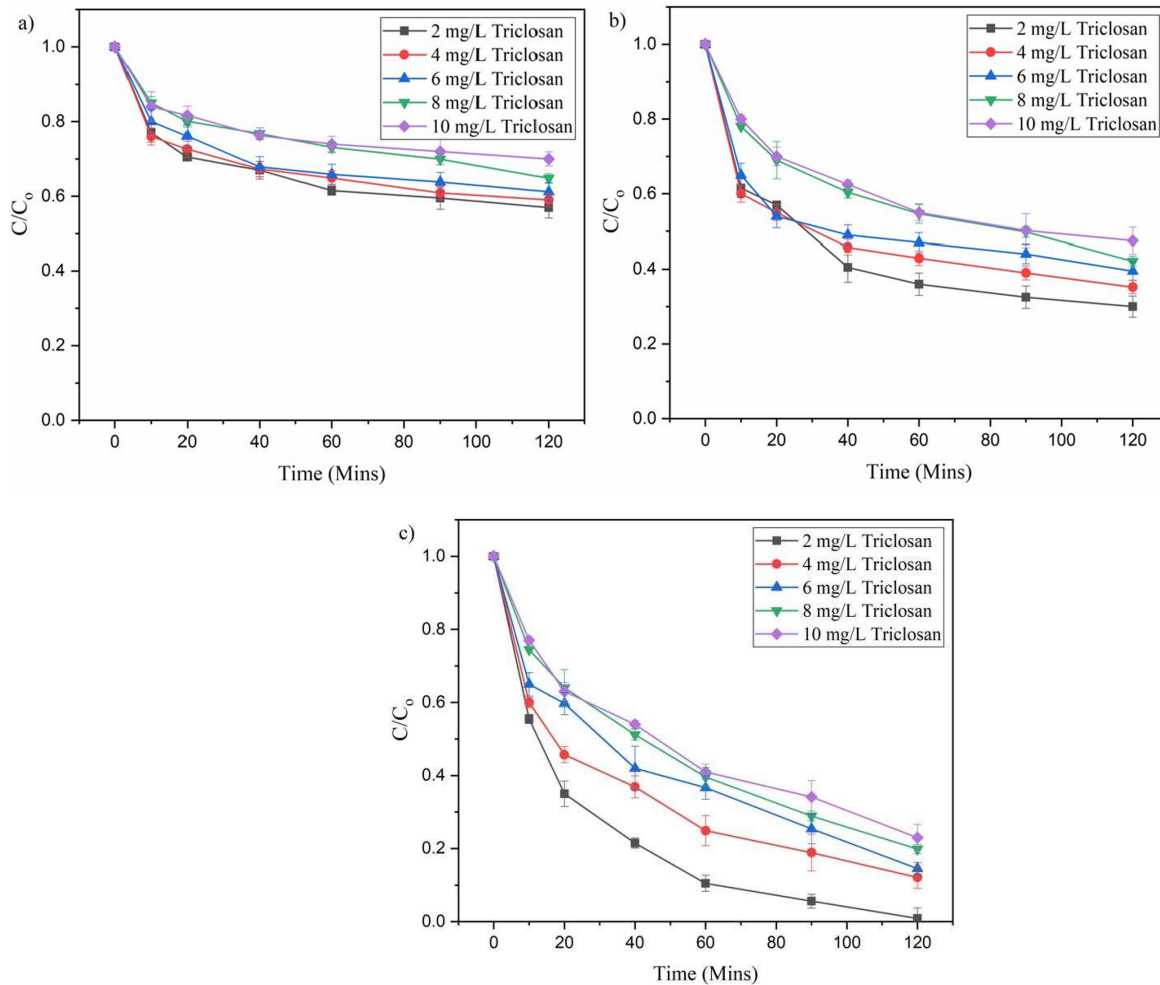


**Figure 4.12: Effect of Initial concentration of Triclosan during Fenton's oxidation with *Macaranga peltata* Laterite Iron Oxide Nanoparticles (GMpLaNP)**

#### 4.3.5 Effect of pH on Fenton's Oxidation of Triclosan

In Fenton's oxidation treatment regulation of pH is very much essential. Fenton's oxidation processes are influenced by the pH of the solution, which affects the hydroxyl radical production rate and  $\text{Fe}^{2+}$  concentration. The different values of pH varied from 3 to 5 were considered for the investigation for the optimization.

A range of pH values from 3 to 5 is used for the oxidation experiments with initial triclosan concentrations of 2mg/L,  $\text{H}_2\text{O}_2 = 300$  mg/L, and synthesized nano iron as 1 g/L. The maximum removal was observed at pH 3. Many studies have proved that the removal of organic contaminants is higher at pH 3 in Fenton's oxidation process (Chaturvedi and Katoch, 2020; Khataee and Pakdehi, 2014).

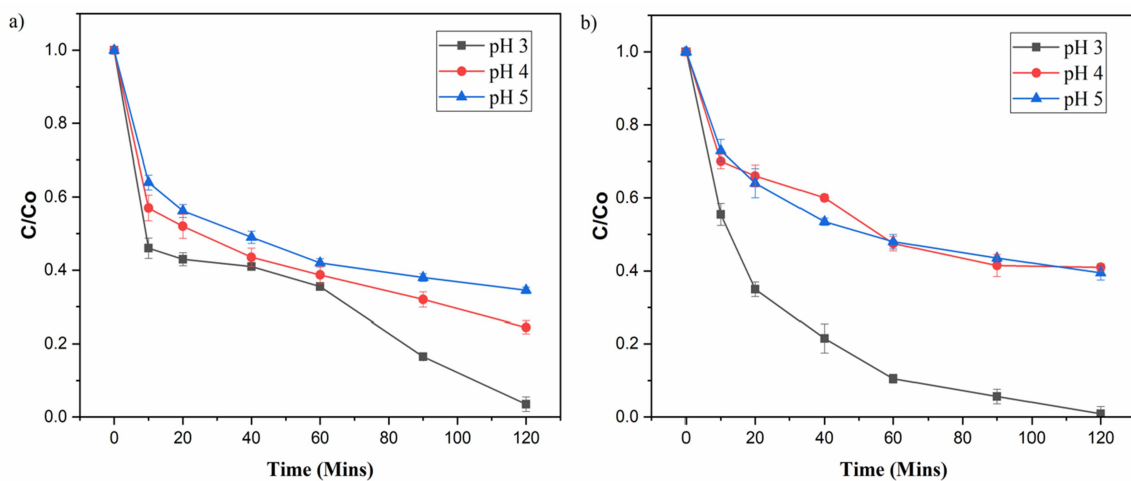


**Figure 4.13: Effect of pH during Fenton's oxidation with a) *Psidium guajava* Laterite Iron Oxide Nanoparticles (GPsLaNP) b) *Macaranga peltata* Laterite Iron Oxide Nanoparticles (GMpLaNP)**

As the pH increases the degradation of triclosan decreases as shown in Figure 4.13 (a) and Figure 4.13 (b) for green synthesized laterite-based *Psidium guajava* nanoparticles and green synthesized laterite-based *Macaranga peltata* nanoparticles respectively. The

degradation of triclosan at different pH using GLaFeNP is presented in Table 4.9. At pH 4 and pH 5, the degradation rate was lesser when compared to pH 3 that is because the number of active sites decreases as there is an increase in pH. At higher pH, the adsorption process takes place, and the generation of •OH radicals is reduced due to the formation of ferric hydroxide complexes, which prevent further reactions (Kuang et al., 2013; Sangami and Manu, 2017).

Ferrous ions are reported to be produced more rapidly at an acidic pH of 3 for GLaFeNP (Shahwan et al., 2011). The hydrated ferrous ions get transformed into the colloidal ferric species forming the ferric hydroxyl complexes at a more neutral pH range. The efficiency gets reduced as the pH gets increases. The pH got varied from 3.0 to 4.4 which favored the oxidation process forming the hydroxyl radicals. (Burbano et al., 2005; Kang and Hwang, 2000). A rise in pH has been detected as a result of ferrous oxidation and ferric precipitation and thereby reducing the treatment efficiency.

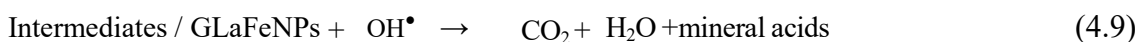
**Table 4.9: Maximum degradation of triclosan at various pH**

GLaNP (1 g/L)	% Removal of TCS		
	pH 3	pH 4	pH 5
GPsLaNP	96.5	75.5	65.5
GMpLaNP	99.1	65.5	59

#### 4.3.6 Effect of Treatment Time on Fenton's Oxidation of Triclosan

In the generation of •OH radicals time also plays an important role in the reaction. The reaction time was varied from 10 to 120 minutes in the present study with the optimum conditions of pH = 3, GLaFeNPs = 1 g/L, and H<sub>2</sub>O<sub>2</sub> = 300mg/L. The maximum degradation occurs within 20 minutes for GPsLaNP and the degradation follows gradually till 120 minutes for the GMpLaNP. Through the process, ferrous iron

concentrations have decreased with GPsLaNP, while ferric iron concentrations have increased. Iron stays in ferric form for the first 20 minutes of the treatment when using GMpLaNP. As a result, leaching and oxidation-reduction occurred continuously throughout the treatment. Degradation may occur due to adsorption, OH radical generation, and mineralization. Initially, the triclosan gets adsorbed to the surface of GLaFeNPs then there will be a generation of •OH radicals followed by mineralization products due to the reaction between triclosan and •OH radicals (Eq (4.4)- Eq(4.9)).



As illustrated in Eq (4.6) the oxidants react with Fe<sub>2</sub>O<sub>3</sub> and Fe<sub>3</sub>O<sub>4</sub> gets oxidized to Fe<sup>2+</sup> and Fe<sup>3+</sup> ions and finally, there will be a release of hydroxyl radicals (Garrido-Ramírez et al., 2010; Sangami and Manu, 2017; Xue et al., 2009). A reaction between OH radicals and triclosan on the surface of GLaFeNPs leads to the mineralization of the compound as shown in Eq (4.8) and Eq (4.9). In the solution, generated Fe<sup>2+</sup> and Fe<sup>3+</sup> react with water to generate oxyhydroxide ((Eq. 10) and Eq (4.11)), which is also able to adsorb triclosan.

#### 4.3.7 Effect of Iron on Fenton's Oxidation of Triclosan

In the Fenton reactions, reactive radicals are generated by redox reactions which involve iron ions, they are the center of Fenton reactions. By complexing iron ions or by changing their redox cycle, organic compounds or their degradation intermediates can affect the activity of iron ions. Figure 4.14, Figure 4.15, and Figure 4.16 represent the

total iron, ferrous, and ferric iron leached out of GLaFeNPs respectively during the treatment process which is proportional to the degradation of triclosan. The results indicate that a maximum of 327mg/L of iron leached out of nanocatalyst at an optimum condition contributed to a maximum of 96.5% triclosan degradation using GPsLaNP and 99.1% removal in GMpLaNP with the liberation of 336mg/L of total iron during the investigation. In the beginning, it was found that the ferrous form of iron was more later it was converted into a ferric form of iron. Initially, the leached ferrous ions produce the hydroxyl radicals and attack the organic pollutants, hence there will be a reduction in the pollutant concentration. There is an inconsistent change in iron form as a result of triclosan degradation. There is a drop in ferrous iron concentration with GPsLaNP while the ferric iron concentration was observed to increase throughout the process. With GMpLaNP as a catalyst, the ferric form of iron remains constant after the first 20 minutes of the treatment. This confirms leaching and oxidation–reduction occurred during the treatment continuously. It is necessary to maintain a high ORP value in Fenton’s oxidation process as a controlling parameter (Wu & Wang, 2012).

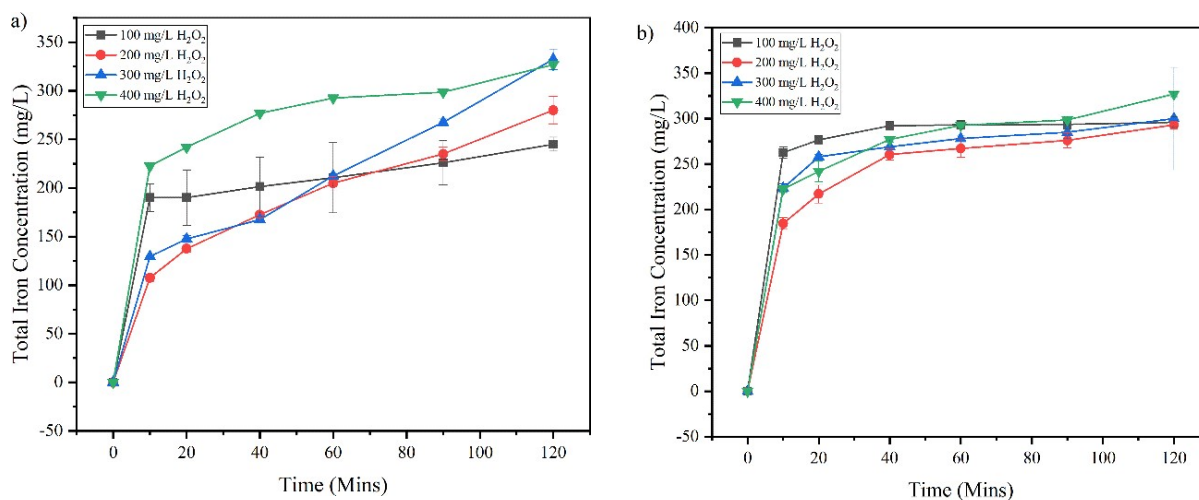


**Figure 4.14: Total Iron variation during Fenton’s oxidation of Triclosan with**  
**a) *Psidium guajava* Laterite Iron Oxide Nanoparticles (GPsLaNP)**  
**b) *Macaranga peltata* Laterite Iron Oxide Nanoparticles (GMpLaNP)**

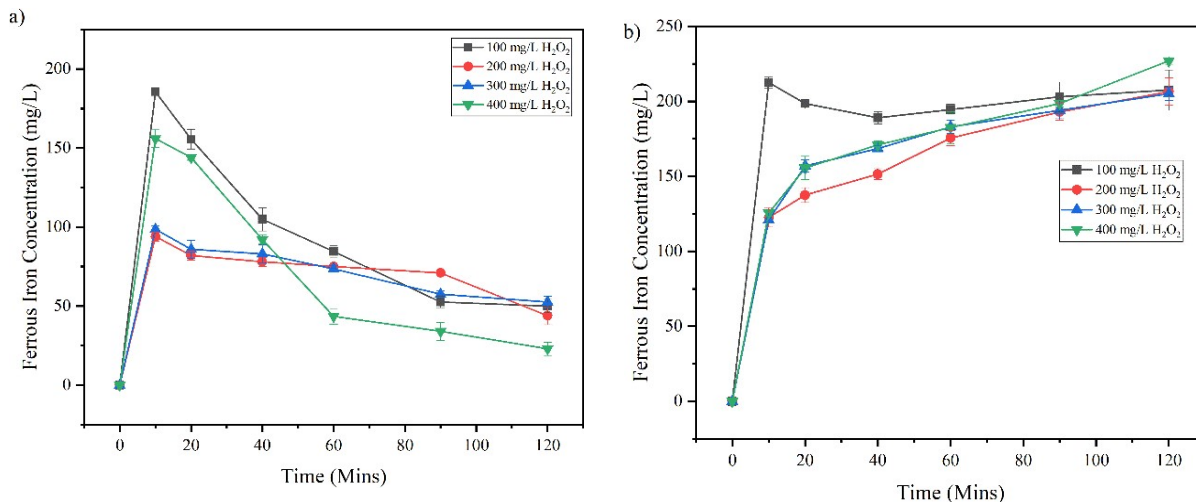


**Figure 4.15: Ferrous Iron variation during Fenton's oxidation of Triclosan with**  
**a) *Psidium guajava* Laterite Iron Oxide Nanoparticles (GPsLaNP)**  
**b) *Macaranga peltata* Laterite Iron Oxide Nanoparticles (GMpLaNP)**

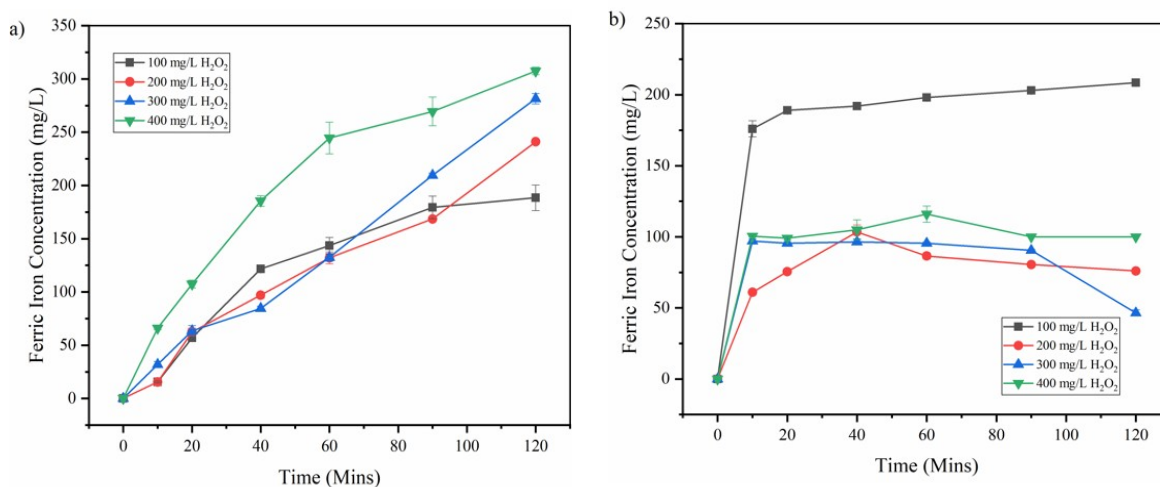


**Figure 4.16: Ferric Iron variation during Fenton's oxidation of Triclosan with**  
**a) *Psidium guajava* Laterite Iron Oxide Nanoparticles (GPsLaNP)**  
**b) *Macaranga peltata* Laterite Iron Oxide Nanoparticles (GMpLaNP)**

#### 4.3.8 Degradation Kinetics

To examine the reaction kinetics involved in the entire treatment process, experiments were performed in optimal conditions of pH= 3, GLaFeNPs = 1 g/L, H<sub>2</sub>O<sub>2</sub> = 300mg/L, then the obtained results were plotted graphically.

The kinetic fit for both iron nanoparticles is shown in figure 4.17 (a) and figure 4.17 (b). The process can be described by a pseudo-first-order rate kinetic model, based on kinetic studies (Boussahel et al., 2007; Chen et al., 2017b; S. Kang et al., 2016) which were done as shown in Eq (4.12).

$$\ln C_0/C = -Kt \quad (4.12)$$

Where  $C_0$  is the concentration of triclosan at t min and C is the initial concentration of triclosan at 0 min. K is a first-order rate constant-- and presents the slope of the decay curve. It is observed that the rate constant for the degradation of triclosan using GPsLaNP and GMpLaNP was 0.0226/min and 0.0355/min with  $R^2$  of 0.9339 and 0.9877 respectively. The result indicates that the degradation efficiency is more using GMpLaNP than GPsLaNP. It has also been reported that other studies on the degradation of triclosan have shown pseudo-first-order kinetic models with rate constants of 0.214 to 0.964/min (Orhon et al., 2017b), 0.083 to 0.092 /min (So et al., 2019), 0.0118 to 0.0457 /Min (Peng et al., 2019).

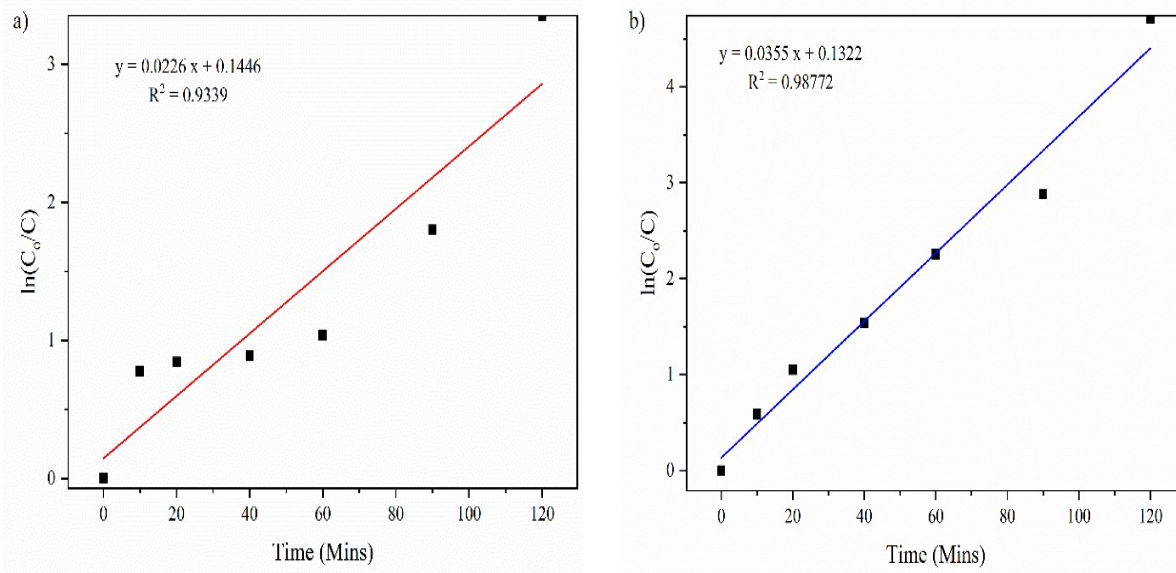


**Figure 4.17: Linear fit for Fenton's oxidation of Triclosan with a) *Psidium guajava* Laterite Iron Oxide Nanoparticle (GPsLaNP) b) *Macaranga peltata* Laterite Iron Oxide Nanoparticle (GMpLaNP)**

During the mineralization process, there will be a generation of byproducts. Sires et al., (2007) investigated the suitability of electro-Fenton's oxidation in the degradation of both triclosan and trichlorocarbon and identified oxalic acid, formic acid, and maleic acid as degradation products with 2,4-dichlorophenol, 4-chlorocatechol, and chlorohydroquinone as hydroxylated derivatives (Sires et al., 2007). Munoz et al., (2012) identified three major degradation compounds on Fenton's oxidation of triclosan and claim p-hydroquinone of triclosan forms when OH radicals attack triclosan in para-position while 2,4- DCP and 4-CC forms when the OH radical attacks to triclosan in the ortho- position leading to the opening of one of the aromatic rings. Chen et al., found the following transformation products during the degradation of triclosan by ozonation were 2,4-dichlorophenol, chloro- catechol, mono-hydroxy-triclosan, and di-hydroxy-triclosan (Chen et al., 2012). A study conducted by Song et al., (2012) found harmful dichlorophenol accumulation. During the electro-Fenton degradation dichlorohydroquinone, 2,4-dichlorophenol, 2,7-dichlorodibenzodioxin were formed as mineralization products

(Espinoza et al., 2019). As per the study conducted by Peng et al., (2016) found eight compounds out of which  $C_{12}H_7O_3Cl_3$ ,  $C_{12}H_7O_4Cl_3$ ,  $C_{12}H_5O_4Cl_3$ ,  $C_{12}H_8O_3Cl_2$ ,  $C_6H_5O_2Cl$ ,  $C_6H_4OCl_2$  are major byproducts.

#### 4.3.9 Reuse and Recoverability Studies

Chemical reactions are driven by catalysts, which are reusable because they are not consumed in the process. The possibility of recovering and reusing the catalyst after separation from the reaction mixture is a key aspect of any catalytic process. In the present study, the reusability of the catalyst was conducted for five cycles.

**Table 4.10: Reusability of GLaFeNPs on Fenton's oxidation of Triclosan**

Cycle	GPsLaNP based Fenton's Oxidation			GMpLaNP based Fenton's Oxidation		
	Triclosan Degradation (%)	k/Min	R <sup>2</sup>	Triclosan Degradation (%)	k/Min	R <sup>2</sup>
1	95.8	0.0225	0.9572	93.0	0.0200	0.9842
2	94.2	0.0202	0.9626	91.0	0.0175	0.9757
3	93.1	0.0207	0.9885	88.0	0.0154	0.9667
4	86.0	0.0171	0.9936	83.0	0.0131	0.9782
5	81.0	0.015	0.9859	81.0	0.0141	0.9902

Recoverability and reuse of spent catalyst studies have been shown in Figures 4.19 (a) and 4.19 (b) for GLaFeNPs. The reusability of Green Laterite-based Iron oxide Nano Particles on Fenton's oxidation of Triclosan is tabulated in Table 4.10. A drop in the degradation efficiency by 15.5% and 18.1% for GPsLaNP and GMpLaNP by the end of the fifth cycle marks the limit of catalyst reuse. It is evident that k and triclosan removal efficiency decreases with increasing cycles. Due to the presence of dissolved oxygen in water, iron corrosion occurs more quickly than in air, and iron hydroxides easily leach out from the nano iron particles. This further attacks the metal inside the core, which

reduces the catalyst's efficiency and results in the loss of metallic iron (Bokare et al., 2008).

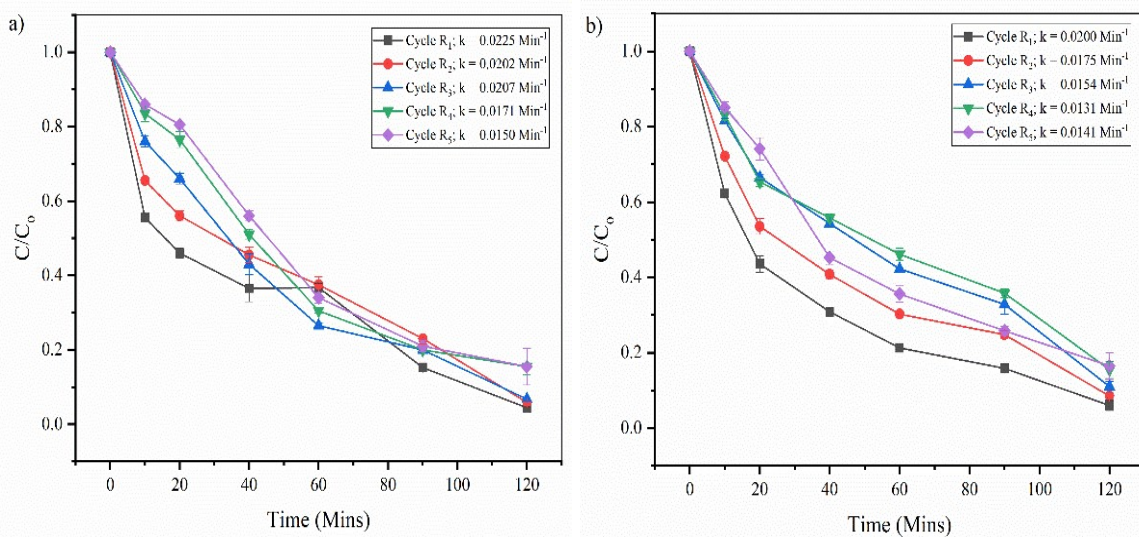


**Figure 4.18: Reusability on Fenton's oxidation of Triclosan with a) *Psidium guajava* Laterite Iron Oxide Nanoparticles (GPsLaNP) b) *Macaranga peltata* Laterite Iron Oxide Nanoparticles (GMpLaNP)**

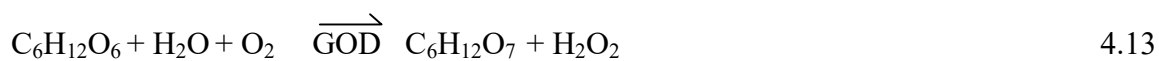
**Table 4.11: Overview of Fenton's oxidation of Triclosan with different iron nanoparticles**

Catalyst	First order kinetics	Triclosan removal (%)	$R^2$
<i>Psidium guajava</i> Iron Oxide Nanoparticles	$y = 0.0226x + 0.1446$	96.5	0.9339
<i>Makaranga Peltata</i> Iron Oxide Nanoparticles	$y = 0.0355x + 0.1322$	99.1	0.98772

#### 4.4 BIO-FENTON'S OXIDATION OF TRICLOSAN

The bio-Fenton processes generate  $H_2O_2$  by oxidizing glucose using glucose oxidase (GOD) as a biocatalyst and then generate hydroxyl radicals by consuming  $H_2O_2$  which reacts with  $Fe^{2+}$ . Fenton's oxidation works well in the acidic pH, which is practically a bit difficult to maintain the same. To overcome this bio-Fenton can be implemented. In

addition to being a sustainable method with lesser power consumption, bio-Fenton has the capability of producing hydrogen peroxide in situ, thereby reducing the overall cost of the process. To generate hydrogen peroxide as a main product or by-product, enzymes like glucose oxidase and alcohol oxidase must be capable to catalyze the reaction. An enzyme called glucose oxidase is most commonly used in the bio-Fenton process, which forms D-glucono-1,5 lactone by oxidizing glucose, as well as hydrogen peroxide as a by-product as shown in Eq (4.13) to Eq (4.15) (Ravi et al., 2020).



In the present study, bio-Fenton was implemented for the optimized condition of the Fenton process. In this process, glucose oxidase in the presence of glucose was applied for in situ production of hydrogen peroxide, and simultaneously hydroxyl radicals produced from Fenton's reaction were used for the degradation of Triclosan.

The optimized condition of Fenton's oxidation was considered for the bio-Fenton process. The parameters considered for this were Glucose concentration (1 – 2 g/L) and glucose oxidase (1000 U/L and 2000 U/L). The effect of substrate concentration, pH, and enzyme concentration was investigated.

#### **4.4.1 Optimization of Hydrogen Peroxide Production from Glucose Oxidase and Glucose**

The different concentrations of glucose oxidase (GOD) and glucose were used for the production of hydrogen peroxide. Figure 4.19 presents hydrogen peroxide production with different concentrations of glucose oxidase and glucose. The production of hydrogen peroxide is increased with the increase in the initial concentration of glucose. It is because glucose can be oxidized stoichiometrically to produce H<sub>2</sub>O<sub>2</sub> due to substrate

availability (Ravi et. al., 2020). The amount of  $H_2O_2$  production increased with time. The  $H_2O_2$  generation was increased with an increase in the glucose concentration. For 1.5 g/L of glucose, 330 mg/L of  $H_2O_2$  was generated with 30 minutes of contact time. As the GOD concentration increased, the production of  $H_2O_2$  also increased. For further study, 1.5 g/L of glucose and 1000U/L of GOD were used. As time increased the production of  $H_2O_2$  reached 2000mg/L for 2 g/L of glucose and 1000U/L of GOD.

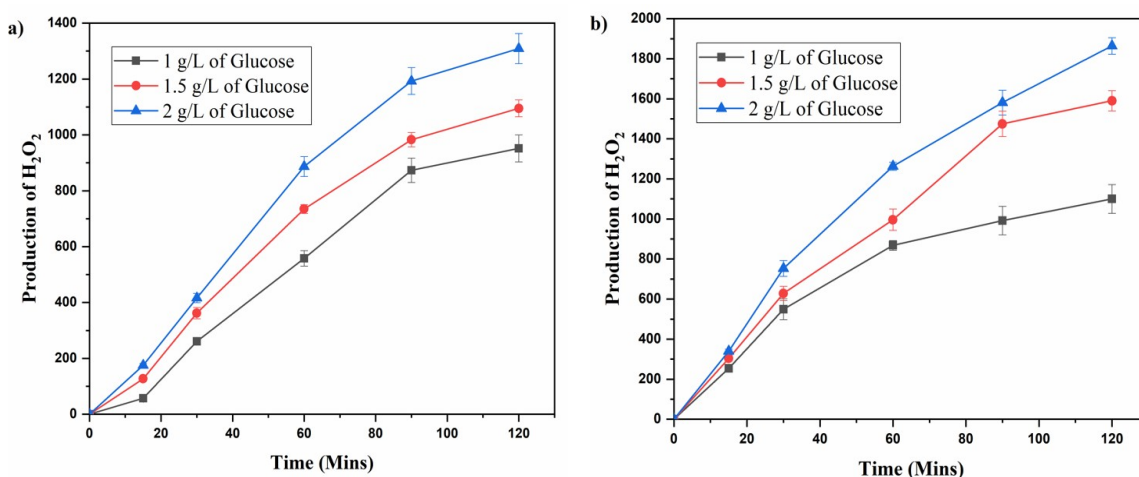


**Figure 4.19: Production of  $H_2O_2$  with different concentrations of glucose**

**(a) 1000U/L Enzyme (b) 2000U/L Enzyme**

#### 4.4.2 Bio Fenton's Process of Triclosan Using GPsLaNP and GMpLaNP

The concentration of Triclosan was taken as 2 mg/ L and catalyst concentration as 1g/L for bio-Fenton's study. Here glucose oxidase with glucose was utilized for the production of hydrogen peroxide. At the same time, the hydroxyl radicals generated were used for the degradation of Triclosan. The oxidative degradation of triclosan by the bio-Fenton process using GLaFeNPs is represented in Figure 4.20. The variation of the pH (3, 5.5, 7) was considered for the degradation study. Fenton's process mainly works on acidic pH to remove the pollutant. At neutral pH, the reaction is occurring due to the availability of  $Fe^{2+}$  due to the chelating effect of gluconic acid (Ravi et al., 2020). The bio-Fenton process provides the platform for the chelation of iron to occur when the GOD is added to glucose. Table 4.12 presents the bio-Fenton's degradation of triclosan using GLaFeNP's.

**Table 4.12: Bio-Fenton's degradation of triclosan at various pH**

GLaFeNP (1 g/L)	% Removal of TCS			Rate Constant /Min		
	pH 3	pH 5.5	pH 7	pH 3	pH 5.5	pH 7
GPsLaNP	35.5	78	59.2	0.0034	0.0119	0.0068
GMpLaNP	47	80.5	60.5	0.0046	0.0133	0.0071

The decrease in reaction rate at pH values higher than 5.5 is due to iron hydroxide ( $\text{Fe}(\text{OH})_3$ ) formation; in this form, iron disintegrates hydrogen peroxide into water and oxygen (Elhami et. al., 2015). On the other hand, the higher and lower pH values disrupt the enzymatic reaction, so there is an optimal pH value of 5.5 for enzyme activity and the degradation process.

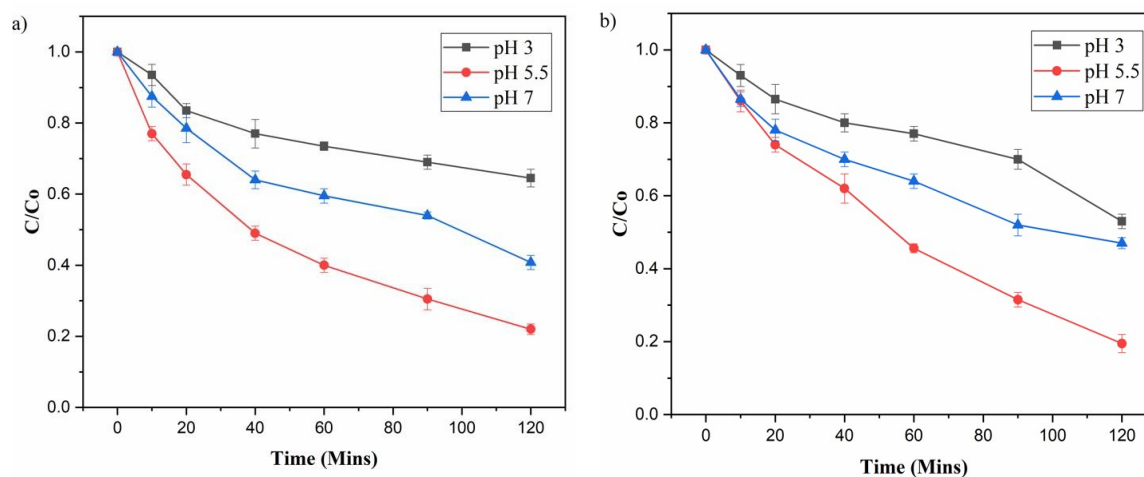


**Figure 4.20: Oxidative degradation of Triclosan by Bio-Fenton process a) *Psidium guajava* Laterite Iron Oxide Nanoparticles (GPsLaNP) b) *Macaranga peltata* Laterite Iron Oxide Nanoparticles (GMpLaNP)**

#### 4.4.3 Degradation Kinetics for Bio-Fenton Process

Further to know the effect of both the nanoparticles, degradation kinetics was studied and it is plotted in Figure 4.20 and was observed to follow the pseudo-first-order kinetics. The

degradation kinetic plot for maximum degradation of Triclosan fitted a pseudo first order kinetic model with an  $R^2$  of 0.9775 and 0.9962 at pH 5.5 for *Psidium guajava* Laterite Iron Oxide Nanoparticles and *Macaranga peltata* Laterite Iron Oxide Nanoparticles respectively. The rate constants obtained are 0.0119/ Min and 0.0133/ Min which are almost equal as shown in Figure 4.21 indicating a less pronounced effect of green synthesized *Psidium guajava* and *Makaranga peltata* iron oxide nanoparticles.

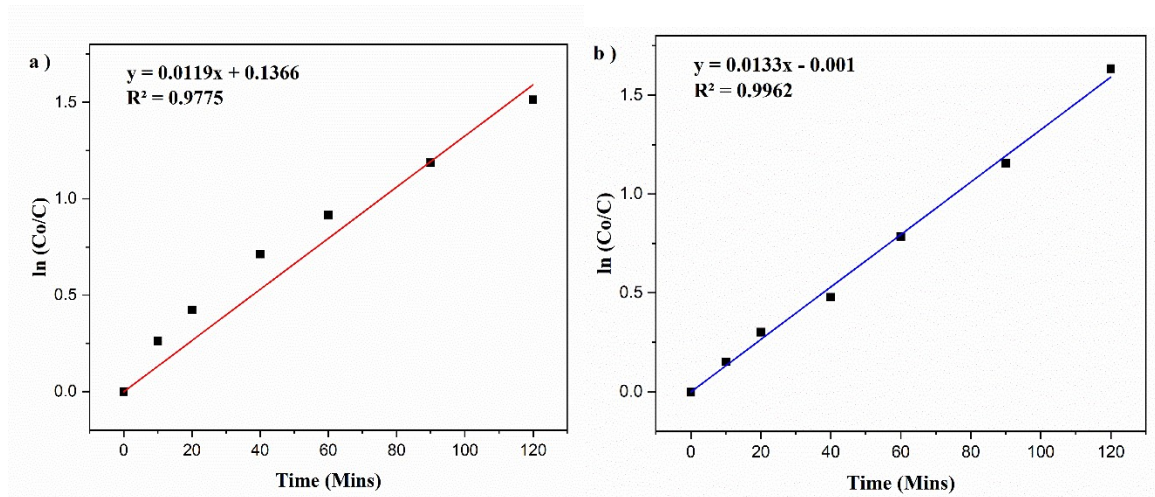


**Figure 4.21: Linear fit for Bio Fenton's oxidation of Triclosan with a) *Psidium guajava* Laterite Iron Oxide Nanoparticles (GPsLaNP) b) *Macaranga peltata* Laterite Iron Oxide Nanoparticles (GMpLaNP)**



## CHAPTER 5

### SUMMARY AND CONCLUSIONS

The iron nanoparticles for Fenton's oxidation application were synthesized using laterite iron as a precursor and *Psidium guajava* and *Macaranga peltata* leaf extracts. The iron nanoparticles are sustainable, because it is synthesized by locally available materials. The synthesized GLaFeNPs were characterized and it was used as a catalyst in the triclosan degradation by Fenton's process. The FESEM analysis found the agglomerated spherical particles arranged in groups for GPsLaNP and agglomerated spherical particles with clear edges for GMpLaNP with 27.6% iron by weight and 19% iron by weight respectively. The BET analysis shows a surface area of 11.76 and 11.707 m<sup>2</sup>/g respectively for GPsLaNP and GMpLaNP. The XRD results confirm the presence of Fe<sub>2</sub>O<sub>3</sub>, Fe<sub>3</sub>O<sub>4</sub> and polyphenols, along with the confirmation of functional groups with FTIR results. Triclosan, an emerging pollutant, has been removed effectively by Fenton-like oxidation. The triclosan was degraded using H<sub>2</sub>O<sub>2</sub> as an oxidizing agent and GLaFeNP as a catalyst. At an acidic pH of 3, maximum degradation of 96.5% and 99.1% was observed for GPsLaNP and GMpLaNP with 1.0 g/L of catalyst load and 300 mg/L of H<sub>2</sub>O<sub>2</sub> with 120 minutes of treatment time. Pseudo 1st order reaction kinetics best fits the triclosan degradation using both catalysts. Total iron, ferrous and ferric iron variation during Fenton's oxidation of triclosan with *Psidium guajava* laterite iron oxide nanoparticles (GPsLaNP) and *Macaranga peltata* laterite iron oxide nanoparticles (GMpLaNP) were studied for the optimized condition. The reusability studies confirm that nanocatalysts are efficient for the usage of up to five consecutive cycles with a drop in degradation efficiency of 15.1% and 18.1% with the fifth cycle. The study confirms the use of green synthesized laterite iron nanoparticles in Fenton's degradation of recalcitrant triclosan. GLaFeNP are eco-friendly, easy to prepare, economical, very efficient and reusable catalyst for the degradation of pollutants. Also from the results it can be concluded that there is no much difference in the degradation using GPsLaNP and GMpLaNP.

The bio-Fenton process is one of the promising methods for the degradation of organic pollutants. In the bio-Fenton process biomaterials are used to generate hydrogen peroxide, which will reduce the stocking and transferring risk. Triclosan is degraded using the bio-Fenton process, which involves enzymatic production of hydrogen peroxide in-situ. In this study, several effective parameters were studied. Bio-Fenton was carried out for the optimized condition by varying the pH, Enzyme concentration, and glucose concentration which proves pH 5.5 as optimum with 80.5% removal of triclosan.

### **Scope for the future work**

There is potential for further research in:

- Application of green synthesized laterite-based iron nanoparticles in bio-Fenton's oxidation can be conducted in detail. In the bio-Fenton process, more studies should be carried out to know the efficiency of the system. The bio-Fenton system can be scaled up for evaluation of commercial application feasibility since this study has been performed at a laboratory scale. Also, the lifetime and stability of the bio-Fenton process can be studied further.
- The application of green synthesized laterite-based iron nanoparticles in electro-Fenton can be studied. In the electro-Fenton process, the hydrogen peroxide is generated at the cathode with the help of oxygen or air. In this the effect of pH, dosage of GLaFeNP, electrode materials, the concentration of hydrogen peroxide, pH, current density, and distance between electrodes can be studied in detail.

## REFERENCES

- Afsheen, S., Tahir, M. B., Iqbal, T., Liaqat, A., and Abrar, M. (2018). “Green synthesis and characterization of novel iron particles by using different extracts”. *Journal of Alloys and Compounds*, 732, 935–944. <https://doi.org/10.1016/j.jallcom.2017.10.137>
- Ahmmad, B., Leonard, K., Shariful Islam, M., Kurawaki, J., Muruganandham, M., Ohkubo, T., and Kuroda, Y. (2013). “Green synthesis of mesoporous hematite ( $\alpha$ -Fe<sub>2</sub>O<sub>3</sub>) nanoparticles and their photocatalytic activity”. *Advanced Powder Technology*, 24(1), 160–167. <https://doi.org/10.1016/j.appt.2012.04.005>
- Akhbari, A., Kutty, P. K., Chuen, O. C., and Ibrahim, S. (2019). “A study of palm oil mill processing and environmental assessment of palm oil mill effluent treatment”. *Environmental Engineering Research*, 25(2), 212–221. <https://doi.org/10.4491/eer.2018.452>
- Allmyr, M., McLachlan, M. S., Sandborgh-Englund, G., and Adolfsson-Erici, M. (2006). “Determination of triclosan as its pentafluorobenzoyl ester in human plasma and milk using electron capture negative ionization mass spectrometry”. *Analytical Chemistry*, 78(18), 6542–6546. <https://doi.org/10.1021/ac060666x>
- American Public Health Association, American Water Works Association, Water Pollution Control Federation, (1992), Standard methods for the examination of Water and Wastewater, 18<sup>th</sup> Edition, Washington, D.C, 440-447.
- Amritha, A. S., and Manu, B. (2018). “Degradation of nitroaromatic compounds: a novel approach using iron from laterite soil”. *Applied Water Science*, 8(5), 2016–2019. <https://doi.org/10.1007/s13201-018-0778-7>
- Anupama and Shrihari S. (2018). “Triclosan Removal from Synthetic Wastewater by Tio<sub>2</sub>/UV and O<sub>3</sub>/UV Processes”. *IOSR Journal of Environmental Science*, 12(3), 17–20. <https://doi.org/10.9790/2402-1203021720>

- Anitha, S., Balu, A. R., Balamurugan, S., Suganya, M., Delci, Z., Karthika, M., Kayathiri, C., and Chitra Devi, S. (2021). “A comparative study on the photocatalytic performance of two third order NLO active nanocomposites (NiO-CdO and NiO-CuO) green synthesized using Psidium guajava leaf extract”. *Inorganic Chemistry Communications*, 134(November), 109073.  
<https://doi.org/10.1016/j.inoche.2021.109073>
- Andrades, J. A., Coello, M. D., Quiroga, J. M., and Lojo-I, M. (2021). “Degradation of simazine by photolysis of hydrogen peroxide Fenton and photo-Fenton under darkness, sunlight and UV light”. *Journal of Water Process Engineering*, 42(March).  
<https://doi.org/10.1016/j.jwpe.2021.102115>
- Arbuckle, T. E., Marro, L., Davis, K., Fisher, M., Ayotte, P., Bélanger, P., Dumas, P., LeBlanc, A., Bérubé, R., Gaudreau, É., Provencher, G., Faustma, E. M., Vigoren, E., Ettinge, A. S., Dellarco, M., MacPherson, S., and Fraser, W. D. (2015). “Exposure to free and conjugated forms of bisphenol a and triclosan among pregnant women in the MIREC cohort”. *Environmental Health Perspectives*, 123(4), 277–284.  
<https://doi.org/10.1289/ehp.1408187>
- Behera, S. K., Oh, S. Y., and Park, H. S. (2010). “Sorption of triclosan onto activated carbon, kaolinite and montmorillonite: Effects of pH, ionic strength, and humic acid”. *Journal of Hazardous Materials*, 179(1–3), 684–691.  
<https://doi.org/10.1016/j.jhazmat.2010.03.056>
- Bester, K. (2005). “Fate of triclosan and triclosan-methyl in sewage treatment plants and surface waters”. *Archives of Environmental Contamination and Toxicology*, 49(1), 9–17. <https://doi.org/10.1007/s00244-004-0155-4>
- Bhaskar, S., Manu, B., and Sreenivasa, M. Y. (2019). “Bacteriological synthesis of iron hydroxysulfate using an isolated Acidithiobacillus ferrooxidans strain and its application in ametryn degradation by Fenton’s oxidation process”. *Journal of*

*Environmental Management*, 232, 236–242.

<https://doi.org/10.1016/j.jenvman.2018.11.048>

Bhaskar, S., Manu, B., and Sreenivasa, M. Y. (2021). “Bioremediation of iron from laterite soil using an isolated *Acidithiobacillus ferrooxidans* strain and application of leached laterite iron as Fenton’s catalyst in selective herbicide degradation”.

*PLOS ONE*, 16(3 March), 1–18. <https://doi.org/10.1371/journal.pone.0243444>

Bokare, A. D., Chikate, R. C., Rode, C. V., and Paknikar, K. M. (2008). “Iron-nickel bimetallic nanoparticles for reductive degradation of azo dye Orange G in aqueous solution”. *Applied Catalysis B: Environmental*, 79(3), 270–278.

<https://doi.org/10.1016/j.apcatb.2007.10.033>

Bolade, O. P., Williams, A. B., and Benson, N. U. (2020). “Green synthesis of iron-based nanomaterials for environmental remediation: A review”. *Environmental Nanotechnology, Monitoring and Management*, 13, 100279.

<https://doi.org/10.1016/j.enmm.2019.100279>

Boukhessaim, S., Gacem, A., Khan, S. H., Amari, A., Yadav, V. K., Harharah, H. N., Elkhaleefa, A. M., Yadav, K. K., Rather, S. U., Ahn, H. J., and Jeon, B. H. (2022). “Emerging Trends in the Remediation of Persistent Organic Pollutants Using Nanomaterials and Related Processes: A Review”. *Nanomaterials*, 12(13), 1–23.

<https://doi.org/10.3390/nano12132148>

Boussahel, R., Harik, D., Mammari, M., and Lamara-mohamed, S. (2007). “Degradation of obsolete DDT by Fenton oxidation with zero-valent iron”. 206(May 2006), 369–

372. <https://doi.org/10.1016/j.desal.2006.04.059>

Burbano, A. A., Dionysiou, D. D., Suidan, M. T., and Richardson, T. L. (2005). “Oxidation kinetics and effect of pH on the degradation of MTBE with Fenton reagent”. *Water*

*Research*, 39(1), 107–118. <https://doi.org/10.1016/j.watres.2004.09.008>

- Buth, J.M; Grandbois, M.; Vikeslan P.J.; McNeill, K.; Arnold, W. A. (2009). “Pharmaceuticals and Personal Care Products in the Environment Aquatic Photochemistry of Chlorinated Triclosan Derivatives: Potential Source of Polychlorodibenzo- P –Dioxins”. *Environmental Toxicology and Chemistry*, 28(12), 2555–2563.
- Calafat, A. M., Ye, X., Wong, L. Y., Reidy, J. A., and Needham, L. L. (2008). “Urinary concentrations of triclosan in the U.S. population: 2003-2004”. *Environmental Health Perspectives*, 116(3), 303–307. <https://doi.org/10.1289/ehp.10768>
- Chalew, T. E. A., and Halden, R. U. (2009). “Environmental exposure of aquatic and terrestrial biota to triclosan and triclocarban”. *Journal of the American Water Resources Association*, 45(1), 4–13. <https://doi.org/10.1111/j.1752-1688.2008.00284.x>
- Chandra Pragada, S., and Thalla, A. K. (2021). “Polymer-based immobilized Fe<sub>2</sub>O<sub>3</sub>–TiO<sub>2</sub>/PVP catalyst preparation method and the degradation of triclosan in treated greywater effluent by solar photocatalysis”. *Journal of Environmental Management*, 296(July), 113305. <https://doi.org/10.1016/j.jenvman.2021.113305>
- Chaturvedi, N. K., and Katoch, S. S. (2020). “Evaluation and comparison of Fenton-like oxidation with Fenton’s oxidation for hazardous methoxyanilines in aqueous solution”. *Journal of Industrial and Engineering Chemistry*, 92, 101–108. <https://doi.org/10.1016/j.jiec.2020.08.028>
- Chen, F., Xie, S., Huang, X., and Qiu, X. (2017). “Ionothermal synthesis of Fe<sub>3</sub>O<sub>4</sub> magnetic nanoparticles as efficient heterogeneous Fenton-like catalysts for degradation of organic pollutants with H<sub>2</sub>O<sub>2</sub>”. *Journal of Hazardous Materials*, 322, 152–162. <https://doi.org/10.1016/j.jhazmat.2016.02.073>
- Chen, J., Qu, R., Pan, X., and Wang, Z. (2016). “Oxidative degradation of triclosan by potassium permanganate: Kinetics, degradation products, reaction mechanism, and

- toxicity evaluation”. *Water Research*, 103, 215–223. <https://doi.org/10.1016/j.watres.2016.07.041>
- Chen, X., Richard, J., Liu, Y., Dopp, E., Tuerk, J., and Bester, K. (2012). “Ozonation products of triclosan in advanced wastewater treatment”. *Water Research*, 46(7), 2247–2256. <https://doi.org/10.1016/j.watres.2012.01.039>
- Constantin, L. A., Nitoi, I., Cristea, N. I., and Constantin, M. A. (2018). “Possible degradation pathways of triclosan from aqueous systems via TiO<sub>2</sub> assisted photocatalysis”. *Journal of Industrial and Engineering Chemistry*, 58, 155–162. <https://doi.org/10.1016/j.jiec.2017.09.020>
- Cusioli, L. F., Quesada, H. B., Barbosa de Andrade, M., Gomes, R. G., and Bergamasco, R. (2021). “Application of a novel low-cost adsorbent functioned with iron oxide nanoparticles for the removal of triclosan present in contaminated water”. *Microporous and Mesoporous Materials*, 325(June). <https://doi.org/10.1016/j.micromeso.2021.111328>
- Dann, A. B., and Hontela, A. (2011). “Triclosan: Environmental exposure, toxicity and mechanisms of action”. *Journal of Applied Toxicology*, 31(4), 285–311. <https://doi.org/10.1002/jat.1660>
- Dayan, A. D. (2007). “Risk assessment of triclosan [Irgasan®] in human breast milk”. *Food and Chemical Toxicology*, 45(1), 125–129. <https://doi.org/10.1016/j.fct.2006.08.009>
- Desbrow, C. E. J. R., Routledge, E. J., Brighty, G. C., Sumpter, J. P., and Waldock, M. (1998). “Identification of estrogenic chemicals in STW effluent. 1. Chemical fractionation and in vitro biological screening”. *Environmental science and technology*, 32(11), 1549-1558.
- Devatha, C. P., Thalla, A. K., and Katte, S. Y. (2016). “Green synthesis of iron

- nanoparticles using different leaf extracts for treatment of domestic waste water”. *Journal of Cleaner Production*, 139, 1425–1435.
- Dhillon G.S., Kaur S., Pulicharla R, Brar S.K., Cledón , Verma M, Surampalli R.Y., (2015), "Triclosan: Current Status, Occurrence, Environmental Risks and Bioaccumulation Potential", *Int. J. Environ. Res. Public Health*, 12, 5657-5684
- Eisenberg, G. M. (1943). “Colorimetric Determination of Hydrogen Peroxide”. *Industrial and Engineering Chemistry*, 327–328.
- Elhami, V., and Karimi, A. (2017). “*Advances in Environmental Technology Preparation of Kissiris / TiO<sub>2</sub> / Fe<sub>3</sub>O<sub>4</sub> / GOx biocatalyst : Feasibility study of MG decolorization*”. 3(2016), 111–117.
- Elhami, V., Karimi, A., and Aghbolaghy, M. (2015). “Preparation of heterogeneous bio-Fenton catalyst for decolorization of Malachite Green”. *Journal of the Taiwan Institute of Chemical Engineers*, 56, 154–159. <https://doi.org/10.1016/j.jtice.2015.05.006>
- Ertit Taştan, B., and Dönmez, G. (2015). “Biodegradation of pesticide triclosan by *A. Versicolor* in simulated wastewater and semi-synthetic media”. *Pesticide Biochemistry and Physiology*, 118, 33–37. <https://doi.org/10.1016/j.pestbp.2014.11.002>
- Eskandarian, M., Mahdizadeh, F., Ghalamchi, L., and Naghavi, S. (2014). “Bio-Fenton process for Acid Blue 113 textile azo dye decolorization: Characteristics and neural network modeling”. *Desalination and Water Treatment*, 52(25–27), 4990–4998. <https://doi.org/10.1080/19443994.2013.810325>
- Fernandes, M., Shareef, A., Kookana, R., Gaylard, S., Hoare, S., and Kildea, T. (2011). “The distribution of triclosan and methyl-triclosan in marine sediments of Barker Inlet, South Australia”. *Journal of Environmental Monitoring*, 13(4), 801–806.

<https://doi.org/10.1039/c0em00612b>

- Fidelis, M. Z., Abreu, E., Dos Santos, O. A. A., Chaves, E. S., Brackmann, R., Dias, D. T., and Lenzi, G. G. (2019). “Experimental design and optimization of triclosan and 2,8-diclorodibenzeno-p-dioxina degradation by the Fe/Nb<sub>2</sub>O<sub>5</sub>/UV system”. *Catalysts*, 9(4), 1–18. <https://doi.org/10.3390/catal9040343>
- Folmar, L. C., Denslow, N. D., Rao, V., Chow, M., Crain, D. A., Enblom, J., Marcino, J., and Guillette Jr, L. J. (1996). “Vitellogenin induction and reduced serum testosterone concentrations in feral male carp (*Cyprinus carpio*) captured near a major metropolitan sewage treatment plant”. *Environmental Health Perspectives*, 104(10), 1096–1101.
- Gao, J. F., Wu, Z. L., Duan, W. J., and Zhang, W. Z. (2019). “Simultaneous adsorption and degradation of triclosan by Ginkgo biloba L. stabilized Fe/Co bimetallic nanoparticles”. *Science of the Total Environment*, 662, 978–989. <https://doi.org/10.1016/j.scitotenv.2019.01.194>
- García-Espinoza, J. D., Robles, I., Gil, V., Becerril-Bravo, E., Barrios, J. A., and Godínez, L. A. (2019). “Electrochemical degradation of triclosan in aqueous solution. A study of the performance of an electro-Fenton reactor”. *Journal of Environmental Chemical Engineering*, 7(4), 103228. <https://doi.org/10.1016/j.jece.2019.103228>
- Garrido-Ramírez, E. G., Theng, B. K. G., and Mora, M. L. (2010). “Clays and oxide minerals as catalysts and nanocatalysts in Fenton-like reactions - A review”. *Applied Clay Science*, 47(3–4), 182–192. <https://doi.org/10.1016/j.clay.2009.11.044>
- Groiss, S., Selvaraj, R., Varadavenkatesan, T., and Vinayagam, R. (2017). “Structural characterization, antibacterial and catalytic effect of iron oxide nanoparticles synthesised using the leaf extract of *Cynometra ramiflora*”. *Journal of Molecular Structure*, 1128, 572–578. <https://doi.org/10.1016/j.molstruc.2016.09.031>

- Heidler, J., and Halden, R. U. (2007). “Mass balance assessment of triclosan removal during conventional sewage treatment”. *Chemosphere*, 66(2), 362–369. <https://doi.org/10.1016/j.chemosphere.2006.04.066>.
- Hernández-Leal, L., Temmink, H., Zeeman, G., and Buisman, C. J. N. (2011). “Removal of micropollutants from aerobically treated grey water via ozone and activated carbon”. *Water Research*, 45(9), 2887–2896. <https://doi.org/10.1016/j.watres.2011.03.009>
- Huber, D. L. (2005). “Synthesis, properties, and applications of iron nanoparticles”. *Small*, 1(5), 482–501. <https://doi.org/10.1002/smll.200500006>
- Ibrahim, R. K., Hayyan, M., AlSaadi, M. A., Hayyan, A., and Ibrahim, S. (2016). “Environmental application of nanotechnology: air, soil, and water”. *Environmental Science and Pollution Research*, 23(14), 13754–13788. <https://doi.org/10.1007/s11356-016-6457-z>
- Ikehata, K., El-Din, M. G., and Snyder, S. A. (2008). “Ozonation and advanced oxidation treatment of emerging organic pollutants in water and wastewater”. *Ozone: Science and Engineering*, 30(1), 21–26. <https://doi.org/10.1080/01919510701728970>
- Ikehata, K., Jodeiri Naghashkar, N., and Gamal El-Din, M. (2006). “Degradation of aqueous pharmaceuticals by ozonation and advanced oxidation processes: A review”. *Ozone: Science and Engineering*, 28(6), 353–414. <https://doi.org/10.1080/01919510600985937>
- Inaba, K., Doi, T., Isobe, N., and Yamamoto, T. (2006). “Formation of bromo-substituted triclosan during chlorination by chlorine in the presence of trace levels of bromide”. *Water Research*, 40(15), 2931–2937. <https://doi.org/10.1016/j.watres.2006.05.031>
- Jagini, S., Konda, S., Bhagawan, D., and Himabindu, V. (2019). “Emerging contaminant (triclosan) identification and its treatment: a review”. *SN Applied Sciences*, 1(6), 1–

15. <https://doi.org/10.1007/s42452-019-0634-x>

Jobling, S., Nolan, M., Tyler, C. R., Brighty, G., and Sumpter, J. P. (1998). “Widespread sexual disruption in wild fish”. *Environmental Science and Technology*, 32(17), 2498–2506. <https://doi.org/10.1021/es9710870>

Kahoush, M., Behary, N., Cayla, A., and Nierstrasz, V. (2018). “Bio-Fenton and Bio-electro-Fenton as sustainable methods for degrading organic pollutants in wastewater”. *Process Biochemistry*, 64 (September 2017), 237–247. <https://doi.org/10.1016/j.procbio.2017.10.003>

Kang, S., Liu, S., Wang, H., and Cai, W. (2016). “Enhanced degradation performances of plate like micro / nanostructured zero valent iron to DDT”. *Journal of Hazardous Materials*, 307, 145–153. <https://doi.org/10.1016/j.jhazmat.2015.12.063>

Kang, Y. U. N. W., and Hwang, K. (2000). “Effects of Reaction conditions on the oxidation efficiency in the Fenton Process”. *Wat. Res.*, 34(10), 2786–2790.

Karale, R., Manu, B., and Shrihari, S. (2013). “Degradation of toxic 2-aminopyridine pharmaceutical compound from aqueous environments using advanced Fenton and photo-Fenton oxidation processes”. *Int J Adv Technol Civ Eng*, 2, 34-38.

Karimi, A., Aghbolaghy, M., Khataee, A., and Shoa Bargh, S. (2012). “Use of enzymatic bio-fenton as a new approach in decolorization of malachite green”. *The Scientific World Journal*, 2012(1). <https://doi.org/10.1100/2012/691569>

Kasthurba, A. K., Santhanam, M., and Achyuthan, H. (2008). “Investigation of laterite stones for building purpose from Malabar region, Kerala, SW India - Chemical analysis and microstructure studies”. *Construction and Building Materials*, 22(12), 2400–2408. <https://doi.org/10.1016/j.conbuildmat.2006.12.003>

Khan, E., Wirojanagud, W., and Sermsai, N. (2009). “Effects of iron type in Fenton reaction on mineralization and biodegradability enhancement of hazardous organic

- compounds”. *Journal of Hazardous Materials*, 161(2–3), 1024–1034.  
<https://doi.org/10.1016/j.jhazmat.2008.04.049>
- Khataee, A. R., and Pakdehi, S. G. (2014). “Removal of sodium azide from aqueous solution by Fenton-like process using natural laterite as a heterogeneous catalyst: Kinetic modeling based on nonlinear regression analysis”. *Journal of the Taiwan Institute of Chemical Engineers*, 45(5), 2664–2672.  
<https://doi.org/10.1016/j.jtice.2014.08.007>
- Khataee, A., Salahpour, F., Fathinia, M., Seyyedi, B., and Vahid, B. (2015). “Iron rich laterite soil with mesoporous structure for heterogeneous Fenton-like degradation of an azo dye under visible light”. *Journal of Industrial and Engineering Chemistry*, 26, 129–135. <https://doi.org/10.1016/j.jiec.2014.11.024>
- Klamerth, N., Miranda, N., Malato, S., Agüera, A., Fernández-Alba, A. R., Maldonado, M. I., and Coronado, J. M. (2009). “Degradation of emerging contaminants at low concentrations in MWTPs effluents with mild solar photo-Fenton and TiO<sub>2</sub>”. *Catalysis Today*, 144(1–2), 124–130. <https://doi.org/10.1016/j.cattod.2009.01.024>
- Klamerth, N., Rizzo, L., Malato, S., Maldonado, M. I., Agüera, A., and Fernández-Alba, A. R. (2010). “Degradation of fifteen emerging contaminants at µg/L–1 initial concentrations by mild solar photo-Fenton in MWTP effluents”. *Water Research*, 44(2), 545–554. <https://doi.org/10.1016/j.watres.2009.09.059>
- Klavarioti, M., Mantzavinos, D. and Kassinos, D. (2009). “Removal of residual pharmaceuticals from aqueous systems by advanced oxidation processes”. *Environment international*, 35 (2). pp. 402–417.
- Kuang, Y., Wang, Q., Chen, Z., Megharaj, M., and Naidu, R. (2013). “Heterogeneous Fenton-like oxidation of monochlorobenzene using green synthesis of iron nanoparticles”. *Journal of Colloid and Interface Science*, 410, 67–73.  
<https://doi.org/10.1016/j.jcis.2013.08.020>

- Kumar K.R, Rohini P., Md A.R., Devi Y.P., (2015), "A Review on Occurrence, Fate And Toxicity Of Triclosan", 4(07), 336-369
- Langdon, K. A., Warne, M. S. J., Smernik, R. J., Shareef, A., and Kookana, R. S. (2012). "Field dissipation of 4-nonylphenol, 4-t-octylphenol, triclosan and bisphenol A following land application of biosolids". *Chemosphere*, 86(10), 1050–1058. <https://doi.org/10.1016/j.chemosphere.2011.11.057>
- Lee, D. G., Zhao, F., Rezenom, Y. H., Russell, D. H., and Chu, K. H. (2012). "Biodegradation of triclosan by a wastewater microorganism". *Water Research*, 46(13), 4226–4234. <https://doi.org/10.1016/j.watres.2012.05.025>
- Li, M., Xu, G., Guan, Z., Wang, Y., Yu, H., and Yu, Y. (2019). "Synthesis of Ag/BiVO<sub>4</sub>/rGO composite with enhanced photocatalytic degradation of triclosan". *Science of the Total Environment*, 664, 230–239. <https://doi.org/10.1016/j.scitotenv.2019.02.027>
- Lin, Y., Jin, X., Owens, G., and Chen, Z. (2019). "Simultaneous removal of mixed contaminants triclosan and copper by green synthesized bimetallic iron/nickel nanoparticles". *Science of the Total Environment*, 695, 133878. <https://doi.org/10.1016/j.scitotenv.2019.133878>
- Lindström, A., Buerge, I. J., Poiger, T., Bergqvist, P. A., Müller, M. D., and Buser, H. R. (2002). "Occurrence and environmental behavior of the bactericide triclosan and its methyl derivative in surface waters and in wastewater". *Environmental Science and Technology*, 36(11), 2322–2329. <https://doi.org/10.1021/es0114254>
- Liu, B., and Liu, X. (2004). "Direct photolysis of estrogens in aqueous solutions". *Science of the Total Environment*, 320(2–3), 269–274.
- Liu, H., Cao, X., Liu, G., Wang, Y., Zhang, N., Li, T., and Tough, R. (2013). "Photoelectrocatalytic degradation of triclosan on TiO<sub>2</sub> nanotube arrays and toxicity

change”. *Chemosphere*, 93(1), 160–165.  
<https://doi.org/10.1016/j.chemosphere.2013.05.018>

Liu, J., Wang, J., Zhao, C., Hay, A. G., Xie, H., and Zhan, J. (2016). “Triclosan removal in wetlands constructed with different aquatic plants”. *Applied Microbiology and Biotechnology*, 100(3), 1459–1467. <https://doi.org/10.1007/s00253-015-7063-6>

Liu, Y., Zhu, X., Qian, F., Zhang, S., and Chen, J. (2014). “Magnetic activated carbon prepared from rice straw-derived hydrochar for triclosan removal”. *RSC Advances*, 4(109), 63620–63626. <https://doi.org/10.1039/c4ra11815d>

Luo, C., Ma, J., Jiang, J., Guan, C., Pang, S., Shi, Y., Zhai, X., and Wu, D. (2017). “Degradation of triclosan by UV/H<sub>2</sub>O<sub>2</sub>: Kinetics and reaction mechanism”. 49, 26–31. <https://doi.org/10.11918/j.issn.0367-6234.2017.02.005>

Luo, Z., He, Y., Zhi, D., Luo, L., Sun, Y., Khan, E., Wang, L., Peng, Y., Zhou, Y., and Tsang, D. C. W. (2019). “Current progress in treatment techniques of triclosan from wastewater: A review”. *Science of the Total Environment*, 696, 133990. <https://doi.org/10.1016/j.scitotenv.2019.133990>

M. Verma, P. V. Raj, H. R. Chandrasekhar, J. V. Rao and N. Udupa, "Screening of plant *Macaranga peltata* for its antioxidant, antimicrobial and cytotoxicity activity," 2009 International Conference on Biomedical and Pharmaceutical Engineering, 2009, pp. 1-3, doi: 10.1109/ICBPE.2009.5384086.

Madubuonu, N., Aisida, S. O., Ahmad, I., Botha, S., Zhao, T. kai, Maaza, M., and Ezema, F. I. (2020). “Bio-inspired iron oxide nanoparticles using *Psidium guajava* aqueous extract for antibacterial activity”. *Applied Physics A: Materials Science and Processing*, 126(1), 1–8. <https://doi.org/10.1007/s00339-019-3249-6>

Malakootian, M., Yaseri, M., and Faraji, M. (2019). “Removal of antibiotics from aqueous solutions by nanoparticles: a systematic review and meta-analysis”. *Environmental*

*Science and Pollution Research*, 26(9), 8444–8458. <https://doi.org/10.1007/s11356-019-04227-w>

Malato, S., Blanco, J., Alarcón, D. C., Maldonado, M. I., Fernández-Ibáñez, P., and Gernjak, W. (2007). “Photocatalytic decontamination and disinfection of water with solar collectors”. *Catalysis Today*, 122(1–2), 137–149. <https://doi.org/10.1016/j.cattod.2007.01.034>

Manu, B., and Mahamood, S. (2011). “Enhanced degradation of paracetamol by UV-C supported photo-Fenton process over Fenton oxidation”. *Water Science and Technology*, 64(12), 2433–2438. <https://doi.org/10.2166/wst.2011.804>

Martínez-Zapata, M., Aristizábal, C., and Peñuela, G. (2013). “Photodegradation of the endocrine-disrupting chemicals 4n-nonylphenol and triclosan by simulated solar UV irradiation in aqueous solutions with Fe(III) and in the absence/presence of humic acids”. *Journal of Photochemistry and Photobiology A: Chemistry*, 251, 41–49. <https://doi.org/10.1016/j.jphotochem.2012.10.009>

Martínez, S., Morales-Mejía, J. C., Hernández, P. P., Santiago, L., and Almanza, R. (2014). “Solar photocatalytic oxidation of Triclosan with TiO<sub>2</sub> immobilized on volcanic porous stones on a CPC pilot scale reactor”. *Energy Procedia*, 57(55), 3014–3020. <https://doi.org/10.1016/j.egypro.2014.10.337>

Mellon, M.G. and Woods, J.T., (1941). “Thiocyanate Method for Iron: A Spectrophotometric Study”. *Industrial and Engineering Chemistry Analytical Edition*, 13, 551-554.

Meenakshi Verma, N. K., Thakar, M., Subrahmanyam, V. M., Rao, V., and Dhanaraj Vasant Raj P, S. A. (2013). “Investigation of Anti Bacterial and Anti Fungal Potentials of Macaranga Peltata”. *International Journal of Current Research and Review*, 5(7), 26–32.

- Methatham, T., Ratanatamskul, C., and Lu, M. C. (2012). "Oxidation of 2,4,4'-trichloro-2'-hydroxydiphenyl ether (triclosan) by Fenton's reagents with the electrochemical system". *Sustainable Environment Research*, 22(6), 371–377.
- Mondal, P., Anweshan, A., and Purkait, M. K. (2020). "Green synthesis and environmental application of iron-based nanomaterials and nanocomposite: A review". *Chemosphere*, 259, 127509. <https://doi.org/10.1016/j.chemosphere.2020.127509>
- Moustafa, M., and Shams Al Din, R. (2017). "Green Synthesis and Characterization of Iron-Oxide Nanoparticles By Guava Aqueous Leaves Extract for Doxorubicin Drug Loading". *Journal of Bioscience and Applied Research*, 3(4), 177–180. <https://doi.org/10.21608/jbaar.2017.126138>
- Munoz, M., de Pedro, Z. M., Casas, J. A., and Rodriguez, J. J. (2012). "Triclosan breakdown by Fenton-like oxidation". *Chemical Engineering Journal*, 198–199, 275–281. <https://doi.org/10.1016/j.cej.2012.05.097>
- Mutiyar, P. K., Gupta, S. K., and Mittal, A. K. (2018). "Fate of pharmaceutical active compounds (PhACs) from River Yamuna, India: An ecotoxicological risk assessment approach". *Ecotoxicology and Environmental Safety*, 150(August 2017), 297–304. <https://doi.org/10.1016/j.ecoenv.2017.12.041>
- Nakada, N., Shinohara, H., Murata, A., Kiri, K., Managaki, S., Sato, N., and Takada, H. (2007). "Removal of selected pharmaceuticals and personal care products (PPCPs) and endocrine-disrupting chemicals (EDCs) during sand filtration and ozonation at a municipal sewage treatment plant". *Water Research*, 41(19), 4373–4382. <https://doi.org/10.1016/j.watres.2007.06.038>
- Neyens, E., and Baeyens, J. (2003). "A review of classic Fenton's peroxidation as an advanced oxidation technique". *Journal of Hazardous Materials*, 98(1–3), 33–50. [https://doi.org/10.1016/S0304-3894\(02\)00282-0](https://doi.org/10.1016/S0304-3894(02)00282-0)

- Okutverici, A., Yilmaz, L., Yetis, U., and Dilek, F. B. (2016). "Triclosan removal by NF from a real drinking water source - Effect of natural organic matter". *Chemical Engineering Journal*, 283, 330–337. <https://doi.org/10.1016/j.cej.2015.07.065>
- Okuda, T., Kobayashi, Y., Nagao, R., Yamashita, N., Tanaka, H., Tanaka, S., Fujii, S., Konishi, C. and Houwa, I. (2008). "Removal efficiency of 66 pharmaceuticals during wastewater treatment process in Japan". *Water Science and Technology*, 57 (1). pp. 65–71.
- Oliveira, R., Domingues, I., Grisolia, C. K., and Soares, A. M. V. M. (2009). "Effects of triclosan on zebrafish early-life stages and adults". *Environmental Science and Pollution Research*, 16(6), 679–688. <https://doi.org/10.1007/s11356-009-0119-3>
- Orhon, K. B., Orhon, A. K., Dilek, F. B., and Yetis, U. (2017). "Triclosan removal from surface water by ozonation - Kinetics and by-products formation". *Journal of Environmental Management*, 204, 327–336. <https://doi.org/10.1016/j.jenvman.2017.09.02>
- Orvos, D. R., Versteeg, D. J., Inauen, J., Capdevielle, M., Rothenstein, A., and Cunningham, V. (2002). "Aquatic toxicity of triclosan". *Environmental Toxicology and Chemistry*, 21(7), 1338–1349. <https://doi.org/10.1002/etc.5620210703>
- Öztamer, M., and Çokay, E. (2017). "Degradation of Triclosan by Photo-Fenton like Oxidation". *Deu Muhendislik Fakultesi Fen ve Muhendislik*, 19(56), 583–598. <https://doi.org/10.21205/deufmd.2017195655>
- Pal, P. (2018). "Treatment and Disposal of Pharmaceutical Wastewater: Toward the Sustainable Strategy". *Separation and Purification Reviews*, 47(3), 179–198. <https://doi.org/10.1080/15422119.2017.1354888>
- Patil, S. P., and Rane, P. M. (2020). "Psidium guajava leaves assisted green synthesis of metallic nanoparticles: a review". *Beni-Suef University Journal of Basic and Applied*

*Sciences*, 9(1), 1–7. <https://doi.org/10.1186/s43088-020-00088-2>

Peng, J., Zhang, Y., Zhang, C., Miao, D., Li, J., Liu, H., Wang, L., and Gao, S. (2019). “Removal of triclosan in a Fenton-like system mediated by graphene oxide: Reaction kinetics and ecotoxicity evaluation”. *Science of the Total Environment*, 673, 726–733. <https://doi.org/10.1016/j.scitotenv.2019.03.354>

Pignatello, J. J., Oliveros, E., and MacKay, A. (2006). “Advanced oxidation processes for organic contaminant destruction based on the fenton reaction and related chemistry”. *Critical Reviews in Environmental Science and Technology*, 36(1), 1–84. <https://doi.org/10.1080/10643380500326564>

Prabhakar, R., Samadder, S. R., and Jyotsana. (2017). “Aquatic and terrestrial weed mediated synthesis of iron nanoparticles for possible application in wastewater remediation”. *Journal of Cleaner Production*, 168, 1201–1210. <https://doi.org/10.1016/j.jclepro.2017.09.063>

Prousek, J. (1995). “Fenton reaction after a century”. *Chemické Listy*, 89(1), 11–21.

Qu, Z. G., He, X. C., Lin, M., Sha, B. Y., Shi, X. H., Lu, T. J., and Xu, F. (2013). “Advances in the understanding of nanomaterial-biomembrane interactions and their mathematical and numerical modeling”. *Nanomedicine*, 8(6), 995–1011. <https://doi.org/10.2217/nnm.13.81>

Rafqah, S., Wong-Wah-Chung, P., Nelieu, S., Einhorn, J., and Sarakha, M. (2006). “Phototransformation of triclosan in the presence of TiO<sub>2</sub> in aqueous suspension: Mechanistic approach”. *Applied Catalysis B: Environmental*, 66(1–2), 119–125. <https://doi.org/10.1016/j.apcatb.2006.03.004>

Ramaswamy, B. R., Shanmugam, G., Velu, G., Rengarajan, B., and Larsson, D. J. (2011). “GC–MS analysis and ecotoxicological risk assessment of triclosan, carbamazepine and parabens in Indian rivers”. *Journal of hazardous materials*, 186(2-3), 1586–1593.

- Ravi, S., Lonappan, L., Touahar, I., Fonteneau, É., Vaidyanathan, V. K., and Cabana, H. (2020). "Evaluation of bio-fenton oxidation approach for the remediation of trichloroethylene from aqueous solutions". *Journal of Environmental Management*, 270(May). <https://doi.org/10.1016/j.jenvman.2020.110899>
- Ren, G., Shi, Y., Cai, Y., Yuan, L., Wu, K., Ouyang, M., and Zheng, K. (2022). "Removal of triclosan from water by sepiolite supported bimetallic Fe/Ni nanoparticles". *Environmental Technology (United Kingdom)*, 43(21), 3319–3328. <https://doi.org/10.1080/09593330.2021.1921050>
- Ren, Y. Z., Franke, M., Anschuetz, F., Ondruschka, B., Ignaszak, A., and Braeutigam, P. (2014). "Sonochemical degradation of triclosan in water". *Ultrasonics Sonochemistry*, 21(6), 2020–2025. <https://doi.org/10.1016/j.ultsonch.2014.03.028>
- Renganathan, J., S, I. U. H., Ramakrishnan, K., Ravichandran, M. K., and Philip, L. (2021). "Spatio-temporal distribution of pharmaceutically active compounds in the River Cauvery and its tributaries, South India". *Science of the Total Environment*, 800, 149340. <https://doi.org/10.1016/j.scitotenv.2021.149340>
- Saez, C., de Vidales, M. J. M., Canizares, P., Cotillas, S., Llanos, J., Perez, J. F., and Rodrigo, M. A. (2014). "Irradiated electrochemical processes for the removal of persistent organic pollutants from waters and wastewaters". *CHEMICAL ENGINEERING*, 41.
- Sanchez-Prado, L., Llompart, M., Lores, M., García-Jares, C., Bayona, J. M., and Cela, R. (2006). "Monitoring the photochemical degradation of triclosan in wastewater by UV light and sunlight using solid-phase microextraction". *Chemosphere*, 65(8), 1338–1347. <https://doi.org/10.1016/j.chemosphere.2006.04.025>
- Sangami, S., and Manu, B. (2017a). "Optimization of Fenton's oxidation of herbicide dicamba in water using response surface methodology". *Applied Water Science*, 7(8), 4269–4280. <https://doi.org/10.1007/s13201-017-0559-8>

- Sangami, S., and Manu, B. (2017b). “Synthesis of Green Iron Nanoparticles using Laterite and their application as a Fenton-like catalyst for the degradation of herbicide Ametryn in water”. *Environmental Technology and Innovation*, 8, 150–163. <https://doi.org/10.1016/j.eti.2017.06.003>
- Sangami, S., and Manu, B. (2018). “Catalytic efficiency of Laterite based FeNPs for the mineralization of mixture of herbicides in water”. *Environmental Technology*, 0(0), 1–30. <https://doi.org/10.1080/09593330.2018.1449899>
- Sedighe Arabi, Hamid Akbari Javar, and M. K. (2016). “Preparation and Characterization of Modified Polyethyleneimine Magnetic Nanoparticles for Cancer Drug Delivery”. *Journal of Nanomaterials*, 2016(8), 174–179.
- Selvaraj, R., Pai, S., Murugesan, G., Pandey, S., Bhole, R., Gonsalves, D., Varadavenkatesan, T., and Vinayagam, R. (2021). “Green synthesis of magnetic  $\alpha$ -Fe<sub>2</sub>O<sub>3</sub> nanospheres using *Bridelia retusa* leaf extract for Fenton-like degradation of crystal violet dye”. *Applied Nanoscience (Switzerland)*, 11(8), 2227–2234. <https://doi.org/10.1007/s13204-021-01952-y>
- Shahwan, T., Abu Sirriah, S., Nairat, M., Boyaci, E., Eroğlu, A. E., Scott, T. B., and Hallam, K. R. (2011). “Green synthesis of iron nanoparticles and their application as a Fenton-like catalyst for the degradation of aqueous cationic and anionic dyes”. *Chemical Engineering Journal*, 172(1), 258–266. <https://doi.org/10.1016/j.cej.2011.05.103>
- Singer, H., Müller, S., Tixier, C., and Pillonel, L. (2002). “Triclosan: Occurrence and fate of a widely used biocide in the aquatic environment: Field measurements in wastewater treatment plants, surface waters, and lake sediments”. *Environmental Science and Technology*, 36(23), 4998–5004. <https://doi.org/10.1021/es025750i>
- Sirés, I., Oturan, N., Oturan, M. A., Rodríguez, R. M., Garrido, J. A., and Brillas, E. (2007). “Electro-Fenton degradation of antimicrobials triclosan and triclocarban”.

*Electrochimica Acta*, 52(17), 5493–5503.

<https://doi.org/10.1016/j.electacta.2007.03.011>

So, H. L., Lin, K. Y., and Chu, W. (2019). “Triclosan removal by heterogeneous Fenton-like process: Studying the kinetics and surface chemistry of Fe<sub>3</sub>O<sub>4</sub> as catalyst”.

*Journal of Environmental Chemical Engineering*, 7(5).

<https://doi.org/10.1016/j.jece.2019.103432>

Soil Engineering and Rock Mechanics Sectional Committee, B. 23. (1982). *Indian*

*Standard METHODS OF TEST FOR SOILS (IS : 2720 ( Part XXV ) - 1982)*. 1–7.

<https://law.resource.org/pub/in/bis/S03/is.2720.25.1982.pdf>

Somchaidee, P., and Tedsree, K. (2018). “Green synthesis of high dispersion and narrow size distribution of zero-valent iron nanoparticles using guava leaf (*Psidium guajava* L) extract”. *Advances in Natural Sciences: Nanoscience and Nanotechnology*, 9(3).

<https://doi.org/10.1088/2043-6254/aad5d7>

Song, Z., Wang, N., Zhu, L., Huang, A., Zhao, X., and Tang, H. (2012). “ Efficient oxidative degradation of triclosan by using an enhanced Fenton-like process”.

*Chemical Engineering Journal*, 198–199, 379–387.

<https://doi.org/10.1016/j.cej.2012.05.067>

Srivastav, M., Gupta, M., Agrahari, S. K., and Detwal, P. (2019). “Removal of Refractory Organic Compounds from Wastewater by Various Advanced Oxidation Process - A Review”. *Current Environmental Engineering*, 6, 8–16.

<https://doi.org/10.2174/2212717806666181212125216>

Snyder S.A. (2008), "Occurrence, Treatment, and Toxicological Relevance of EDCs and Pharmaceuticals in Water", *Ozone: Science and Engineering*, 30, 65–69

Vasquez, M. I., Lambrianides, A., Schneider, M., Kümmerer, K., and Fatta-kassinos, D. (2014). “Environmental side effects of pharmaceutical cocktails : What we know and

- what we should know”. *Journal of Hazardous Materials*, 279, 169–189.  
<https://doi.org/10.1016/j.jhazmat.2014.06.069>
- Vieno, N. M., Härkki, H., Tuhkanen, T., and Kronberg, L. (2007). “Occurrence of pharmaceuticals in river water and their elimination in a pilot-scale drinking water treatment plant”. *Environmental Science and Technology*, 41(14), 5077–5084.  
<https://doi.org/10.1021/es062720x>
- Wang, S., Wang, X., Poon, K., Wang, Y., Li, S., Liu, H., Lin, S., and Cai, Z. (2013). “Removal and reductive dechlorination of triclosan by *Chlorella pyrenoidosa*”. *Chemosphere*, 92(11), 1498–1505.  
<https://doi.org/10.1016/j.chemosphere.2013.03.067>
- Wang, T., Jin, X., Chen, Z., Megharaj, M., and Naidu, R. (2014). “Green synthesis of Fe nanoparticles using eucalyptus leaf extracts for treatment of eutrophic wastewater”. *Science of the Total Environment*, 466–467, 210–213.  
<https://doi.org/10.1016/j.scitotenv.2013.07.022>
- Weng, X., Owens, G., and Chen, Z. (2020). “Synergetic adsorption and Fenton-like oxidation for simultaneous removal of ofloxacin and enrofloxacin using green synthesized Fe NPs”. *Chemical Engineering Journal*, 382(July 2019), 122871.  
<https://doi.org/10.1016/j.cej.2019.122871>
- Wert, E. C., Rosario-Ortiz, F. L., and Snyder, S. A. (2009). “Effect of ozone exposure on the oxidation of trace organic contaminants in wastewater”. *Water Research*, 43(4), 1005–1014. <https://doi.org/10.1016/j.watres.2008.11.050>
- Wilson, B. A., Smith, V. H., Denoyelles, F., and Larive, C. K. (2003). “Effects of three pharmaceutical and personal care products on natural freshwater algal assemblages”. *Environmental Science and Technology*, 37(9), 1713–1719.  
<https://doi.org/10.1021/es0259741>

- Wu, H., and Wang, S. (2012). Impacts of operating parameters on oxidation-reduction potential and pretreatment efficacy in the pretreatment of printing and dyeing wastewater by Fenton process. *Journal of Hazardous Materials*, 243, 86–94. [+https://doi.org/10.1016/j.jhazmat.2012.10.030](https://doi.org/10.1016/j.jhazmat.2012.10.030)
- Xue, X., Hanna, K., and Deng, N. (2009). Fenton-like oxidation of Rhodamine B in the presence of two types of iron (II, III) oxide. *Journal of Hazardous Materials*, 166(1), 407–414. <https://doi.org/10.1016/j.jhazmat.2008.11.089>
- Yang, B., Ying, G.-G. G., Zhao, J.-L. L., Zhang, L.-J. J., Fang, Y.-X. X., and Nghiem, L. D. (2011). Oxidation of triclosan by ferrate: Reaction kinetics, products identification and toxicity evaluation. *Journal of Hazardous Materials*, 186(1), 227– 235. <https://doi.org/10.1016/j.jhazmat.2010.10.106>
- Yin, Y., Wu, H., Jiang, Z., Jiang, J., and Lu, Z. (2022). Degradation of Triclosan in the Water Environment by Microorganisms: A Review. *Microorganisms*, 10(9), 1713. <https://doi.org/10.3390/microorganisms10091713>
- Ying G.G. and Kookana R.S., (2007), "Triclosan in wastewaters and biosolids from Australian wastewater treatment plants", *Environment International*, 33, 199–205
- Yueh, M. F., and Tukey, R. H. (2016). “Triclosan: A Widespread Environmental Toxicant with Many Biological Effects”. *Annual Review of Pharmacology and Toxicology*, 56, 251–272. <https://doi.org/10.1146/annurev-pharmtox-010715-103417>
- Zhang, Z., Li, J., Luan, C., Wang, H., Cheng, X., Fang, L., Wang, L., Zhao, B., Ma, C., Zhang, H., Li, C., and Xu, J. (2020). “Preparation and characterization of palladium/polypyrrole-reduced graphene oxide/foamed nickel composite electrode and its electrochemical dechlorination of triclosan”. *Arabian Journal of Chemistry*, 13(2), 3963–3973. <https://doi.org/10.1016/j.arabjc.2019.04.006>
- Zhao, C., Xie, H. J., Xu, J., Xu, X., Zhang, J., Hu, Z., Liu, C., Liang, S., Wang, Q., and

Wang, J. (2015). Bacterial community variation and microbial mechanism of triclosan (TCS) removal by constructed wetlands with different types of plants. *Science of the Total Environment*, 505, 633–639.  
<https://doi.org/10.1016/j.scitotenv.2014.10.053>

Zinatloo-Ajabshir, S., Salavati-Niasari, M., and Zinatloo-Ajabshir, Z. (2016). “Nd<sub>2</sub>Zr<sub>2</sub>O<sub>7</sub>-Nd<sub>2</sub>O<sub>3</sub> nanocomposites: New facile synthesis, characterization and investigation of photocatalytic behavior”. *Materials Letters*, 180, 27–30.  
<https://doi.org/10.1016/j.matlet.2016.05.094>

## **LIST OF PUBLICATIONS BASED ON PRESENT WORK**

1. Rashmishree K N, Bhaskar S, Shrihari S, Arun Kumar Thalla, “Green synthesis of laterite iron-based nanocatalysts using Psidium guajava and Macaranga peltata plant extract for its catalytic application in Fenton’s oxidation of triclosan” , Clean Technologies and Environmental Policy, Volume 1, Issue:12, March - 2023.
2. Rashmishree K N, Bhaskar S, Shrihari S, Arun Kumar Thalla,“Extraction of iron from laterite soil and green synthesis of laterite Nano iron catalyst (GLaNICs) for its application as Fenton's catalyst in the degradation of triclosan.” Water Science and Technology, Volume:86, Issue: 12, Page No. 3195-3204, November - 2022.
3. Rashmishree K N, Shrihari S, Arun Kumar Thalla,“Removal of micro-pollutants using green synthesized Nano iron particles by the advanced oxidation process”, Poll Res. , Volume: 40, Issue: 3: Page No.884-892, February - 2021.

## **LIST OF CONFERENCE**

1. “Green synthesis of Laterite – based Iron oxide nanoparticles using Makaranga peltata leafextract for its application as Fenton’s catalyst in the degradation of triclosan” presented in3rd International Conference on Chemical, Bio and Environmental Engineering (CHEMBIOEN 2022) held at Department of Chemical Engineering, B V Raju Institute of Technology, Narsapur in collaboration with Dr B R Ambedkar National Institute of Technology, Jalandhar on November 2022.

## RESUME

Name : Mrs. RASHMISHREE K. N.  
Permanent Address : W/O Komalesh Rao P  
#2022, Vijinapura Extention,  
Ramamurthy Nagar, Bangalore 560016  
Contact Number : +918971141387  
Email id: : rashu.kn87@gmail.com

## ACADEMIC QUALIFICATIONS

Degree	Specialization	INSTITUTION	DURATION	% MARKS
PhD	Environmental Engineering	NITK, Surathkal	2015-2023	8.77 (CGPA)
M.Tech	Environmental Engineering	NITK, Surathkal	2009-2011	8.03 (CGPA)
B.E	Civil Engineering	KVGCE, Sullia	2005-2009	69.57 %

## PUBLICATIONS

- Green synthesis of laterite iron-based nanocatalysts using *Psidium guajava* and *Macaranga peltata* plant extract for its catalytic application in Fenton's oxidation of triclosan", Clean Technologies and Environmental Policy, Volume 1, Issue:12, March - 2023.

- “Green synthesis of granular activated carbon/zinc ferro nanocomposites-based bioleached laterite iron (BLaFe) for the removal of Rhodamine B in water using adsorption–Fenton's oxidation process”, *Water Practice and Technology*, Volume 18, Issue: 3, Page No. 665-676. February – 2023.
- “Extraction of iron from laterite soil and green synthesis of laterite Nano iron catalyst (GLaNICs) for its application as Fenton's catalyst in the degradation of triclosan.” *Water Science & Technology*, Volume: 86, Issue: 12, Page No. 3195-3204, November - 2022.
- “Sustainable replacement of EDTA–Biojarosite for commercial iron in the Fenton's and UV–Fenton's degradation of Rhodamine B—a process optimization using Box–Behnken method”. *Water Science & Technology*, Volume: 86, Issue: 8, Page No. 2008-2019, October- 2022.
- “Removal of micro-pollutants using green synthesized Nano iron particles by the advanced oxidation process”, *Poll Res.* , Volume: 40, Issue: 3: Page No.884-892, February - 2021.
- “Determination of water quality of Vengaihnakere lake and Varthur lake, Bangalore”, *IJRET*, e-ISSN: 2395-0056, Volume: 05, Issue: 06, June -2018.
- “Study of Leachate Management in Municipal Solid Waste Management System”, *IERJ*, e-ISSN No: 2454 - 9916, Volume: 03, Issue: 06, June -2017.
- “Production of Bio Gas using Kitchen Waste”, *IJRET*, e-ISSN No: 2319 - 1163, Volume: 05 Issue: 06, June -2016.

#### **CONFERENCE ATTENDED**

- “Green synthesis of Laterite – based Iron oxide nanoparticles using Makaranga peltata leaf extract for its application as Fenton’s catalyst in the degradation of triclosan” presented in 3<sup>rd</sup> International Conference on Chemical, Bio & Environmental Engineering (CHEMBIOEN 2022) held at Department of Chemical Engineering, B V Raju Institute of Technology, Narsapur in collaboration

with Dr B R Ambedkar National Institute of Technology, Jalandhar on 4<sup>th</sup> - 5<sup>th</sup> November 2022.

- “Treatment of Leachate using Low-Cost Materials” presented in 2<sup>nd</sup> International Conference on Recent Research Emerging Trends in Mechanical and Civil Engineering (ICRRETMCE – 2018) held at Reva University on 13<sup>th</sup> - 14<sup>th</sup> July 2018.